CHALMERS

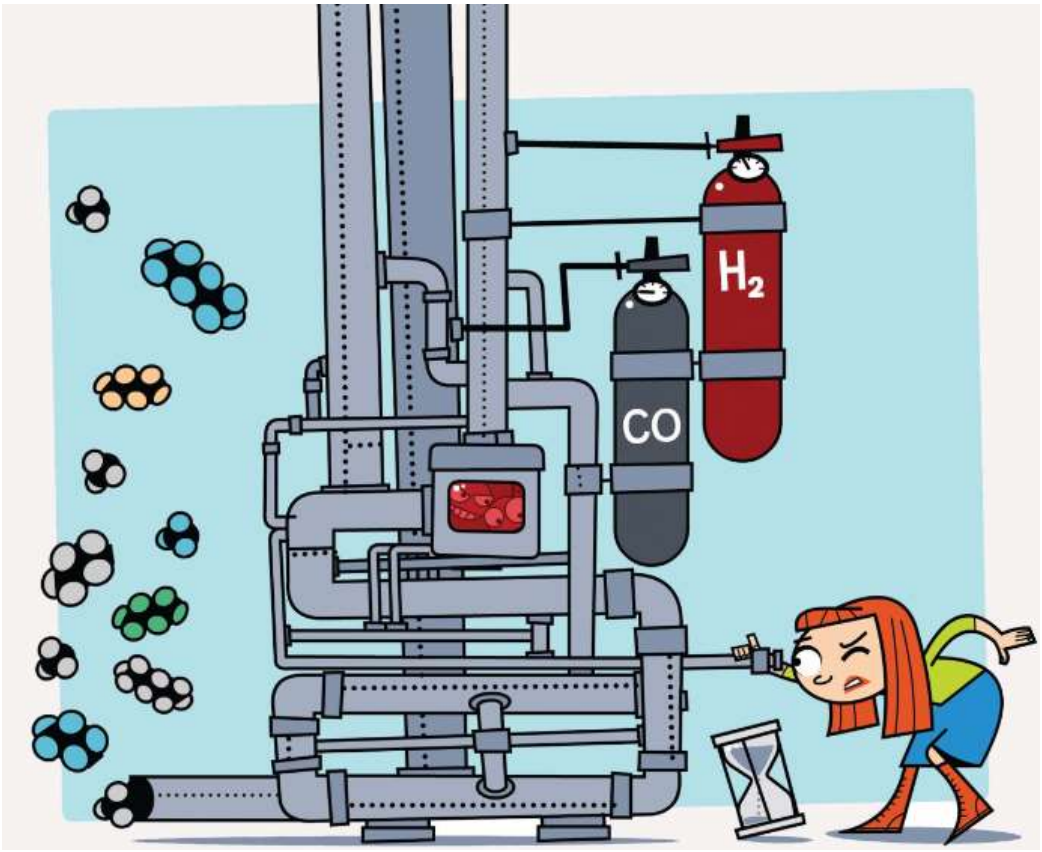

Process synthesis and design of low temperature Fischer-Tropsch crude production from biomass derived syngas

Master's Thesis within the Sustainable Energy Systems programme

MADDALENA PONDINI

MADELINE EBERT

Department of Energy and Environment
Division of Heat and Power Technology
CHALMERS UNIVERSITY OF TECHNOLOGY
Göteborg, Sweden 2013

MASTER'S THESIS

Process synthesis and design of low temperature Fischer-Tropsch crude production from biomass derived syngas

Master's Thesis within the Sustainable Energy System programme

MADDALENA PONDINI

MADELINE EBERT

SUPERVISOR(S):

Matteo Morandin

EXAMINER

Karin Pettersson

Department of Energy and Environment

Division of Heat and Power Technology

CHALMERS UNIVERSITY OF TECHNOLOGY

Göteborg, Sweden 2013

Process synthesis and design of low temperature Fischer-Tropsch crude production from biomass derived syngas
Master's Thesis within the Sustainable Energy Systems programme
MADDALENA PONDINI
MADELINE EBERT

Department of Energy and Environment
Division of Heat and Power Technology
Chalmers University of Technology
SE-412 96 Göteborg
Sweden
Telephone: + 46 (0)31-772 1000

Cover:
Drawn by Itamar Daube; http://www.itamardaube.com
http://blogs.rsc.org/gc/2011/08/05/green-chemistry-volume-13-issue-8-online-now/, checked: 11.06.2013.

Chalmers Reproservice
Göteborg, Sweden 2013

Process synthesis and design of low temperature Fischer-Tropsch crude production from biomass derived syngas
Master's Thesis in the *Sustainable Energy Systems* programme

MADDALENA PONDINI
MADELINE EBERT
Department of Energy and Environment
Division of Heat and Power Technology
Chalmers University of Technology

ABSTRACT

The production of biofuels via a low temperature Fischer-Tropsch synthesis could potentially increase the utilization of biofuels without having to change the currently used combustion engines. Furthermore, the upgrading process needed to convert the FT-crude obtained just after the synthesis into commercial motor fuels could be done in a state-of-the-art refinery. In addition, current infrastructures would still be suitable for the distribution of the FT-fuels.

To gain knowledge about this synthesis, a model has been developed with particular focus on the FT-synthesis of hydrocarbons from biomass derived syngas. The general Biomass-To-Liquid process would also include the upstream gasification process which converts biomass into syngas and the further upgrading of the FT-crude into diesel and gasoline. The main features of this model are: a chain growth probability, α, dependent on temperature, H_2 and CO mole fraction, a concomitant production of olefins and paraffins considered and kinetics of the FT-synthesis reaction taken into account.

The starting point of the modelled processes is a cleaned syngas which was previously derived from biomass through a gasification process. This syngas is then converted into a FT-crude stream. However, not all of the H_2 and CO in the fresh syngas is converted in the FT-synthesis. Therefore, it can be recycled into the reactor to increase the overall conversion. Alternatively, the light hydrocarbons in the syngas obtained after crude condensation can be reformed to H_2 and CO, thus increasing the fresh syngas available for the synthesis. To avoid a build-up of inert components, some of the recycled stream is purged. Four different process configurations have been modelled and analysed in this work. They differ by the way the syngas loop is handled (with and without reformer) and by the final utilization of the purge gas (simple combustion in a boiler or used to fuel a gas turbine for power production).

This work discusses the results of a parametric study of the different configurations in order to investigate the impact of the reactor operating temperature, pressure and of the desired CO conversion on different indicators. Within this study the product distribution has been investigated according to the characteristics required for products in the carbon ranges of interest. Catalyst amount and reactor volume needed to achieve a certain CO conversion have been calculated as well as efficiencies of the process using different system boundaries. The electricity balance of the processes has also been considered for further evaluation. The results highlight that there is a trade-off between the quality and quantity of FT-crude production and the reactor size which mainly depends on the temperature. With an increase in temperature the reactor volume decreases, however, the amount of long chain hydrocarbons decreases as well and the production of C_{1-4} is favoured. This gives a less valuable product stream. The same trend is applicable for the system and conversion efficiency of the modelled process.

Due to the applied model for the chain growth probability (α) of the hydrocarbons, the pressure only has a minor impact except for the electricity consumption. It can be generally concluded that the electricity demand of the FT synthesis process increases with the pressure. It is furthermore shown that the same impact on the electricity consumption can be observed with an increase of the CO conversion within the FT reactor. Considering the impact of an upgrading process for the recirculating gas flow, it can be concluded that the utilisation of a reformer helps to a large extent to reduce the need for a water gas shift prior the synthesis step. However, with the syngas composition considered in this work (similar to that of a biomass indirect gasifier product gas) the reformer's contribution is not enough to completely avoid this part of the system.

The model of the FT-reactor provided by this study can be used in the future to investigate a more complete process where the syngas production, e.g. by biomass gasification, as well as the following upgrading of the FT-crude to motor fuels is also included. The major advantage of this model with respect to other literature models is that kinetic has been taken into account.

Keywords: Low temperature Fischer-Tropsch, Process Synthesis, biofuel, autothermal reformer

SOMMARIO

La produzione di biofuels attraverso la sintesi di Fischer-Tropsch di bassa temperatura offre la possibilità di un aumento nell'utilizzo di biofuels senza la necessità di apportare modifiche ai motori a combustione comunemente usati. Inoltre il processo di upgrading richiesto per la trasformazione dell'FT-crude ottenuto dalla sintesi in combustibili a livello commerciale può essere attuato utilizzando unità di processo già esistenti. In aggiunta le attuali infrastrutture sarebbero ancora adatte alla distribuzione degli FT-fuels.

Per acquisire più familiarità con questo processo di sintesi un modello è stato sviluppato con particolare attenzione alla sintesi di idrocarburi FT da syngas derivato da biomassa. In generale il processo Biomass-To-Liquid (BTL) includerebbe anche la gassificazione a monte che converte la biomassa nel syngas e l'ulteriore upgrading dell'FT-crude in diesel e benzine. Le caratteristiche più importanti di questo modello sono: la probabilità di crescita della catena idrocarburica α che dipende dalla temperatura e dalle frazioni molari di H_2 e CO, una produzione concomitante di olefine e paraffine e la cinetica della reazione di sintesi di FT tenuta in considerazione.

Il punto di partenza del processo modellato è un syngas pulito derivato precedentemente da biomassa attraverso la gassificazione. Questo syngas è poi convertito in FT-crude. Tuttavia non tutto l'H_2 e il CO contenuti nel syngas sono convertiti nella sintesi di FT, quindi può essere ricircolato nel reattore per aumentare la conversione complessiva. In alternativa gli idrocarburi leggeri in questo syngas ottenuti dopo la condensazione del greggio posso essere riformati in H_2 e CO per aumentare il syngas disponibile per la sintesi. Per evitare un crescita di componenti inerti una parte del flusso di ricircolo è separato come gas di scarto. Quattro configurazioni sono state modellate e analizzate in questo studio e si differenziano dalla modalità con cui il ricircolo è gestito (con e senza reformer) e dall'utilizzo finale del gas di scarto (semplice combustione in una caldaia o usato per alimentare una turbina a gas per la produzione di elettricità).

Questo studio mostra i risultati ottenuti da uno studio parametrico delle diverse configurazioni al fine di analizzare l'impatto delle condizioni operative della sintesi di FT, ossia temperatura, pressione e conversione del CO, su diversi indicatori. Attraverso questo studio la distribuzione dei prodotti è stata osservata in linea con le caratteristiche richieste per i prodotti negli intervalli di numero di Carbonio richiesti. La quantità di catalizzatore e il volume del reattore per ottenere una certa conversione del CO sono stati calcolati così come le efficienze del processo con diversi limiti di sistema. Anche il bilancio di elettricità dei processi è stato considerato per ulteriori valutazioni. I risultati sottolineano che c'è un trade-off tra qualità e quantità di FT-crude prodotti e il design del reattore che dipende principalmente dalla temperatura. Con una crescita nella temperatura il volume del reattore diminuisce insieme alla quantità di idrocarburi di catena lunga mentre la produzione di C_{1-4} è favorita.

Lo stesso andamento si può riscontrare nell'efficienza di sistema ed efficienza di conversione del processo in questione. A causa del modello scelto per la probabilità di crescita della catena idrocarburica α la pressione ha un'influenza scarsa sulla maggior parte delle valutazioni fatte a parte quelle riguardanti la produzione e il consumo di elettricità. Si può in generale concludere che il consumo del processo di sintesi di FT cresce con la pressione e di conseguenza il surplus di elettricità nei casi con turbina a gas diminuisce. I risultati mostrano anche che lo stesso impatto sul consumo di elettricità risulta con un aumento della conversione del CO nel reattore FT. Considerando l'impatto di un processo di upgrading per il gas di ricircolo si può concludere che l'utilizzo di un reformer aiuta per gran parte a ridurre l'apporto di idrogeno da parte del reattore di shift prima della sezione di sintesi. Nonostante questo, con la composizione del gas di sintesi adottata (simile a quella di un gas da gassificazione indiretta di biomassa) il contributo del reformer non è sufficiente a evitare completamente questa parte del sistema.

Il modello di sintesi di FT fornito da questo studio può essere utilizzato nel futuro per l'analisi di processi più complessi dove la produzione di syngas, e.g. attraverso la gassificazione di biomassa, così come il successivo processo di upgrading sono inclusi. Il vantaggio più evidente di questo modello rispetto ad altri modelli da letteratura consiste nell'aver tenuto in considerazione la cinetica della reazione.

Parole chiave: Fischer-Tropsch di bassa temperatura, sintesi, biomassa, reforming auto termico

ZUSAMMENFASSUNG

Die Erzeugung von Biobrennstoffen durch eine Niedertemperatur Fischer-Tropsch (FT) Synthese hat das Potenzial die Anwendung von Biobrennstoffen zu erhöhen. Ein besonderer Vorteil ist, dass es nicht notwendig ist die aktuell verwendeten Motoren zu verändern. Darüber hinaus kann die Veredelung dieser FT-Rohöle mit Raffinerien nach dem heutigen Stand der Technik durchgeführt werden. Zusätzlich ist die jetzige Infrastruktur auch anwendbar für die Verteilung von FT-Motorbrennstoffen.

Um das Wissen über den FT-Syntheseprozess zu erhöhen wurde ein Model entwickelt, das sich besonders auf die FT-Synthese von Kohlenwasserstoffen aus Biomasse konzentriert. Der generelle Biomass-To-Liquid Prozess würde darüber hinaus die vorherige Vergasung der Biomasse umfassen, wie auch den Veredelungsprozess der FT-Rohöle zu Diesel und Benzin.

Die Hauptmerkmale dieses Models umfassen: die Kettenwachstumswahrscheinlichkeit α, welche abhängig von der Temperatur und der Syngaszusammensetzung ist, die gleichzeitige Erzeugung von Paraffinen und Olefinen wie auch die Reaktionskinetik der FT-Synthese.

Das Model beginnt mit einem gereinigten Syngas, welches aus einer Biomassevergasung gewonnen wurde. Dieses Syngas wird daraufhin zu FT-Rohöl umgewandelt. Da jedoch H2 und CO nicht komplett umgewandelt werden, wird dieser Teil des Produktstroms rezirkuliert, wodurch sich die Gesamtumwandlung erhöht. Eine Alternative für den rezirkulierenden Strom ist die darin enthaltenen kurzen Kohlenwasserstoffe wieder zu H2 und CO zu reformieren. Um einen Aufbau inerter Bestandteile zu verhindern wird ein Teil des rezirkulierenden Stroms entweder ein einem Kessel verbrannt oder in einer Gasturbine zu zusätzlichen Stromerzeugung verwendet.

Diese Arbeit diskutiert die Ergebnisse einer Paramterstudie auf die unterschiedlichen Konfigurationen, um den Einfluss der Arbeitstemperatur, des Arbeitsdruckes und der gewünschten CO-Umwandlung auf verschiedene Indikatoren zu untersuchen. In dieser Arbeit wurde zum einen die Produktverteilung für die gewünschten Kettenlängenbereiche untersucht, wie auch die notwendige Katalysatormenge und die Reaktorgröße. Darüber hinaus wurden verschiedene Prozesseffizienten mit unterschiedlichen Systemgrenzen wie auch die Strombilanz berechnet. Die Ergebnisse zeigen dass ein Kompromiss zwischen der Qualität und Quantität der FT-Rohölproduktion und der Reaktorgröße gefunden werden muss. Dieser Kompromiss wird hauptsächlich durch die Temperatur bestimmt, da mit einem Anstieg der Temperatur das Reaktorvolumen verringert wird, allerdings führt dies auch zu einer geringeren Produktion von langkettigen Kohlenwasserstoffen. Ein ähnlicher Trend wurde für die System und Umwandlungseffizienz ermittelt.

Da das angewendete empirische Model für die Kettenwachstumswahrscheinlichkeit α nicht von Druck abhängig ist, hat dieser nur einen geringen Einfluss außer auf den Stromverbrauch. Es kann generell zusammengefasst werden, dass der Stromverbrauch des Prozesses mit steigendem Druck wie auch steigender CO-Umwandlung zunimmt. Zuletzt wurde der Einfluss der Reformierung des rezirkulierenden Stroms auf die Anwendung einer vorgelagerten Wassergas-Shift-Reaktion untersucht.

Das Model der FT-Synthese, das in dieser Arbeit entwickelt wurde, kann in der Zukunft verwendet werden um weitere komplexere Prozesse zu untersuchen, die unter anderem auch die Biomassevergasung oder den Veredelungsprozess umfassen. Der hauptsächliche Vorteil dieses Modells liegt in der integrierten Betrachtung der Reaktionskinetik.

Schlüsselwörter: Niedertemperatur Fischer-Tropsch, Prozesssynthese, Biobrennstoffe, Autotherme Reformierung

Contents

Abbreviations

a ..... Reaction constant [mmol/min g_{cat} MPa^2]

A ..... ash content

ASF ..... Anderson-Schulz-Flory

b ..... Reaction constant [1/MPa]

bbl ..... barrel

BTL ..... Biomass-to-Liquid

C ..... Carbon

CFB ..... Circulating Fluidized Bed

CSTR ..... Continuous Stirred Tank Reactor

CTL ..... Coal-to-Liquid

d ..... Catalyst density in FT-reactor [$kg_{cat}/m^3_{reactor}$]

E_A ..... Activation energy [kJ/mol]

FC ..... fixed coal

FT ..... Fischer-Tropsch

g_{cat} ..... Mass of catalyst [g]

GCC ..... Grand Composite Curve

GT ..... Gas Turbine

GTL ..... Gas-to-Liquid

HHV ..... Higher Heating Value

HTFT ..... High Temperature Fischer-Tropsch

k_0. ..... Reaction constant [mol/s kg_{cat} bar^2]

k_1 ..... Reaction constant [1/bar]

LTFT ..... Low Temperature Fischer-Tropsch

M ..... moisture content

M_n ..... Molar distribution

n ..... Carbon number

O/P ..... α-Olefin / n-Paraffin

p_i ..... Partial pressure of component i

p_{tot} ..... Total pressure of stream [bar]

r_{CO} ..... Reaction rate [mol/dm^3 s]

R_{CO} ..... Carbon monoxide reaction rate [mol/s kg_{cat}]

R_p ..... Propagation rate

R_t ..... Termination rate

SAS ..... Sasol Advanced Synthol process

S_{C5+} ..... Selectivity for hydrocarbons with n > 5
SMDS ..... Shell Middle Distillate Synthesis
SSBR ..... Sasol Slurry Bed Reactor
T ..... Temperature
V ..... Reactor volume [m^3]
$W_{e,net}$ ..... Net electricity
WGS ..... Water-Gas-Shift reaction
VM ..... volatile matter
W_n ..... Weight distribution
α ..... Chain growth probability
γ_i ..... mole fraction of component i
ΔH_{ads} ..... Adsorption energy [kJ/mol]
η_{CG} ..... Cold gas efficiency
η_{conv} ..... Conversion efficiency
η_{System} ..... System efficiency
χ_{CO} ..... CO conversion
Θ ..... Carnot Factor

1 Introduction

> *"In Sweden the market share of diesel cars grew from below 10 percent in 2005 to 62 percent in 2011 despite a closing gap between pump prices on diesel oil and gasoline, and diesel cars being less favored than ethanol and biogas cars in terms of tax cuts and other subsidies offered to ‘‘environment cars’’." (Kågeson 2013)*

This statement is in unison with the facts shown in Figure 1-1. The energy use in the car sector in Sweden has been generally increasing in the years apart from the period between 2007 and 2009 due to the beginning of the economic crisis. The values in the graph represent a part of the total energy use in the transport sector (123 TWh in 2012) which includes also aviation, maritime traffic and rail traffic (Swedish Energy Agency 2013). It can be stated that the percentage of renewable motor fuels has also been increasing but a further push is needed in order to be able to make the share of conventional car fuels become even lower.

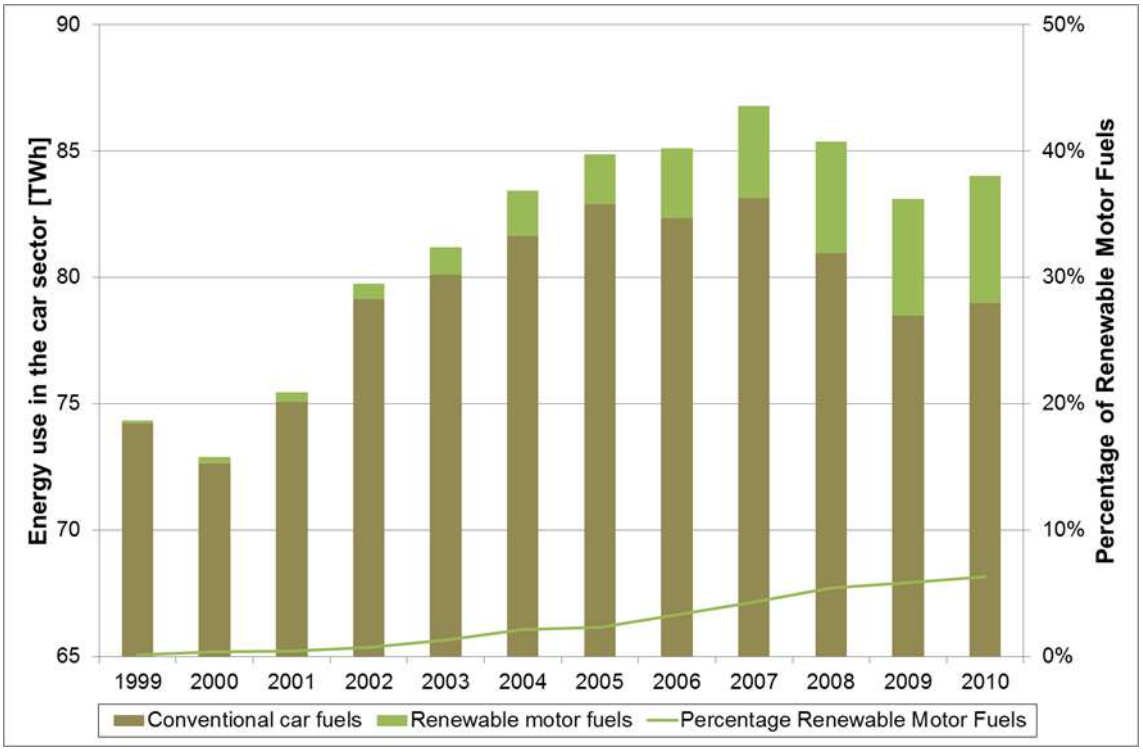

Figure 1-1: Trend in the energy use (TWh) of the car sector - comparing the renewable with conventional motor fuels (Swedish Energy Agency 2013)

There are different technologies available nowadays to promote a further increase of renewable motor fuels. Generally, biofuels can be divided according to their feedstock into: first, second, third and fourth generation biofuels. Table 1-1 shows the characteristics for the different renewable biofuel generations.

Table 1-1: Comparison of different generation biofuels based on their feedstock and produced fuel (Fatih Demirbas 2009)

Generation	Feedstock	Fuel example
First	Sugar, starch, vegetable oils	Bioalcohols, biodiesel, biogas
Second	Non-food crops, wheat, straw, wood, solid waste, energy crop	Bioalcohols, FT-diesel, DME
Third	Algae	Vegetable oil, biodiesel
Fourth	Vegetable oil, biodiesel	Biogasoline

First generation biofuels already reached full commercialization and are widely used nowadays. However, due to the use of food biomass their production raises sustainability questions (Naik et al. 2010). Third and fourth generation biofuels are being investigated but commercialization seems unfeasible within the next 10 years (Guczi and Erdôhelyi 2012). The most interesting option in shorter terms appears to be the second generation type. Within the different possible technologies to produce second generation biofuels the Fischer-Tropsch (FT) process will be investigated further in this study.

In general, it can be said that the FT-synthesis is a catalyst supported polymerisation which converts CO and H_2 into a wide range of liquid hydrocarbons (Yuan et al. 2011; Reichling and Kulacki 2011; Lu and Lee 2007). These hydrocarbons can then be further upgraded and converted in motor fuels and other chemicals.

The development of the FT-synthesis dates back into the early 19^{th} century and since then it has mainly been used with coal (Coal-to-liquid (CTL)) or natural gas (Gas-to-Liquid (GTL)) as feedstock (Dry 2004). However, recent research focuses on the use of biomass (Biomass-to-Liquid (BTL)) as an input to the upstream gasification process. The gasification produces a syngas which afterwards is converted within the FT-synthesis into hydrocarbons, the so called FT-crude. This FT-crude can either consist mainly of gasoline and olefins or of diesel and waxes depending on the FT-operation temperature. A downstream upgrading step of this FT-crude is needed in order to transform it into motor fuels (FT-fuels) that are suitable for market applications and therefore could help to decrease the share of conventional motor fuels.

These products are of special interest due to the absence of sulphur and the low content of aromatics[1], which make the fuel suitable for the combustion in conventional diesel and gasoline engines with the advantage of lower local emission levels (Calemma et al. 2010; Tijmensen et al. 2002). Furthermore, FT-fuels can be blended with conventional motor fuels. This makes it possible to use the current fuel infrastructure (Luque et al. 2012). All of these facts would lead to an increase in the percentage of renewable motor fuels in Sweden without the need to purchase a special "environment car". Furthermore, due to the very low amount of impurities the FT-fuels produced by the BTL process might be of special interest with the tightening of clean fuel regulations by the EU in the upcoming years (Euro 5 and Euro 6) (European Parliament 2007).

[1] Aromatics are an unwanted diesel component since they decrease the cetane number of the diesel fraction, a value that should rather be high in order to have a good combustion quality Dry (1981).

1.1 Objective of the thesis

The purpose of this master thesis is to gain knowledge about low temperature FT synthesis processes, the composition of the FT-crude product, and general techno-economic aspects of the process.

To achieve this goal steady-state models of different FT synthesis processes using biomass derived syngas as feedstock is built. Those models will be simulated with Aspen Plus, which holds the possibility to model a wide variety of chemical processes.

1.2 Methodological Approach

Based on the issue that regards fuels requirements underlined in the previous section, the present work aims at gaining knowledge about one of the possible solutions identified for the production of renewable motor fuels: the Fischer-Tropsch process. Therefore, a literature review has been carried out in Chapters 2 and 3 beginning from the early phase of application of this process to the technological characteristics that make it so peculiar.

In order to be able to understand the various factors that contribute to the achievement of the desired products, Aspen Plus is used as tool for process modelling and simulation. The starting point for this technical part is a model by Johan Isaksson from the Heat and Power Technology Division at Chalmers which is based on Hamelinck et al. (2004). From this a new model has been developed based on different assumptions related particularly to the product distribution. The choice of such model has been based on the probability of gaining products in the range of diesel and waxes which can be further upgraded into motor fuels. A further look into the olefin content has been taken into account together with an empirical equation for the alpha chain growth probability, both implemented through an MS-Excel file used as a calculator block for the Aspen simulation. Supplementary assumptions regarding reactor type, catalyst and kinetic model have been added during the elaboration of the whole simulation process and are outlined in Section 4.1. In the follow up of those assumptions a base configuration including the recycle of unconverted syngas to improve the overall conversion of the process was obtained. Different possibilities have been identified at this point involving either the purge from the recycle or the recycle itself. In Section 4.2 the different configurations developed are explained in detail.

A parametric study is conducted with pressure, temperature and CO conversion as varying parameters. The influence of different syngas composition is not taken into consideration since the gasification of biomass has not been included in the simulation. The parametric study is described in more detail in Section 4.3 where the indicators included in this study have been pointed out. In general the main outputs of the process such as the composition of the FT-crude stream, electricity and heat streams have been analysed as well as the efficiencies of the process itself. Another key factor that has been relevant to show was the catalyst amount and reactor volume which are directly related. At last, the interpretation and discussion of the results are outlined in Chapter 5 followed by conclusions gained from the evaluations made around the process in Chapter 6.

2 Introduction to the Fischer-Tropsch process

2.1 History and Development

The FT-reaction was discovered in the 1920s by Franz Fischer and Hans Tropsch and first applied as an alternative way to convert various gaseous products (mainly syngas) into a wide variety of hydrocarbon products, but further adjustments and developments were needed in order to make it relevant for a commercial use (Fatih Demirbas 2009).

In 1936 the first commercial FT-plant with an overall capacity of about 660 000 t/y was commissioned in Germany. The plant was built to supply Germany with an oil substitute due to the shortage of oil resources and the abundance of coal during the Second World War. FT-products accounted for about 9% of the total production capacity in Germany during this time (Dry 2004).

In 1940 a high temperature FT-plant utilizing an iron-based catalyst and converting natural gas to FT-liquids was operated in Brownsville, Texas (Luque et al. 2012). However, due to economical and operational problems the plant was shut down in the late 1950s already (Schulz 1999; Sie and Krishna 1999). In the same time period a coal-based FT-plant was constructed in Sasolburg, South Africa. The interest in the FT-process was mainly fuelled by the cheap coal available in South Africa wherefore the Sasol 1 plant was able to withstand the decreasing interest in FT due to cheap gas and oil supplies from the Middle East (Schulz 1999).

Over the years four different types of reactors have been commercially employed. Their development took place due to the increasing potential of large-scale production of synthetic fuels after the Second World War. The multitubular fixed bed reactor called ARGE was created by Lurgi and Ruhrchemie and had a production capacity of about 50 tonnes per day (around 400 bbl[2]/day). Another type of reactor applied was the high temperature circulating fluidized bed one, known as Synthol, whose products were mainly gasoline and light olefins. Later on, the Sasol Advanced Synthol (SAS) reactor has been developed, a fixed fluidized bed with similar operating conditions as the Synthol reactor but at half the capital cost and size for the same capacity. The fourth reactor design is the low temperature slurry reactor which operates in a three-phase system where an excellent contact between the different phases is achieved. This kind of reactor is nowadays gaining more relevance in the business of FT-technology especially because of the high interest in its commercial products such as clean diesel, waxes and paraffins (Lu and Lee 2007).

The original Sasol 1 plant in Sasolburg had both ARGE low temperature FT-technology (LTFT) and Synthol high temperature FT (HTFT) technology operating in parallel. The former was mainly addressed to the production of heavier products like diesel and waxes while the latter was more towards petrol (gasoline) (Steynberg and Dry 2004). Scaled-up reactors with a capacity of 6 500 bbl/day were later installed in Sasol 2 and Sasol 3 which were located in the Secunda Complex and began operation in 1980 and 1982. These two technologies applied fluidized bed reactors and they mainly produced motor gasoline and diesel although chemicals were also included. Their realization took place just after the oil crises in the 1970s and with these two projects the Secunda Complex consisted of 16 circulating fluidized bed (CFB) reactors each of 7 500 bbl/day capacity. The Secunda plant went through a series of subsequent changes, the most important consisted in the replacement of the existing CFB Synthol reactors with 8 SAS reactors, after the first commercial example of SAS was realized in 1989 (Chang 2000). As SAS produced also ammonia and other chemicals this helped the process to lose its identity as fuel-only refinery.

[2] bbl = barrels

This trend towards chemical products faced a slow down when the first commercial high temperature FT from natural gas was constructed. It was 1993 when a GTL plant built by PetroSa (Mossgas) and settled in Mossel Bay, South Africa, started operation. This plant makes use of an iron catalyzed Synthol reactor and exploits offshore natural gas as a feed.

Improvements to the capacity of the Arge reactor have been realized with the multitubular reactor applied in the Shell Middle Distillate Synthesis (SMDS) process which converts syngas from natural gas into heavy, waxy FT-products. The first SMDS plant was built in Bintulu, Malaysia and started operation in 1993 but its production hasn't been as fortunate as the one of the latest Sasol plants especially due to a high drop in oil prices in the middle of the 90s.

To give an overview Table 2-1 shows FT-plants that have been installed worldwide. However, most of these plants are not utilizing biomass as a feedstock.

Table 2-1: Overview of worldwide FT-plants (Luque et al. 2012)

Company	Country	Capacity [barrels/day]	Raw material	Status	Catalyst type
Sasol	South Africa	150.000	Coal	In operation	Fe/K
	China	2 x 80.000	Coal	Abandoned	—
	Australia	30.000	Natural gas	Study	—
	Nigeria	34.000	Natural gas	Under construction	—
	Qatar	34.000	Natural gas	In operation	Co/Al2O3
Shell	Malaysia	14.700	Natural gas	In operation	Co/SiO2
	Qatar	140.000		In operation	Proprietary Co-based
	Indonesia	75.000		Study	—
	Iran	70.000		Abandoned	—
	Egypt	75.000		Study	—
	Argentina	75.000		Study	—
	Australia	75.000		Study	—
Shell Choren	Germany	300	Biomass	In operation	—
Mossgas	South Africa	22.500	Natural gas	In operation	Fe/K
EniTechnologie	Italy	20	Natural gas	In operation	—
BP	USA	300	Natural gas	In operation	Proprietary Co-based
Rentech	USA	1.000	Natural gas	In operation	Proprietary Fe-based
	South Africa	10.000		Study	—
	Bolivia	10.000		Under construction	—
Rentech pertamina	Indonesia	15.000	Natural gas	Study	—
Syntroleum	USA	70	Natural gas	Closed	—
	Australia	11.500	Natural gas	Under construction	—
	Chile	10.000	Natural gas	Study	—
	Peru	5.000	Natural gas	Study	—
Syntrol.-Tyson Foods	USA	5.000	Biomass	In operation	Proprietary catalyst
Gazprom syntroleum	Russia	13.500	Natural gas	Study	—
Repsol-YPF	Bolivia	13.500	Natural gas	Study	—
Syntroleum	Bolivia	90.000		Study	—
ExxonMobil	Qatar	90.000	Natural gas	Abandoned	—
Conoco	Qatar	60.000	Natural gas	In operation	Proprietary catalyst
	USA	400		In operation	—
Bioliq	Germany	—	Biomass	Under construction	—

In the following section one possible BTL process will be discussed in more detail to highlight the differences between the BTL process and the longer developed CTL and GTL processes.

2.2 Overview of the Fischer-Tropsch BTL process

In this particular BTL process the biomass feedstock is converted into FT crude through a sequence of process steps that significantly resemble the more consolidated CTL case. An overview of the process steps is shown in Figure 2-1 below. The process starts with a pre-treatment of the biomass. Since the moisture content (M) of biomass is a lot higher than that of coal, as shown in Table 2-2, the biomass has to be dried first. The drying process of biomass is considered to be the most important step within the pre-treatment of biomass. Dry biomass not only increases the conversion efficiency of the gasifier it also lowers the hydrogen content in the rawgas, which is negative for the FT-synthesis (Jin Hu 2012). The subsequent grinding process is equal to the grinding of coal.

Table 2-2: Ultimate and proximate analysis of different feedstocks (Vassilev et al. 2010)

	Ulimate Analysis (waf)					Proximate Analysis (a.d.)			
Feedstock	**C**	**O**	**H**	**N**	**S**	**VM**	**FC**	**M**	**A**
Wood and woody biomass	52.1	41.2	6.2	0.4	0.08	62.9	6.5	4.7	0.1
Natural biomass	51.1	41.4	6.2	1.1	0.2	64.4	16	14.7	4.9
Peat	56.3	36.2	5.8	1.5	0.2	57.8	24.3	14.6	3.3
Coal	78.2	13.6	5.2	1.3	1.7	30.8	43.9	5.5	19.8
Lignite	64	23.7	5.5	1	5.8	32.8	25.7	10.5	31
Sub-bituminous coal	74.4	17.7	5.6	1.4	0.9	33.4	34.1	8.2	24.3
Bituminous coal	83.1	9.5	5	1.3	1.1	29.1	52.6	3.1	15.2

waf - water, ash free VM - volatile matters M - moisture content
a.d. - as delivered FC - fixed coal A - ash content

After the preparation, the biomass is gasified (Dry 2004) into a rawgas mainly consisting of H_2, CO, CO_2 and CH_4. According to Le Chatelier's principle the production of H_2 and CO is favoured with an increase in temperature. However, to avoid agglomeration the temperature cannot be increased too high (Göransson et al. 2011). Depending on the gasification technology different moisture contents can be found in the rawgas as well as impurities such as H_2S, NH_3 and TAR (higher boiling substances) (Tijmensen et al. 2002; Milne et al. 1998; Göransson et al. 2011). Tijmensen et al. (2002) suggest maximum impurity values as shown in Table 2-3. The study compares the impurity weight percentage of a rawgas produced from poplar wood with the maximum amount suitable for the FT-synthesis.

The amount of TAR could be reduced with a higher residence time of the gas within the gasification reactor. However, this would require an increased bed height under the premise to not to alter the gas velocity (Göransson et al. 2011).

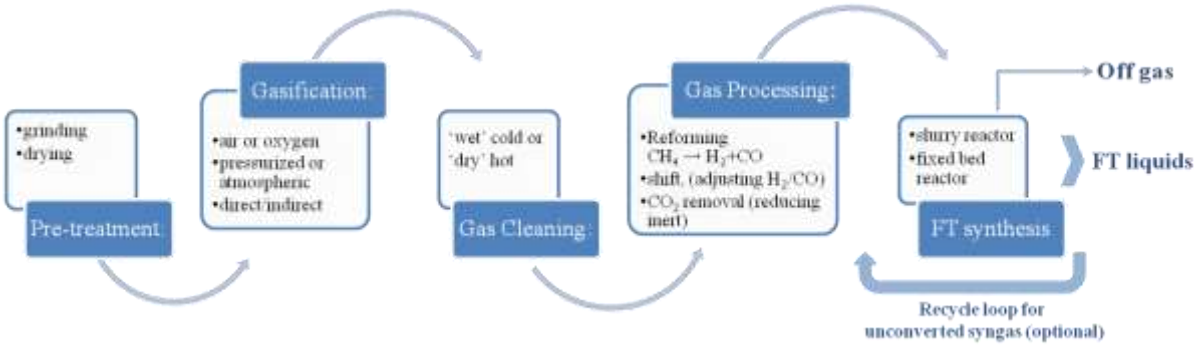

Figure 2-1: Schematic view of the key components for converting biomass to FT-crude which can be further upgraded to motor fuels (cf. Tijmensen et al. 2002)

Borg et al. (2011) figured out in one of his studies that sulfur generally has a negative effect on the activity of catalysts within the Fischer-Tropsch reactor. As listed in Table 2-2 the sulfur content in biomass, however, is considerably lower than the content in coal. Therefore, the cost of a subsequent sulfur cleaning process should be weighed against the costs for replacing the catalyst in shorter intervals (Borg et al. 2011). In case a high sulfur biomass or coal is used as a feedstock the gasification is followed by selective separation of sulfur components, possibly coupled with a Claus sulfur recovery system.

Table 2-3: Exemplary impurity values of components presenting the raw gas after gasification and the maximum tolerated amount for FT-synthesis (Tijmensen et al. 2002)

Impurity	Poplar wood [wt%]	Assumed cleaning requirement [ppb]	Cleaning efficiency	Required cleaning steps
Ash (particulates)	1.33	0	> 99.9 %	Cyclone seperator, bag filters/scrubber
N (HCN + NH_3)	0.47	20	> 99.9 %	Scrubber (possible with H2SO4), Sulfinol D also removes HCN and NH_3
S (H_2S + COS)	0.01	10	> 99.9 %	Srubber, possibly COS hydrolisation unit or Sulfinol D necessary, ZnO guard bed
Alkalis	0.1	10	> 99.9 %	During cooling down alkalis condense on particulates, possibly also on vessels (and thereby polluting them)
Cl (HCl)	0.1	10	> 99.9 %	Absorbed by dolomite in tar cracker (if used), reaction with particulates in bag filter, scrubber (possibly with NaOH)
Tars	-[a]	0	> 99.9 %	Condense on particulates and vessels (and thereby polluting them) when syngas is cooled below 500°C

[a] - Not known, but order of magnitude is g/Nm^3.

The last step before the actual FT-synthesis is of utmost importance as optimal syngas conditions for the conversion process should be achieved. In case the gasification produces a rawgas with a high CH_4 content this CH_4 should at least be partially reformed to H_2 and CO according to the following chemical reaction:

$$CH_4 + ½\ O_2 \rightarrow 2\ H_2 + CO \qquad [2\text{-}1]$$

Consecutively, the H_2/CO ratio within the syngas is adjusted in a shift-reactor. The main reaction for this process is called Water-Gas-Shift reaction (WGS):

$$CO + H_2O \rightarrow H_2 + CO_2 \qquad [2\text{-}2]$$

Estimates of suitable syngas compositions are listed in Table 2-4 in which the required H_2/CO ratios for different FT-synthesis processes are shown according to Dry (2010).

Table 2-4: H_2/CO ratio depending on the temperature and catalyst

	LTFT		HTFT
Catalyst	iron-based	cobalt-based	iron-based
H_2/CO ratio	1.65	2.15	1

LTFT: 220 - 250 °C, HTFT: 320 - 350 °C

The cleaned syngas is finally converted into hydrocarbons of different chain length within the FT-synthesis reactor, which is most commonly either a fixed bed or a slurry reactor (Tijmensen et al. 2002). The different reactor types are discussed in Section 3.3. The composition of the so-called FT-liquid varies from methane, which is most of the times not desired but unavoidable, to long-chain hydrocarbons. The hydrocarbons are mainly in form of paraffins, while olefins are present in smaller amounts (Calemma et al. 2010; Dry 2010; van der Laan and Beenackers 1998). Oxygenated compounds may also appear such as aldehydes and alcohols, though in smaller quantities compared to hydrocarbons (Dry 2004). The actual composition of the FT-liquid depends on the process parameters temperature and pressure, as well as on the reactor type and catalyst used.

A part of the syngas might not be fully converted, concluding in an off gas stream. This one can either be recirculated (high conversion mode) or be totally or partially used for combined heat and power applications as for example in a gas turbine thus leading to smaller conversion of the syngas into FT-liquids (Tijmensen et al. 2002). Alternatively the off gas can undergo other reforming and synthesis processes.

The FT-liquid obtained from the reactor is usually referred to as FT-crude as it can be further upgraded into more specific products for market applications (mainly because it should resemble liquid fuels of similar characteristics of those commonly produced from crude oil).

The long-chained hydrocarbons can be hydrocracked into diesel which is of excellent quality since the impurities (e.g. sulfur) have been removed upstream. In particular, the FT-diesel is free of nitrogen which could otherwise contribute to NO_x formation during combustion in car engines which implies that much cleaner exhaust gases are obtained from automobiles than when burning conventional diesel.

If the process yields hydrocarbon compositions more similar to gasoline, very little aromatic compounds are found (e.g. benzene share less than 1 % is reported). For fossil gasoline the amount of this carcinogenic compound is much higher (Dry 2010).

3 Fischer-Tropsch Synthesis

In general, it can be said that the FT-synthesis is a catalyst supported polymerisation which converts CO and H_2 into a wide range of liquid hydrocarbons (Yuan et al. 2011; Reichling and Kulacki 2011; Lu and Lee 2007). These hydrocarbons can be further upgraded and converted in motor fuels and other chemicals. According to Lu and Lee (2007), however, there are four main reasons behind the fact that FT-synthesis has not been widely utilized yet:

A wide range of hydrocarbons is produced due to a limitation in selectivity.

- The catalyst is deactivated easily.
- The capital costs are high.
- The carbon and thermal efficiency are lower than other syngas applications

The following sections discuss briefly the theoretical background concerning the FT-synthesis reactions, the types of catalysts and reactors, and possible FT-crude upgrading steps.

3.1 Thermodynamic background

The FT-synthesis process is highly exothermic. According to Sie and Krishna (1999) the FT-synthesis follows this general form:

$$CO + 2\ H_2 \rightarrow \text{“-}CH_2\text{-“} + H_20 \qquad [3\text{-}1]$$

The term “-CH_2-“ stands for the product which mainly consists of paraffins (saturated hydrocarbons) and olefins (unsaturated hydrocarbons). The more specific building reactions are defined as the following:

$$n\ CO + (2n+1)\ H_2 \rightarrow C_nH_{2n+2} + n\ H_2O \qquad [3\text{-}2]$$

$$n\ CO + 2n\ H_2 \rightarrow C_nH_{2n} + n\ H_2O \qquad [3\text{-}3]$$

The generalized reaction releases around 150 kJ of heat/mol CO converted (Maitlis and de Klerk 2013). Compared to other catalytic reactions in the oil refining industry this is about one order of magnitude higher (Sie and Krishna 1999; Steynberg and Dry 2004).

It can be generally stated that the paraffin content is higher than the olefin content. However, this is not applicable for the short hydrocarbons C_3 and C_4, as shown in experiments by Rane et al. (2012) or Van der Laan and Beenackers (1999). Dry (1981), furthermore, stated that the olefin amount of C_3 and C_4 can reach up to 90 % of the C_3 and C_4 produced. Shi and Davis (2005) compared in a study experiments of an α-Olefin/n-Paraffin (O/P) ratio model from the literature which shows a strong exponential decrease of olefin content with higher carbon number. This approach follows the general correlation:

$$O/P = e^{-cn} \qquad [3\text{-}4]$$

in which n stands for the carbon number and c is a constant between 0.19 and 0.49. Within the model a value for c of 0.3 was developed whereas Shi and Davis (2005) determined a c value of only 0.15. The comparison of both values is shown in Figure 3-1 as well as for a medium c value of 0.25 for hydrocarbons with a carbon number from 8 to 16 since the models have only been compared in this range within the study.

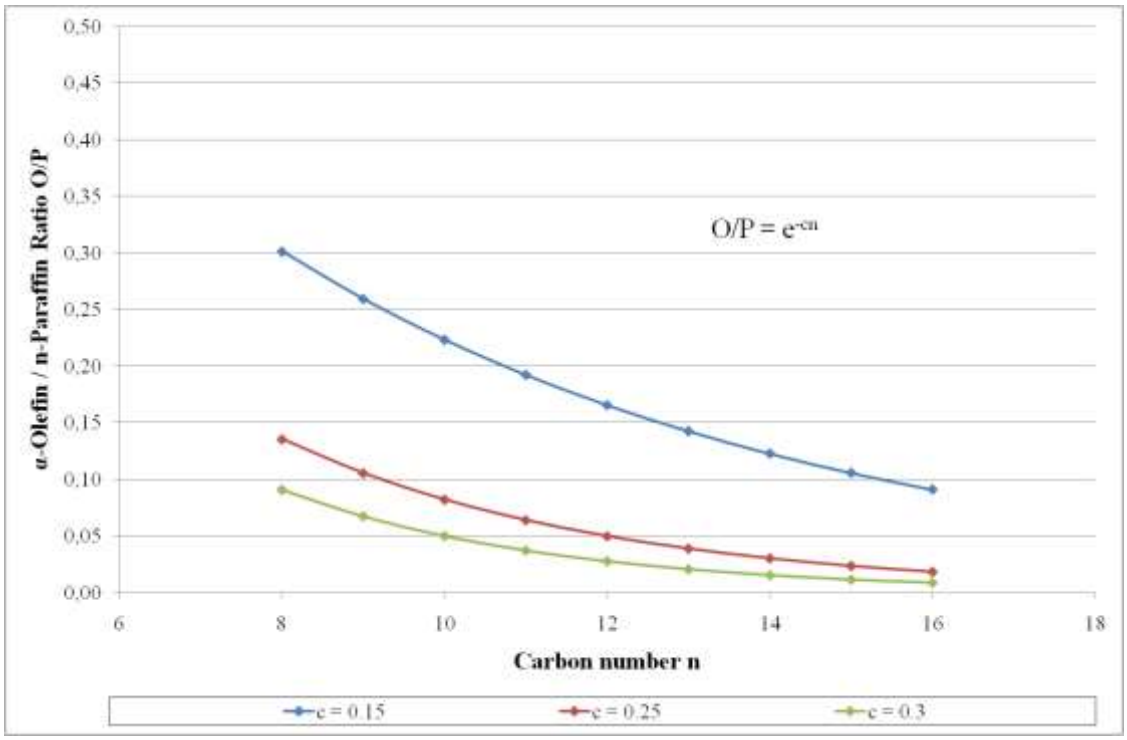

Figure 3-1: Comparison of different c values for the O/P ratio

The distribution of the hydrocarbon chain lengths is indeed the most important criterion to analyse and compare different configurations of the FT-process.

The spread between the different hydrocarbon chain lengths is usually described by means of the Anderson-Schulz-Flory (ASF distribution.

This is based on a Weibull distribution model which is further characterized by a chain growth probability factor α (Tijmensen et al. 2002; Sie and Krishna 1999; Yuan et al. 2011).

The ASF distribution can be shown in its molar (M_n) or mass (W_n) distribution variants (Hamelinck et al. 2004; Ng and Sadhukhan 2011):

$$M_n = \alpha^{n-1} (1-\alpha) \quad [3\text{-}5]$$

$$W_n = \alpha^{n-1} (1-\alpha)^2 n \quad [3\text{-}6]$$

Examples of ASF distributions are shown in Figure 3-2 in which the α-value is varied from 0 to about 1. In particular the hydrocarbons are further clustered in subsets of similar chain-length to represent the naphtha, diesel and waxes shares in the total FT-crude product.

It is apparent that with a higher α-value the selectivity of hydrocarbons of a carbon number greater than 5 increases linearly. Therewith, waxes which are the desirable intermediate product are more extensively formed with an α-value higher than 0.85. Those waxes can afterwards be hydrocracked and upgraded into motor fuels (cf. Section 3.4).

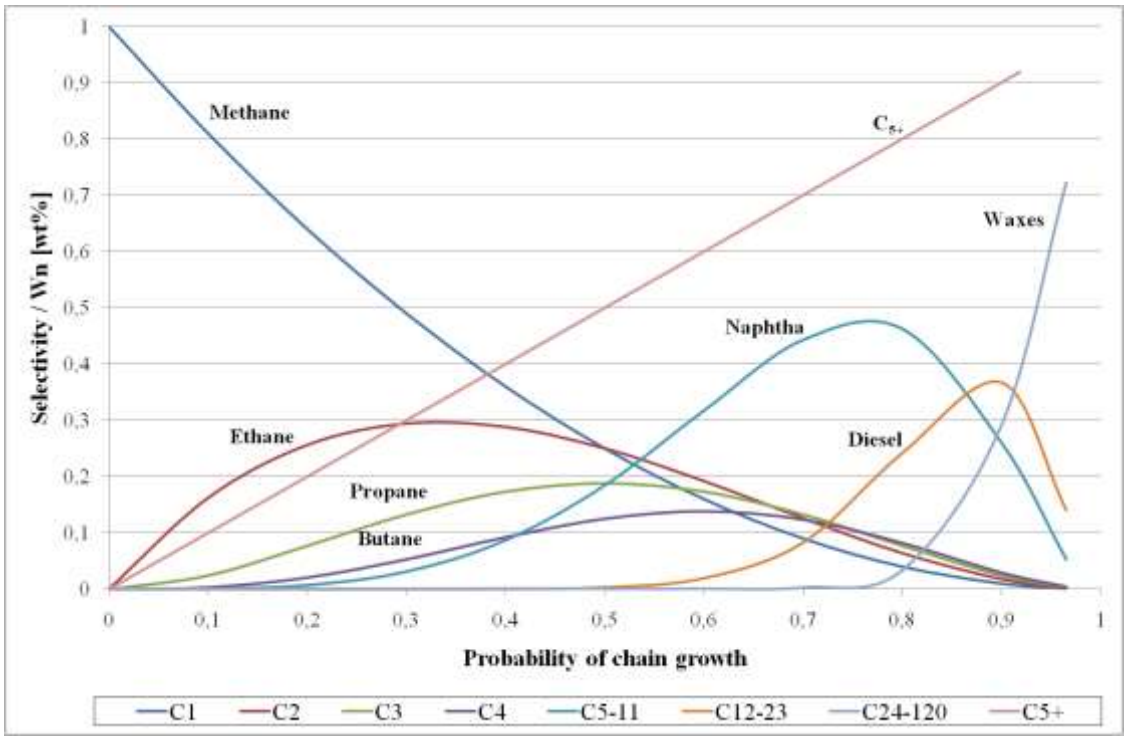

Figure 3-2: Anderson-Schulz-Flory distribution

The α-value does itself not represent an operating parameter but is a useful theoretical tool that allows to simplify the analysis of a rather complex product. The probability of chain growth generally describes the likeliness of a hydrocarbon chain to further grow with CH_2. It can furthermore be expressed as a ratio of the propagation Rp of the chain growth and termination rate Rt according to the following equation (James et al. 2012):

$$\alpha = \frac{R_p}{(R_p + R_t)} \qquad [3\text{-}7]$$

Since these rates are rather abstract and cannot be measured easily scientists have worked on developing empirical correlations for α by combining the dependency on the operation temperature and/or pressure as well as the H_2/CO ratio.

However, experimental research has mainly focused on correlations for cobalt catalysts. One of these correlations was first developed by Yermakova and Anikeev (2000) which is based on different tested equations and several experiments at 533 K and 20 atm over an alumina-supported cobalt catalyst promoted with zirconium:

$$\alpha = A\,\frac{\tilde{a}_{CO}}{\tilde{a}_{CO} + \tilde{a}_{H_2}} + B \qquad [3\text{-}8]$$

where the constants A and B have a value of 0.2332 ± 0.0740 and 0.6330 ± 0.0420, respectively.

However, this correlation is only dependent on the H_2 and CO composition in the syngas. Song et al. (2004) therefore further developed the correlation to be dependent on the operation temperature:

$$\alpha = \left(A\,\frac{\gamma_{CO}}{\gamma_{CO} + \gamma_{H_2}} + B\right)[1 - 0.0039(T - 533)] \qquad [3\text{-}9]$$

where T equals the operation temperature in Kelvin. It is noticeable that Equation [3-9] equals [3-8] if the operation temperature is 260 °C.

Another possible correlation was developed by Hamelinck et al. (2004). It includes a selectivity calculation of the hydrocarbons with a chain length longer than 5 (SC5+) prior to the calculation of α:

$$S_{C5+} = 1.7 - 0.0024\,T - 0.088\,\frac{[H_2]}{[CO]} + 0.18\,([H_2] + [CO] + 0.0078\,p_{tot} \qquad [3\text{-}10]$$

$$\alpha \approx 0.75 - 0.373\,\sqrt{-\log(S_{C5+})} + 0.25\,S_{C5+} \qquad [3\text{-}11]$$

Where T is the operation temperature in Kelvin, p_{tot} is the operating pressure in bar and $[H_2]$ and [CO] are the molar concentrations of H_2 and CO in the feed gas. One of the distinguishing characteristics of this model is the pressure dependence.

3.2 Catalyst basis

In general there are four metals with a sufficient FT-activity as shown in Figure 3-3: Iron (Fe), Cobalt (Co), Nickel (Ni) and Ruthenium (Ru). The most active of the four metals is Ru, however due to its scarcity and high price it is not used in commercial applications. Ni is also normally ruled out as a catalyst base since it has a very high activity towards methanation. This concludes that the selectivity for methane is high whereas the yield for the desired long chain hydrocarbons is low. Iron and cobalt are therefore the only metals used for the catalysts' basis in FT-process of commercial interest (Dry 2010).

Fe	Co	Ni	Ru
M[1]: 55.847	M[1]: 58.9332	M[1]: 58.69	M[1]: 101.07
Rp[2]: 1	Rp[2]: 235	Rp[2]: 140	Rp[2]: 76 000
A[3]: 1	A[3]: 250	A[3]: 150	A[3]: 138 000

[1] molar mass [g/mol]
[2] Retail Price in 2007 in comparison to iron
[3] Activity per surface atom over the lifetime in relation to the activity of iron per surface atom over the lifetime

Figure 3-3: Possible metals for FT-catalysts (cf. van Steen and Claeys 2008)

One of the main advantages for iron-based catalysts is the low price of iron compared to cobalt. As shown in Figure 3-3 Co is more than 200 times more expensive than iron and according to Dry (2010) this can rise up to about 1000 times depending on the source of iron. Due to the low price it is therefore advantageous to use an iron catalyst when the syngas includes a high level of catalyst poisons, e.g. H_2S. Another characteristic of an iron catalyst is the high activity towards an in-situ Water-Gas-Shift (WGS) reaction within the FT-reactor (Lu and Lee 2007). The WGS is mainly balancing the H_2/CO ratio needed for a complete CO conversion. Therefore, a H_2/CO ratio smaller than 2 is sufficient when applying an iron-catalyst leading to the possibility of saving an upstream WGS reactor. For cobalt, however, an upstream WGS shift reactor is inevitable since cobalt has little to no WGS activity (Dry 2010). Due to this the H_2/CO ratio when entering the FT-reactor has to be between 2 and 2.2 to ensure that the H_2 is not the limiting factor for the hydrocarbon production.

It is also shown by Figure 3-3 that cobalt has a 250 times higher hydrocarbon selectivity therefore it is utilized to produce paraffins. Whereas iron based catalysts are less active for a secondary hydrogenation and therefore produce more olefins (Dry 2004). One reason for cobalt having a higher level of conversion is the very low negative impact of water compared to iron-based catalysts (Dry 2004; Luque et al. 2012). According to Luque et al. (2012) a

once-through conversion of 60 – 70 % can be achieved with a Co-based catalyst. To reach such a conversion with a Fe-based catalyst requires the syngas flow to be lower and a high recirculation rate after separating the produced water (Dry 2004). Accordingly, more than one reactor or a larger reactor would be needed to handle the same syngas amount as can be converted with a cobalt-based catalyst (van Steen and Claeys 2008).

The impact of water can also be seen in the kinetic models that have been formulated over the years. Table 3-1 shows different models for iron- and cobalt-based catalysts. In both models for an iron-based catalyst the partial pressure of water P_{H2O} is in the denominator to take into account the negative influence of the partial pressure of water on the CO conversion R_{CO}. The main effect of a high partial pressure of water is the increased oxidation of the catalyst surface which consequently leads to a lower coverage of hydrogen molecules, since hydrogen has a weaker adsorption compared to water (Dry 2010). For cobalt-based models on the other hand the partial pressure of water is not included. According to Yates and Satterfield (1991) the partial pressure of H_2O does not negatively influence the CO conversion. However, it is still important to extract the water in case some unconverted stream is recycled even when utilising a cobalt-based catalyst. Not extracting the water would lead to a water build up and therefore decrease the partial pressure of CO and H_2 significantly since water is a product of every hydrocarbon reaction as can be seen in Equation [3-2] and [3-3]. Consequently, the reaction rate will decrease and accordingly only a small amount of CO would be converted.

Table 3-1: Kinetic expressions for the FT-process (cf. Zimmerman and Bukur 1990; Keyser et al. 2000)

	Catalyst	**Rate law**
Atwood and Bennett (1979) Leib and Kuo (1984) Nettelhoff et al. (1985) Ledakowitcz et al. (1985)	CCI fused iron Fe/Cu/K Precipitated Fe Precipitaed 100 Fe/1.3 K	$-R_{CO} = \frac{k_{FT} P_{CO} P_{H_2}}{P_{CO} + a P_{H_2 O}}$
Huff and Satterfield (1984)	C-73 fused iron	$-R_{CO} = \frac{k_{FT} P_{CO} P_{H_2}^2}{P_{CO} P_{H_2} + b P_{H_2 O}}$
Anderson (1956)	Co/ThO2/kieselguhr	$-R_{CO} = \frac{k_{FT} P_{CO} P_{H_2}^2}{1 + b P_{CO} P_{H_2}^2}$
Yates and Satterfield (1991)	Co/Mo/SiO2	$-R_{CO} = \frac{k_{FT} P_{CO} P_{H_2}}{(1 + b P_{CO})^2}$

The catalyst activity, however, is not only influenced by the partial pressures of the different syngas compounds but also by deactivation mechanisms. The deactivation can be distinguished in inherent and operational mechanisms (van Steen and Claeys 2008).

An inherent deactivation mechanism is the build-up of carbon deposition on the catalyst which is thermodynamically favoured by the operation conditions of the FT-synthesis. Those overlayers might lead to chemical attrition of catalyst particles. Furthermore, it could also happen that surface carbon diffuses into the catalyst grid which would lead to the formation of carbide phases (van Steen and Claeys 2008). However, if a cobalt-based catalyst is supported by ruthenium the carburization is reduced. A possible reason for this phenomenon is the

enhanced hydrogenation rate of the surface carbon due to the extensively higher FT-activity of ruthenium (cf. Figure 3-3).

Operational deactivations on the other hand include deactivation by catalyst poisons such as nitrogen, sulphur or halogenated compounds. Nitrogen compounds, e.g. ammonia or HCN, have a negative effect especially on cobalt-based catalysts. They mainly cause a kinetic inhibition of the CO conversion due to the similar adsorption strength compared to CO. However, there are no records about a permanent deactivation of the FT-catalysts due to nitrogen compounds (van Steen and Claeys 2008). Sulphur on the other hand is a catalyst poison which permanently deactivates a catalyst and which is most likely the main cause for operational deactivation (Dry 2010; van Steen and Claeys 2008).

The third group of catalyst poisons which are likely to be present within biomass derived synthesis gas are halogenated compounds. They are most active with the supporting oxides of the catalyst. Since mostly cobalt is supported with oxides such as SiO_2, TiO_2 or Al_2O_3 cobalt is more prone to be deactivated by halogens (van Steen and Claeys 2008). As a conclusion it can be said, that iron is more resistant against operational deactivation compared to cobalt.

In Table 3-2 the comparison of iron- and cobalt-based catalysts is summarized. It additionally shows that both catalysts can operate stable under optimised conditions but that iron is more favourable for harsh operation conditions especially due to its low price and high resistance against poisons. Cobalt on the other hand needs a generally cleaner syngas and is more active at lower temperatures (Luque et al. 2012).

Table 3-2: Comparison of iron- and cobalt-based catalysts

Factor	Iron-based	cobalt-based
FT-selectivity	+	++
	good selectivity, metal to which others are compared	~250 times higher selectivity than iron
Once through conversion	±	+
	too reach high conversion rates more than one reactor has to be installed in a row	60 - 70 % CO conversion in once through operation mode is possible
low hydrogen content	+	-
	high WGS activity, however additional WGS reactor might still be necessary	low or no WGS activity (H_2/CO ~ 2 is needed) WGS reactor is mandatory
resistance against contaminants	+	-
	cheaper and higher resistance against S and ashes	more expensive than Fe catalyst; advantagous only when gas is thouroughly cleaned and conditioned
resistance against water vapour	±	
	water vapour generally inhibits FT reaction, vapour similarly influences Fe and Co-based catalysts dependent on type of catalyst (supported, unsupported), type of metal (Co, Fe, Ru, etc.), metal particle size and support	
partial pressure of H_2O	-	no impact
	negative impact of partial pressure of water on the CO conversion; water has to be extracted before entering the FT reactor	water should be extracted when in recirculation mode to avoid lowering the partial pressures of the other components
Operation stability	+	
	operates for 6+ months under optimised conditions	
Operational mode	±	±
	harsher and more severe conditions are favorable for Fe-based, since cheaper and more resistant	low-severity conditions favorable for Co-based, since higher activity and selectivity at lower temperatures harsh conditions: Co prone to produce methane

3.3 Reactor Types

The FT-synthesis can either be carried out in a fixed bed, slurry phase or fluidized bed reactor as described by many authors (e.g. Lu and Lee 2007; Sie and Krishna 1999). The different technologies lead to a variety of reactor designs:

- ARGE reactor (Fixed bed multitubular reactor)
- Shell Middle Distillate Synthesis (SMDS) (Fixed bed multitubular reactor)
- Synthol reactor (High temperature circulating fluidized bed reactor)
- SASOL Advanced Synthol (Fixed fluidized bed reactor)
- Sasol Slurry Bed Reactor (SSBR) (Low temperature slurry reactor)

Many authors, furthermore, divide the FT-reactor operation conditions in low temperature (LTFT) and high temperature (HTFT) FT-synthesis (e.g. Steynberg and Dry 2004; Dry 2010; Krylova and Kozyukov 2007). The LTFT operates in a temperature range of 200 – 250 °C and mainly produces hydrocarbons in the diesel and waxes range. Depending on the final product that is desired either an iron- or cobalt-based catalyst is utilized. For HTFT, however, only iron-based catalysts are applied. The temperature span for HTFT processes ranges from 300 – 350 °C which leads to mainly olefins and gasoline as products. Table 3-3 gives an overview of the different LTFT and HTFT characteristics as well as the reactor types which are used in each case.

Table 3-3: Operation characteristics for LTFT and HTFT processes

	LTFT	**HTFT**
Reactor Types	- Multitubular, fixed bed - 3-phase slurry bed	- 2-phase
Temperature	220 – 250 °C	320 – 350 °C
Catalysts	Iron or Cobalt	Iron
Products	Diesel and Waxes	Olefins and Gasoline

According to van Vliet et al. (2009) especially the SMDS and SSBR technology had a high market share in 2007. Therefore, the multitubular and slurry bed reactor will be explained in more detail. However, since both designs operate at LTFT conditions the operation of a high temperature fluidized bed reactor design is described as well to complete the possible reactor types.

3.3.1 Multitubular reactor

The first multitubular fixed bed reactor was developed in Germany after the Second World War ("Mitteldruck Synthese"). It operated at a medium pressure and was run in a once-through mode (Sie and Krishna 1999). In a next step the ARGE reactor was developed; Sasol adopted it in the mid-1950s in the Sasolburg plant, South Africa. It operates with a high recirculation of unconverted syngas and not in a once-through mode anymore. The reactors are designed to produce 400 bbl/day (Sie and Krishna 1999). Sasol has lately decided to replace them with SDMS, the most recent reactor design which has a production capacity of ten times higher than the ARGE reactor (Dry 2010). A plant utilizing this reactor has recently been constructed in Bintulu, Malaysia, which is running on natural gas (Shell MDS Technology and Process).

Figure 3-4 shows the conceptual design of a multitubular reactor on the left side. The reactor consists of many double concentric tubes in which the catalyst is packed and which are surrounded by cooling water. To achieve a high heat transfer narrow tubes and a turbulent gas flow within the tubes are required (Dry 2010). As shown in Figure 3-4 the syngas enters the reactor from the top at which also the feed water inlet and steam outlet is situated. At the bottom a separated hydrocarbon waxes and shorter hydrocarbons stream which is still in gaseous state exits the reactor. The fact that the catalyst is in solid packed form within the tubes simplifies the operation since waxes and catalyst do not have to be separated as they have to in a slurry reactor. The produced waxes are in liquid state under FT-conditions. Therefore they can easily

run down the tube walls and be collected at the bottom of the reactor (Dry 2010). However, multitubular reactors in commercial use consist of thousand of tubes which lead to high construction costs. Additionally, the scale up size is limited due to the high amount of tubes and therefore high weight of the reactor which complicates the transport (Dry 2010).

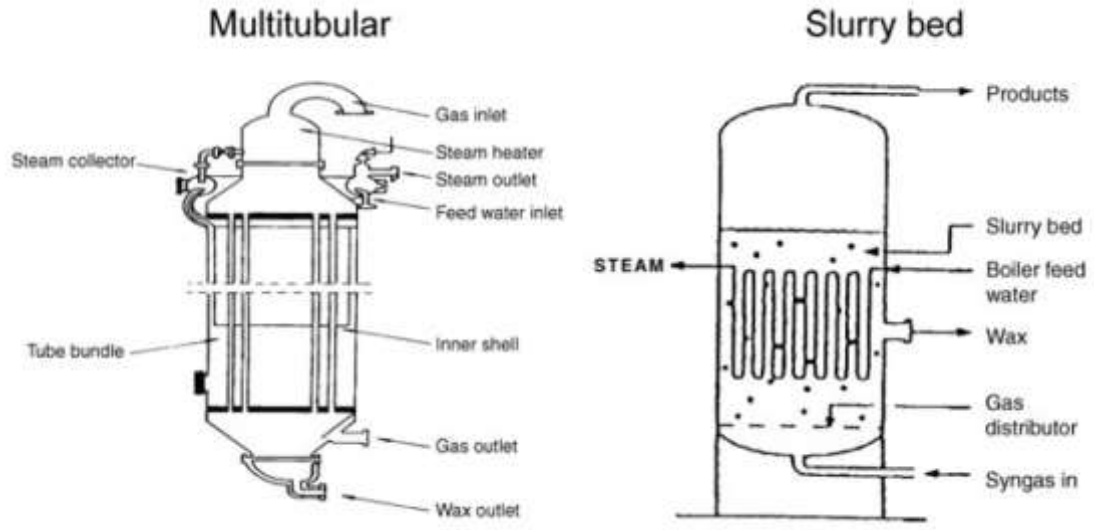

Figure 3-4: Design of multitubular and slurry bed reactors (Dry 2010)

3.3.2 Slurry reactor

The first slurry reactor was similar to the multitubular reactor first developed after the Second World War in Germany by the company BASF ("BASF Schaumverfahren") (Sie and Krishna 1999). In the beginning of the 1990s Sasol developed an internally cooled slurry phase reactor with a capacity of 2 500 bbl/day as an alternative to the ARGE fixed bed reactor. The Sasol Slurry Phase Distillate (SSPD) reactor can nowadays achieve a capacity up to approximately 10 000 bbl/day (Sie and Krishna 1999).

The design of a 3-phase slurry reactor is shown on the right side in Figure 3-4: . The syngas is entering from the reactor bottom and after passing a gas distributor it enters the slurry bed in which the solid catalyst is suspended and dispersed in a liquid with a high thermal capacity. The syngas bubbles through the slurry phase in which a heat exchanger is installed. The product gas exits through the reactor top whereas the catalyst/wax mixture is exiting the reactor on the side. The separation of this mixture is one of the main disadvantages associated with slurry phase reactors since it is complex and expensive. Additionally, it is crucial to thoroughly clean the syngas prior of the reactor since the catalyst particles are fluidized. Namely all particles will be in contact with the syngas and would be damaged or even deactivated (Dry 2010). However, one big advantage is the lower installation and operation costs. The lower operation costs result from lower catalyst consumption and a lower pressure drop within the reactor of less than 1 bar (Tijmensen et al. 2002).

3.3.3 Circulating fluidized bed reactor

The circulating fluidized bed (CFB) technology was mainly utilized in Sasolburg, South Africa, at the Secunda Complex which comprised 16 CFBs each having a capacity of 7 500 bbl/day (Chang 2000). The process was a CTL type and mainly produced motor gasoline and diesel. However, a small part of chemicals was also produced (Luque et al. 2012). In the 1980s those 16 reactors were replaced by eight new Sasol Advanced Synthol (SAS) reactors which used a different fluidized bed technology to produce only gasoline and light olefins (Chang 2000).

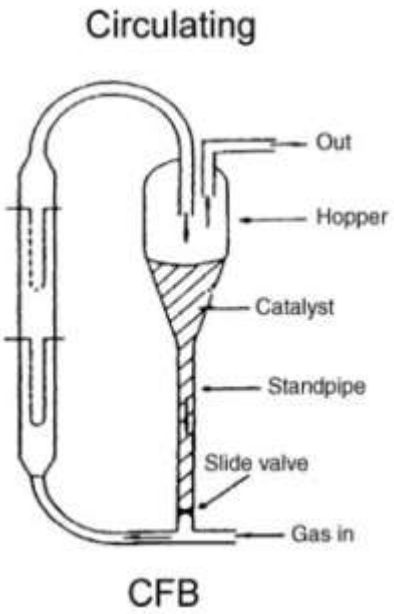

Figure 3-5: Design of a circulating fluidized bed reactor (Dry 2010)

Figure 3-5 shows the design of a two-phase CFB as used in Sasolburg. The syngas enters the reactor from the bottom and gets in contact with the solid circulating catalyst. The exact amount of the catalyst is controlled by a slide valve. The syngas/catalyst mixture streams into the riser in which the reaction takes part. Since it is important to maintain near isothermal conditions heat exchangers are installed within the riser. Those remove up to 40 % of the heat produced (Dry 2010). To ensure that the catalyst leakage is as small as possible the mixture enters a cyclone ("Hopper") in which 99 % of the catalyst is separated from the reacted gas stream. The gas stream afterwards exits the reactor at the top of the cyclone whereas the aerated catalyst falls down within the standpipe and is recycled back into the inlet syngas stream (Dry 2010). To ensure a stable operation it is from utmost importance to guarantee that no syngas flows upwards through the standpipe, therefore it is essential that the differential pressure within the standpipe is always higher than the one in the riser (Dry 2010). However, due to the high temperature within the reactor a carbon deposition at the catalyst can be the result. This leads to a lower density of the catalyst and therefore decreases the differential pressure (Dry 2010). As a result the catalyst lifetime within a CFB is relatively low with 40 – 45 days (Krylova and Kozyukov 2007). Further disadvantages are the bulky and complex design which makes a CFB reactor difficult to control and which also leads to difficulties in scaling (Krylova and Kozyukov 2007).

3.4 Upgrading of FT-crude

According to de Klerk (2007) the refining of FT-crude and crude oil is of comparable complexity. However, FT-crude has more favourable characteristics than crude oil due to the absence of sulphur and nitrogen compounds (cf. Table 3-4). Thus, the overall FT-crude refinery process can be considered to be more environmental friendly (de Klerk 2007).[3]

[3] The sulphur and nitrogen species have to be extracted before the syngas enters the FT-synthesis therefore the emissions are associated with the FT-crude production process.

Table 3-4: Comparison of the components for FT-crude and crude oil (de Klerk 2007)

Property	HTFT[a]	LTFT[b]	Crude oil
Paraffins	> 10 %	major product	major product
Naphthenes	< 1 %	< 1 %	major product
Olefins	major product	> 10 %	none
Aromatics	5 – 10 %	< 1 %	major product
Oxygenates	5 – 15 %	5 – 15 %	< 1 % O (heavy)
Sulphur species	none	none	0.1 – 5 % S
Nitrogen species	none	none	< 1 % N
Water	major by-product	major by-product	0 – 2 %

[a] Sasol Advanced Synthol (Secunda); Synthol CFB (Mossel Bay).
[b] Shell Middle Distillate Synthesis (Bintulu); Sasol Slurry Phase Distillate process (Ras Laffan and Sasolburg); ARGE (Sasolburg)

Table 3-4 also shows that a HTFT-reactor mainly produces olefins and a smaller amount of paraffins. This leads to a higher octane number compared to LTFT crude and conventional crude oil (cf. Table 3-5). The octane number describes the resistance of gasoline against knocking due to the presence of highly branched alkanes. Considering the cetane number, however, the LTFT-crude is evidently favourable especially since the cetane number lies clearly above the EU required one. The high cetane number of LTFT-crude is ascribed to the high amount of linear paraffins and low amount of aromatics (de Klerk 2007) which gives the diesel fuel a better combustion quality during the compression ignition.

Table 3-3: Exemplary cetane and octane number for FT-crude and crude oil (de Klerk 2007; European Parliament 2009)

Property	HTFT	LTFT	Crude oil	EN 590
Cetane number	55	72	56	51 (Minimum)
RON[a]	68	43	25 – 60	95 (Minimum)

[a] Research Octane Number

In addition, de Klerk (2007) scrutinized the complexity of the different upgrading processes for naphtha, distillates and residues in his study and concluded the following:

- Naphtha: It is similar complex for FT-crude and crude oil, however, upgrading of FT-crude to gasoline is more environmental friendly since crude oil upgrading requires aliphatic alkylation and catalytic reforming which need liquid acids and halogenated compounds
- Distillates: The complexity and environmental impact are comparable in their complexity for FT-crude and crude oil
- Residues: The upgrading of crude oil residues is significantly more complex than for FT-crudes since these include olefins which are important for gasoline production. Therefore, at least one carbon rejection technology has to be included which operates at a high temperature (> 440 °C).

All in all, this leads to the conclusion that the FT-crude upgrading is less complex and more environmental friendly. At last, Figure 3-6 gives a schematic overview of a FT-crude upgrading process.

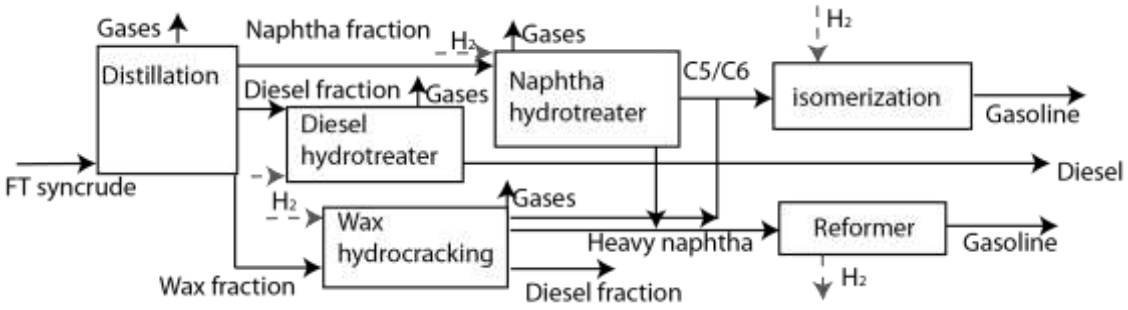

Figure 3-4: Schematic design of the upgrading process of FT-crude (Johansson et al. 2012)

4 Modelling and simulation

4.1 Overview of the modelling assumptions

Before starting to model a process a common equation of state has to be chosen. Within this thesis the "Soave-Redlich-Kwong" is chosen for most of the process. However, to be more precise about the vapour liquid equilibrium within a flash a second section is defined. For this section the "Non-Random to Liquid" equation of state are chosen.

4.1.1 Reactor types

As shown in Section 3.3, the choice for the reactor and catalyst for the FT-synthesis is mainly related to the desired products.

In this study a low temperature slurry reactor was employed in order to obtain mainly diesel and waxes that can subsequently undergo a standard upgrading process in an oil refinery. This choice was also partially dictated by the abundant literature on this reactor type which is crucial when dealing with system modelling if no experimental activity can be performed.

The low operation temperature leads to the linear structure of the alkanes which especially gives the hydrocarbons in the range of C_{10-18} the characteristics of an excellent diesel fuel with a high cetane number (cf. Section 3.4). Furthermore, the zero aromatic content adds the advantage of producing minimal pollution from the end-use application. On the other hand this linearity can be seen as a drawback when considering gasoline as a required product since a high octane number requires branched alkanes and aromatics (Dry 1981).

For these reasons a temperature of 220 °C and a pressure of 20 bar have been adopted as a reference for the base case simulation, these conditions being within the typical ranges of 200-250 °C and 20-60 bar for LTFT (cf. Section 3.3).

Slurry phase reactors have various characteristics that make them suitable for higher yields of long chain hydrocarbons as stated by Schulz (1999), which makes these type of reactors the most suitable for FT-diesel production. In addition efficient heat transfer is promoted which is an advantage due to the exothermic feature of the FT-synthesis process.

For modelling purposes a continuous stirred tank reactor (CSTR) can be adopted for investigating the kinetics of the FT-synthesis. Indeed, as explained later on, the reactor was modelled in Aspen Plus with an RStoich reactor for which the fractional conversion of each reaction is imposed as calculated in an integrated Excel file (cf. Section 4.2.2) according to the estimated chain-length distribution. The estimation of the reactor size and therefore of the gas residence time to achieve the required conversion was instead calculated in parallel.

4.1.2 Catalyst basis

In this work, a cobalt-based reactor was studied mainly due to the large amount of literature data available and due to the higher activity at lower temperatures for high diesel and wax yields compared to iron-based catalysts. As this solution is commonly adopted at a commercial level the studies made in the years led to the predominant development of empirical equations for the determination of the chain growth probability α for cobalt catalysts.

The most famous plants available in this field are nowadays owned by Shell and Sasol which both apply cobalt catalysts for the FT-synthesis. In some studies made on silica supported cobalt catalyst at a reaction temperature of 200 °C showed the high ability of the olefins to readsorb and initiate new chain-growth processes which helps to increase the formation rate

of heavy hydrocarbons (Elbashir 2010). Another good reason for adopting a cobalt-based reactor is the almost inexistent effect of the partial pressure of the product water in the kinetics, which, compared to Fe catalysts, results in a higher conversion of the syngas (Dry 2004).

4.1.3 Alpha correlation

Two different correlations for the chain growth probability α have been introduced in Section 3.1 but a careful analysis of both the models is required in order to be able to determine which one is more suitable.

The model by Song et al. (2004) is described by Equation [3-8] which is listed below again:

$$\alpha = \left(A \frac{\gamma_{CO}}{\gamma_{CO} + \gamma_{H2}} + B\right)[1 - 0.0039(T - 533)] \qquad [4\text{-}1]$$

To calculate α a pressure of 20 atm together with the constant input values below are applied in Equation [4-1]:

- $y_{CO} = 0.23$
- $y_{H2} = 0.46$
- A = 0.2332
- B = 0.633

To highlight the influence of the temperature on the product distribution six different temperature values are used with the aforementioned correlation. The corresponding α-values as well as the temperature levels are shown in Table 4-1.

Table 4-1: Chain growth probability based on Song et al. (2004)

Temperature [°C]	200	210	220	230	240	250
α-value	0.88	0.85	0.82	0.79	0.77	0.74

For calculating the ASF distribution with Equation [3-5] and [3-6] hydrocarbons with a carbon number up till 30 are considered. The resulting weight and molar distribution for the different α-values are displayed in Figure 4-1 and 4-2.

In both graphs it is clearly shown that for high temperatures and consequential low α-values the short chain hydrocarbons are mainly produced. With an increase in chain length the weight and molar distribution decreases and eventually becomes zero. However, with a lower temperature and therefore higher α-value the opposite is the case and a higher amount of long chain hydrocarbons is obtained. This observation corresponds to the information found in the literature and described in Chapter 3 and therefore is suitable for modelling the FT-reactor.

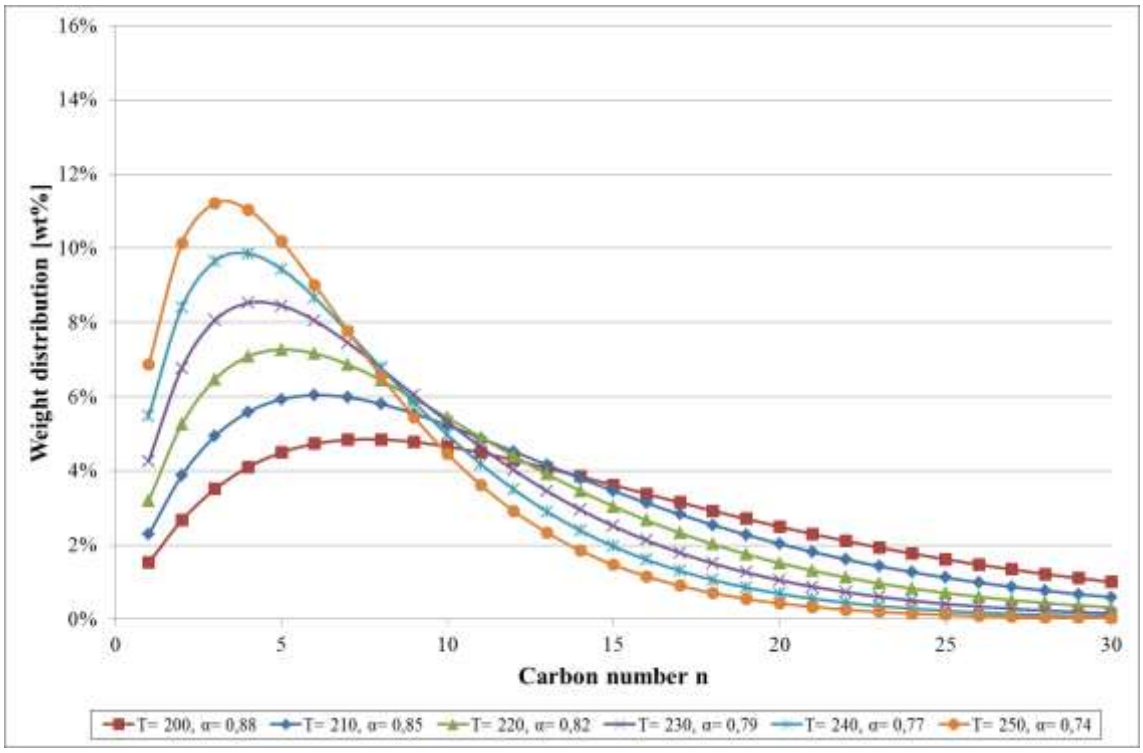

Figure 4-1: Weight distribution W_n based on Song et al. (2004)

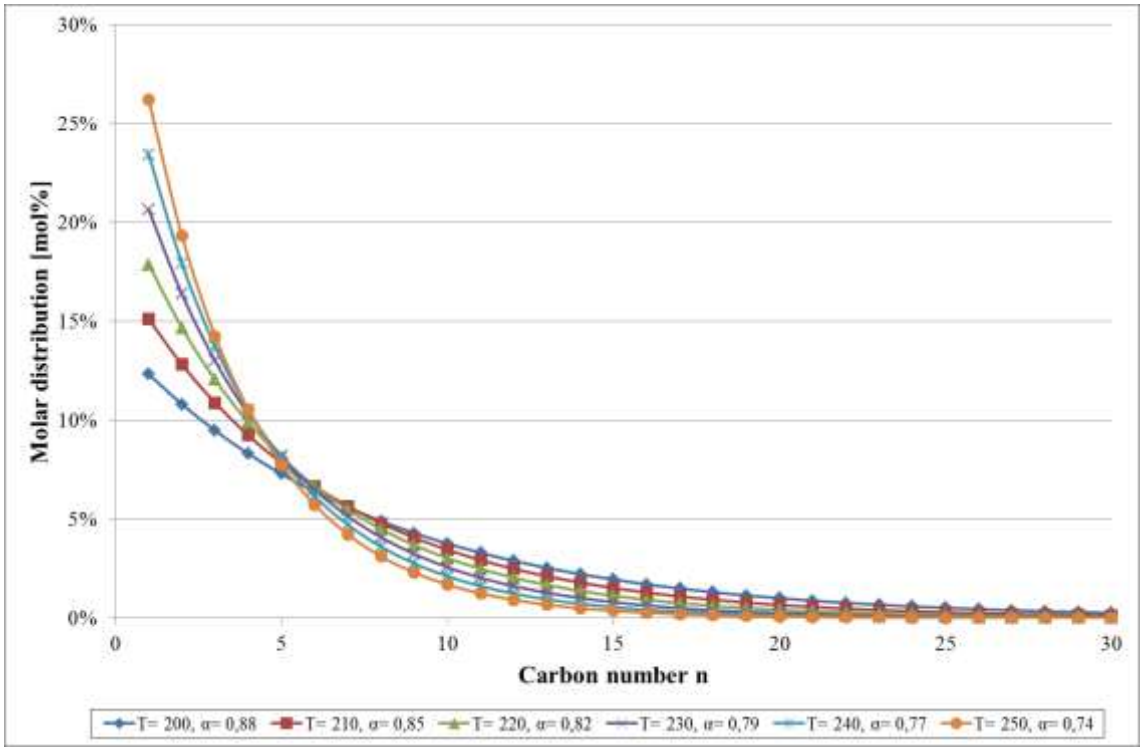

Figure 4-2: Molar distribution M_n based on Song et al. (2004)

The other model investigated is the one developed by Hamelinck et al. (2004) who introduced the dependency on the C_{5+}-selectivity as well as the operation pressure of the α-value.

$$S_{C5+} = 1.7 - 0.0024\,T - 0.088\,\frac{[H_2]}{[CO]} + 0.18\,([H_2] + [CO]) + 0.0078\,p_{tot} \quad [4\text{-}1]$$

$$\alpha \approx 0.75 - 0.373\,\sqrt{-\log(S_{C5+})} + 0.25\,S_{C5+} \quad [4\text{-}2]$$

In order to be able to compare the two models a pressure of 20 atm was applied in this case as well. Furthermore, the following constant values are assumed for the correlation described in Equation [4-2]:

- $H_2/CO = 2$
- $[CO] = 0.23$
- $[H_2] = 0.46$

Table 4-2 shows the C5+ selectivity as well as the α-values for the same temperature levels as for the other model.

Table 4-2: Chain growth probability based on Hamelinck et al. (2004)

Temperature [°C]	200	210	220	230	240	250
Selectivity S_{C5+}	0.67	0.65	0.62	0.60	0.57	0.55
α-value	0.76	0.75	0.74	0.72	0.71	0.70

As for the model of Song et al. (2004) hydrocarbons with a carbon number until 30 are considered and their weight and molar distribution is obtained with the Anderson-Schultz-Flory relations of Equation [3-5] and [3-6]. As can be noticed from Figure 4-3 and 4-4 below this model shows less variation between the curves with varying temperature compared to the distribution by Song et al. (2004). However, the general form also corresponds to the one described in the literature with a high weight percentage of short chain hydrocarbons and a steady decrease towards long chain hydrocarbons

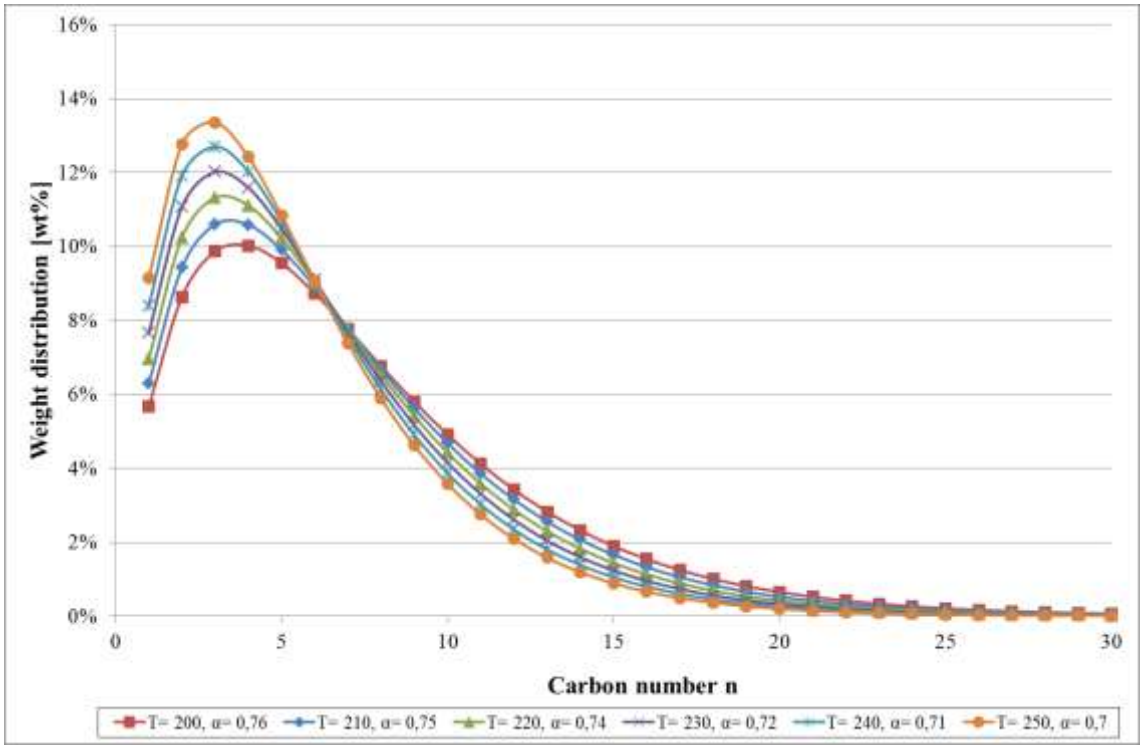

Figure 4-3: Weight distribution W_n based on Hamelinck et al. (2004)

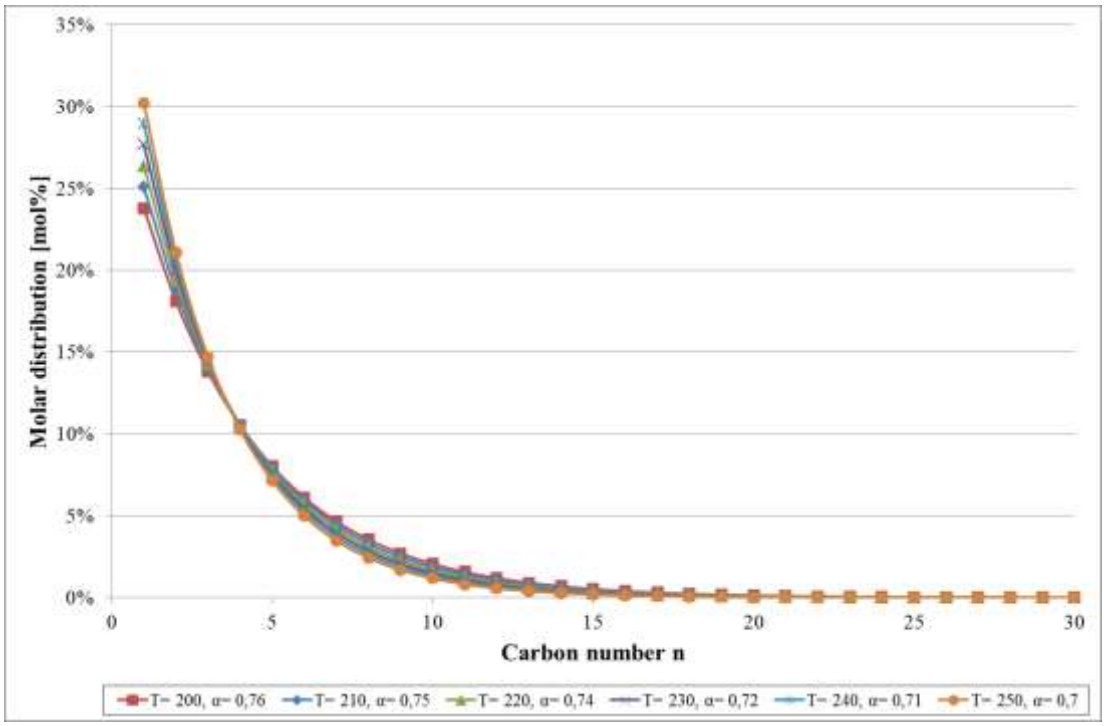

Figure 4-4: Molar distribution M_n based on Hamelinck et al. (2004)

Comparing the two models it can be seen that the model by Song et al. (2004) produces more long chain hydrocarbons than the model of Hamelinck et al. (2004) which is most likely based on different catalyst compositions used during the experiments. Since this thesis aims to obtain a FT-crude consisting of a high amount of long chain hydrocarbons which can be further refined to FT-motor fuels the model by Song et al. (2004) is applied. Furthermore, this model went through various adjustments in the years and the last version was developed in 2004. The values for the constants A and B are assumed to be the averages in the range given, namely 0.2332 and 0.6330 respectively.

4.1.4 Kinetic modelling approach

Kinetics have to be considered in order to be able to determine the weight of the catalyst and the volume of the reactor employed for the synthesis reaction as the reaction rate (R_{CO}) determines either the conversion extent or the reactor size.

The kinetic model developed by Yates and Satterfield (1991) for the carbon monoxide consumption rate R_{CO} is chosen, which is a common reference also in other studies (e.g. Hamelinck et al. 2004). This relation was developed in their study over a range of industrially relevant conditions, which is a good prerequisite for the parametric study that will follow in this report. In particular they showed that the reactor behaves as a continuous stirred tank reactor, as considered in this study which provides data at uniform temperatures and compositions which are also easier to analyze. The cobalt catalyst used is a Co/MgO with SiO_2 support (Yates and Satterfield 1991). Equation [4-4] is the result of their studies on FT-synthesis over cobalt catalyst:

$$-R_{CO} = \frac{a\, p_{CO}\, p_{H_2}}{(1+b\, p_{CO})^2} \qquad [4\text{-}3]$$

where R_{CO} is the carbon monoxide consumption rate [mol/(s kg_{cat})], p_{CO} and p_{H2} are partial pressures of CO and H_2 [bar] and *a* and *b* are kinetic parameters. According to Hamelinck et al. (2004) these parameters are defined as expressed in the equations below.

$$a = k_0 \times \exp\left(\frac{-E_{A,reaction}}{R\,T}\right) \frac{mol}{s\,kg_{cat}\,bar^2} \qquad [4\text{-}4]$$

$$b = k_1 \times \exp\left(\frac{-\Delta H_{ads}}{R\,T}\right) \frac{1}{bar} \qquad [4\text{-}5]$$

R = 8,31 J/(K mol)

In Table 4-3 the kinetic parameters are specified for both solid bed and slurry reactor.

Table 4-3: Kinetic modelling parameters from Hamelinck et al. (2004)

	E_A [kJ/mol]	k_0 [mol/s kg_{cat} bar^2]	ΔH_{ads} [kJ/mol]	k_1 [1/bar]	ρ [$kg_{cat}/m^3_{reactor}$]
Solid bed	68	1,2E+05	192	3,5E-23	1200
Slurry bed	115	1,0E+10	192	3,5E-23	600

Other authors used the model by Yates and Satterfield (1991) as well but developed different expressions for the kinetic parameters a and b. For instance Krishna and Sie (2000) defines these constants with the Equations [4-7] and [4-8] and as regards the properties of the Co/MgO catalyst (21.4 wt.% Co and 3.9 wt.% Mg), they assume ρ_L = 647 kg/m^3.

$$a = 8.8533 \times 10^{-3} \exp\left[4494.41\left(\frac{1}{493.15} - \frac{1}{T}\right)\right] \frac{mol}{s\,kg_{cat}\,bar^2} \qquad [4\text{-}6]$$

$$b = 2.226 \times \exp\left[-8236\left(\frac{1}{493.15} - \frac{1}{T}\right)\right] \frac{1}{bar} \qquad [4\text{-}7]$$

Another example for the application of the kinetic model can be found in the paper by Panahi et al. (2010) in which the constants mentioned above are expressed as follows,

$$a = 8.01368 \times \exp\left(\frac{-37326}{R\,T}\right) \frac{kmol}{s\,kg_{cat}\,MPa^2} \qquad [4\text{-}8]$$

$$b = 1.248 \times 10^{-6} \exp\left(\frac{68402}{R\,T}\right) \frac{1}{MPa} \qquad [4\text{-}9]$$

By comparing these equations at a temperature of 220 °C it is shown that the values for a and b calculated with the approach of Krishna and Sie (2000) is the closest to the original values by Yates and Satterfield (1991). Table 4-4 shows the values for a and b obtained by the different modelling approaches. It can be clearly noticed that the values from Hamelinck et al. (2004) model stand in a remarkable disproportion compared to the other values. The final calculations show that if this model is applied for kinetic evaluations the volume of the reactor is considerably underestimated compared to the other approaches and therefore will not be further considered.

Table 4-4: Comparison of kinetic parameters a and b for different CO conversion rate models

	a **[mmol/min g_{cat} MPa^2]**	**b** **[1/MPa]**
Yates and Satterfield (1991)	53.11	22.26
Hamelinck et al. (2004)	38.99	0.078
Krishna and Sie (2000)	53.12	22.26
Panahi et al. (2010)	53.25	22.14

4.2 Overview of the simulation process

4.2.1 Basic configurations

The FT-synthesis section shown in Figure 4-6 below has been taken as a starting point for the development of the two basic configurations that differ from each other only in relation to the purge stream utilization which is shown in Figure 4-5. The input stream S100 represents the syngas coming from the previous gasification of biomass, its temperature and pressure are fixed to 350 °C and 20 bar respectively (typical conditions prior a high temperature WGS). The assumed mole fractions for the syngas components are shown in Table 4-5. These are typical values for a biomass gasification plant after the gas cleaning steps. It is assumed that the syngas is cleaned from any impurities and went through a desulphurization before entering the final FT-crude synthesis. The mole flow of S100 is assumed to be 1.5 kmol/sec. This value was developed from an iterative scaling process in which the FT-liquid product stream was compared with typical values from built FT-plants (e.g. compare Table 2-1) to back calculate the Syngas inflow

Table 4-5: Mole fraction of the syngas composition

H_2	CO	CO_2	CH_4	H_2O
0.50	0.294	0.093	0.114	0.003

At first S100 is split in SP1 in order to guide part of it through a water gas shift (WGS) reactor, in which the H_2/CO ratio is adjusted to a higher value which should be around 2 to be optimal for the FT-crude synthesis. In particular, in the Aspen models, this value is reached through a "Design Specification" in stream S204 which is achieved by varying the split fraction at SP1. The WGS also requires steam which is assumed to be delivered at 20 bar and 350 °C. The WGS reactor itself is modelled as an adiabatic Gibbs reactor with a pressure drop of 50 mbar. To avoid carbon deposition a H_2O/CO ratio of 3 is considered at the entrance of the reactor by adjusting the flow of the water stream W100. Water is afterwards separated through FLASH1 followed by a Rectisol unit[4] which removes 99 % of CO_2 on a molar basis. The cleaned syngas is sent to the FT-synthesis step for which a RStoich reactor (FTREA) has

[4] a physical adsorption process that uses methanol as a solvent

been chosen to model the hydrocarbons synthesis. Conditions inside the reactor are fixed to a value of 220 °C which is within the LTFT temperature range and a pressure drop of 1 bar (Tijmensen 2002). The calculation block that determines the extent of the synthesis reactions will be further explained in Section 4.2.3. FLASH2 separates the FT-products into three streams: liquid product stream (FTL), water (WOUT2) and a stream consisting mainly of C_{1-4} compounds, CO and H_2 (FTV100). This last stream is further split to purge at least 10% of the gas (FTV110) in order to avoid builds-up of inert compounds inside the reactor. The main purpose of the recycle is to increase the conversion of the unconverted syngas left after the FT-synthesis reaction. The process models of the Aspen Plus flowsheet are described in more detail in Table 4-6.

The use of FTV110 off-gas containing light gases is further distinguished into two solutions leading to two alternative configurations:

- The gas can be burnt in a boiler (cf. Figure 4-5 a).
- The gas can be used to fuel a Gas turbine (cf. Figure 4-5 b).

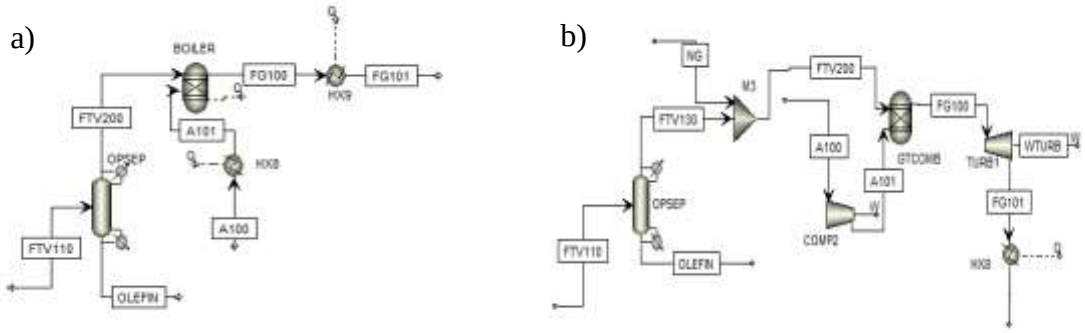

Figure 4-5: Possible purge utilizations: a) Boiler, b) Gas turbine

For both the two options a separator for short chain olefins is applied (OPSEP) with a fixed mole fraction for C_2H_4, C_3H_6 and C_4H_8 in the stream OLEFIN. With today's technologies a purity of up to 99 % can be reached (Da Silva and Rodrigues 2001). Possible technologies include: physical or chemical ab- or adsorption, membrane separation as well as cryogenic or extractive distillation (Eldridge 1993).

In the boiler configuration, air is introduced (stream A100) with a composition of 79 mol-% N_2 and 21 mol-% O_2 and its mole flow is fixed through a calculator block that applies an excess air of 20 %. The combustion is modelled with a Gibbs reactor with an outlet temperature of 1000 °C, the heat available from the reactor representing in this way the radiative share of the combustion heat. The exhaust gases obtained at the Gibbs reactor outlet are afterwards cooled down to 150 °C (stack temperature), this heat representing in this way the convective share of the combustion heat.

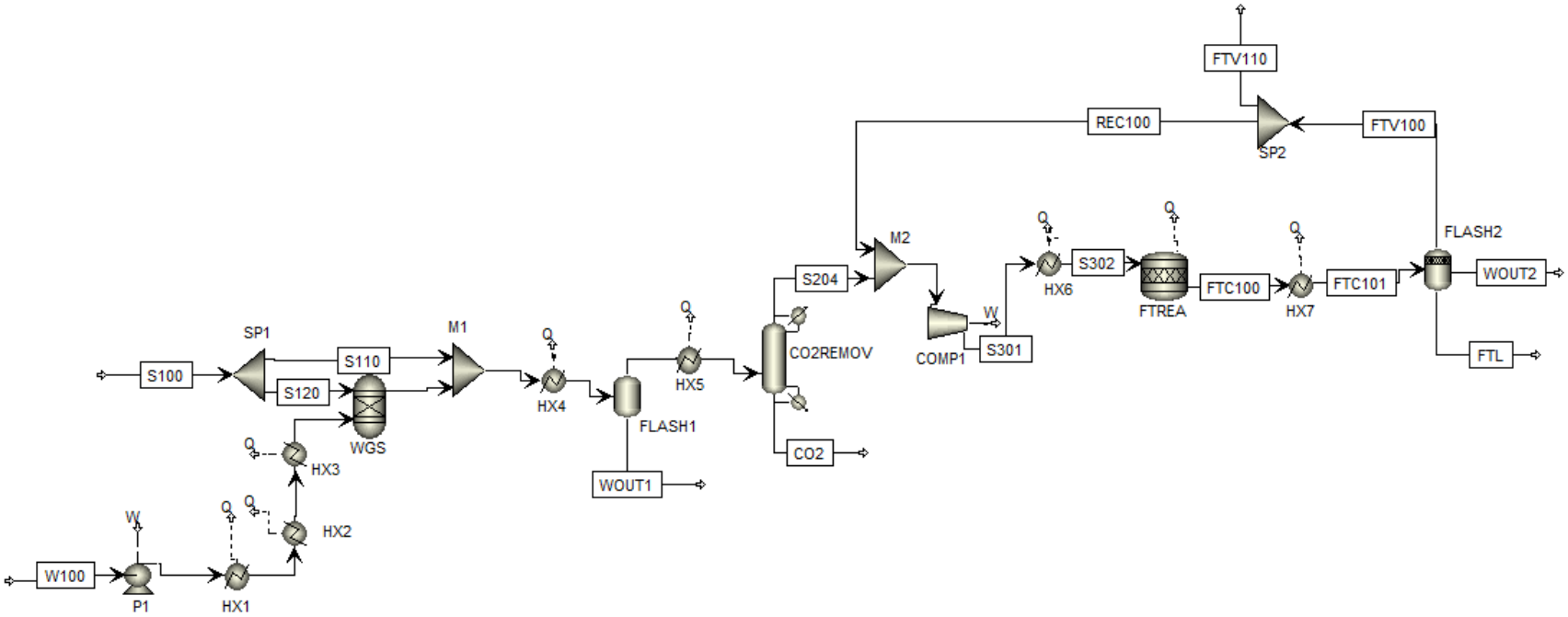

Figure 4-6: Simulation of FT synthesis basic configurations flowsheet in Aspen Plus

Table 4-6: Model description of the basic configurations

Unit	ASPEN plus model	T_{out} [°C]	Pressure [bar]	Other specification
CO2REM	Sep			CO_2 split fraction = 0.99, H_2O split fraction = 1 (stream CO2)
COMP1	Compr		20	Isentropic efficiency = 0.8, Mechanical efficiency = 0.98
FLASH1	Flash2		0	Heat duty = 0 W
FLASH2	Flash3		0	Heat duty = 0 W
FTREA	RStoich	220	-1	
HX1	Heater		0	Vapour fraction = 0
HX2	Heater		0	Vapour fraction = 1
HX3	Heater	350	0	
HX4	Cooler	50	0	
HX5	Cooler	0	0	
HX6	Heater	220	0	
HX7	Cooler	30	0	
M1	Mixer		0	
M2	Mixer		0	
P1	Pump		20	Efficiency = 0.9
SP1	FSplit			Split fraction with Design Spec H_2/CO = 2.15 (stream S204)
SP2	FSplit			Split fraction = 0.9 (stream REC100)
WGS	RGibbs		-0.05	Heat duty = 0 W (Adiabatic reactor), Design Spec H_2O/CO = 3 (varying mole flow W100)
Boiler case				
BOILER	RGibbs	1000	1.2	
HX8	Heater	300	0	
HX9	Cooler	150	0	
OPSEP	Sep			C_{2-4} olefins split fraction = 0.99 (stream OLEFIN)
GT case				
COMP2	Compr		20	Isentropic efficiency = 0.8, Mechanical efficiency = 0.98
GTCOMB	RGibbs		20	Heat duty = 0 W (Adiabatic reactor)
HX8	Cooler	150	0	
M3	Mixer		0	
OPSEP	Sep			C_{2-4} olefins split fraction = 0.99 (stream OLEFIN)
TURB1	Turb		2	Isentropic efficiency = 0.85, Mechanical efficiency = 0.98

Co-firing with natural gas (NG) is considered for a gas turbine (NG is added to the off-gas stream FTV130) in order to have a stable combustion and avoid any modifications in the units required if too low heating value syngas is used. The required flow of compressed air is determined by means of a "Design Specification" to obtain a turbine inlet temperature of 1200 °C. The combustor of the GT (GTCOMB) is modelled as a Gibbs reactor at 20 bar and works as an adiabatic reactor. After the expansion, the products are cooled down to 150 °C (stack temperature).

The two options (boiler and gas turbine) are representative of two different ways to exploit the energy of the purge gas. Eventually in both configurations steam is generated and possibly used to generate electricity. Accordingly, the gas turbine is a way to take advantage of the compressed purge gas for generation of extra power through the expansion of the exhaust gases. The consequences of such different layouts will be further discussed in Chapter 5.

4.2.2 Advanced configurations

A set of "Advanced configurations" is also analysed in this work where the recycled stream is upgraded before being mixed with the fresh syngas coming from the gas cleaning. This is based on the fact that the gas obtained at the top of the first separation stage is rich in light hydrocarbons which cannot be converted into FT-crude through a synthesis step only. This is however possible if these gases are reformed into H_2 and CO which is fresh syngas that can be synthetized. The layout of such advanced FT-synthesis section is shown in Figure 4-7. Still, similar possibilities for the purge gas appear as in the base configuration set which are here not shown again for the sake of brevity but are included in the investigated study cases.

The description of the advanced configuration starts at the recycle stream REC100 since the previous steps are the same as the base case configuration presented in the previous section. REC100 is compressed and sent to an autothermal reformer (ATR) in order to produce hydrogen and carbon monoxide from light hydrocarbons. The reforming process takes place in presence of oxygen (stream O2) and steam (W200). The mole flow of O_2 is regulated by a "Design Specification" that sets the outlet temperature of the ATR to 1000 °C (a typical temperature for the catalytic reformer). The temperature and pressure of the stream are 185°C and 30 bar respectively (Leibbrandt et al. 2013). Steam is injected at 250 °C and a pressure around 38 bar (Leibbrandt et al. 2013). A calculator block determines the quantity of steam needed by applying a steam to carbon ratio of one. The autothermal reformer is modelled as an adiabatic Gibbs reactor after which the reformed products are cooled down to 50 °C and the produced water is removed. Further details about operating conditions of the different blocks in the model are stated in Table 4-7.

The main advantage of this advanced configuration process is related to the increase of the hydrogen content in the recycle stream which allows to reduce the quantity of syngas undergoing the WGS to adjust the H_2/CO ratio of the syngas. Note that this "Design Specification" previously imposed in stream S204 is now adjusting the H_2/CO ratio to a value of 2 in stream S300, i.e. after mixing the syngas from the reformer, once again by changing the split fraction of SP1. In this way it is also possible to compare the flow of stream S120 and see the contribution of the ATR to reduce the WGS extent.

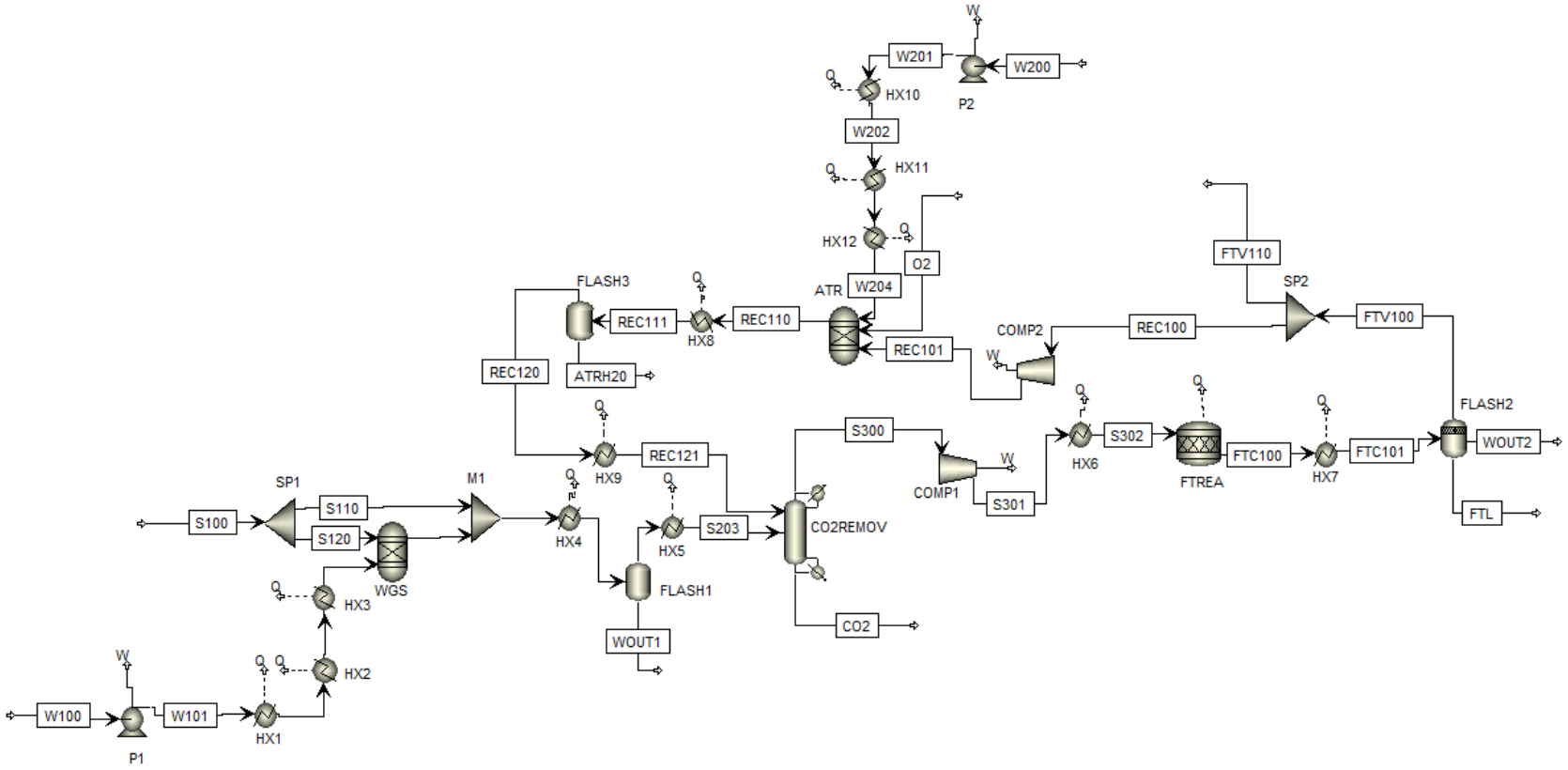

Figure 4-7: Simulation of FT synthesis advanced configurations flowsheet in Aspen Plus

Table 4-7: Model description of the advanced configurations

Unit	ASPEN plus model	T_{out} [°C]	Pressure [bar]	Other specification
ATR	RGibbs			Heat duty = 0 W (Adiabatic reactor), Δp = 5 mbar
CO2REM	Sep			CO_2 split fraction = 0.99, H_2O split fraction = 1 (stream CO2)
COMP1	Compr		20	Isentropic efficiency = 0.8, Mechanical efficiency = 0.98
COMP2	Compr		30	Isentropic efficiency = 0.8, Mechanical efficiency = 0.98
FLASH1	Flash2		0	Heat duty = 0 W
FLASH2	Flash3		0	Heat duty = 0 W
FLASH3	Flash2		0	Heat duty = 0 W
FTREA	RStoich	220	-1	
HX1	Heater		0	Vapour fraction = 0
HX2	Heater		0	Vapour fraction = 1
HX3	Heater	350	0	
HX4	Cooler	50	0	
HX5	Cooler	0	0	
HX6	Heater	220	0	
HX7	Cooler	30	0	
HX8	Cooler	50	0	
HX9	Cooler	0	0	
HX10	Heater		0	Vapour fraction = 0
HX11	Heater		0	Vapour fraction = 1
HX12	Heater	250	0	
M1	Mixer		0	
P1	Pump		20	Efficiency = 0.9
P2	Pump		38	Efficiency = 0.9
SP1	FSplit			Split fraction with Design Spec H_2/CO = 2 (stream S300)
SP2	FSplit			Split fraction = 0.9 (stream REC100)
WGS	RGibbs			Heat duty = 0 W (Adiabatic reactor), Design Spec H_2O/CO = 3 (varying mole flow W100)

4.2.3 FT-calculator block

A rigorous kinetic model of the FT-reactor would require taking into account the synthesis of a large number of hydrocarbons and how the separate reactions participate and compete with each other in the consumption of the fresh syngas. The description of such phenomena through a set of rate laws is extremely complex and researchers instead aggregate the overall synthesis into a single rate law equation. Afterwards the distribution of the hydrocarbons is adjusted through probability distribution models. As this latter approach is of difficult implementation through standard equipment models available in Aspen Plus, the FT-synthesis is modelled as a calculator block. The calculator block is implemented with a MS Excel file. The input part of this file is shown in Figure 4-8.

INPUT VALUES

Manual Input Values							
Alpha Model		C_{1-4} selectivity				CO conversion	Factor for O/P
A	B	C_1	C_2	C_3	C_4		c
0.2332	0.633	8.8%	0.8%	1.18%	1.66%	50%	0.25
			0.07%	2.23%	3.67%		

Source: Song (2004) Source: Rane et al. (2012)

Input Values from Aspen						
Syngas						
Components	mole flow [kmol/s]	mol%	mass flow [kg/s]	mass%	Molar mass M [kg/kmol]	H_2/CO ratio
H_2	11.87	28%	7.42	5%	2	1.97
CO	6.03	14%	51.54	33%	28	
CO_{conv}	3.01	7%	25.77	17%		
CO_2	0.19	0%	88.02	57%	44	
CH_4	23.11	55%	7.7	5%	16	
Molar flow	42.36		154.68			

FT-reactor			
Temperature	220 °C	493.15	K
Pressure	20 bar	2000000	N/m^2

Figure 4-8: Input part of the Excel calculation file for predicting the hydrocarbon distribution within the FT-reactor

First of all "Manual Input Values" have to be defined, which include the α-Model specific constants as well as selectivities of C_{1-4} (expressed in kg_{Cn}/kg_{Cconv}). Those selectivities are average values from the experiments performed by Rane et al. (2012) who studied the influence of different cobalt particle sizes for alumina supported catalysts and specified the relation between hydrocarbon selectivity and the type of catalyst.

These values are needed in order to determine the weight distribution of the C_{1-4} hydrocarbons as they don't follow the ASF curve (cf. Section 3.1) (Van der Laan and Beenackers 1999; Elbashir 2010). For this reason many authors distinguish these selectivities from the one that considers all the compounds higher than C_5 (S_{C5+}). Furthermore, the CO conversion within the FT-reactor has to be manually changed.

Within the second part, the input values which are imported from Aspen Plus are shown (highlighted in green). These are the mole flows of the different compounds as well as the total mole flow and the operating conditions chosen for the FT-reactor. Note that the total mole flow does not need to equal the sum of the H_2, CO, CO_2 and CH_4 flows, the other components such as nitrogen or hydrocarbons which remain in the recirculation being not exported to the Excel file as they do not affect the synthesis.

The actual calculation part is shown in Figure 4-9 in which the blue highlighted cells represent the resulting extent of the single synthesis reaction into paraffins and olefins which are exported to the Aspen Plus stoichiometric reactor.

The calculations within the Excel file are based on the α-model of Song et al. (2004) which is described in more depth in Section 3.1.

In the example shown in Figure 4-9 the α-value equals 0.85. Starting from this value the weight and molar fractions for the hydrocarbons $C_{5\text{-}50}$ can be calculated according to Equation [3-5] and [3-6]. It has been demonstrated that it is possible to calculate the molar distribution from the weight distribution without using both equations. However, M_n and W_n only equal each other if the ASF distribution is also applied for the hydrocarbons $C_{1\text{-}4}$ which is not the case in reality (cf. Section 3.1). Therefore, Equation [3-5] should not be used for calculating M_n but instead M_n should be derived from W_n after adjusting the weight fractions for $C_{1\text{-}4}$.

In order to be able to calculate the molar fractions M_{n_calc} from the weight distribution W_n the molar mass M_{Ctot} of the hydrocarbon mixture is needed. Within a first step the selectivity S_{C5+} for the hydrocarbons with a carbon number of 5 and higher has to be calculated as follows:

$$S_{C_{5+}} = \sum_{n=5}^{50} W_n \qquad [4\text{-}10]$$

This result is needed in order get the sum of the selectivities $S_{C1\text{-}4}$:

$$S_{C_{1-4}} = 1 - S_{C_{5+}} \qquad [4\text{-}11]$$

The weight distribution W_n for $C_{1\text{-}4}$ is calculated with the selectivities for $C_{1\text{-}4}$ as shown in Figure 4-9 by rescaling these values with the sum just determined with Equation [4-2]:

$$W_n = \frac{S_{Cn}}{\sum_{n=1}^{4} S_{Cn}} S_{C_{1-4}} \qquad [4\text{-}12]$$

Since the selectivities are based on the carbon content W_n is expressed in kg_{Cn}/kg_{Ctot}. Thus only the carbon atom mass for each hydrocarbon is relevant for the molar mass:

$$M_{C_n} = M_C * n = 12 * n \qquad [4\text{-}13]$$

in which n stands for the carbon number. With this value the reciprocal of M_{Ctot} can be calculated:

$$\sum_n \frac{W_n}{M_{C_n}} = \frac{1}{M_{C_{tot}}} \qquad [4\text{-}14]$$

And by using the reciprocal value of M_{Ctot} the $M_{n_}$calc is derived from W_n:

$$M_{n\_calc} = \frac{W_n}{M_{C_{tot}}} \qquad [4\text{-}15]$$

Figure 4-10 below shows the comparison of the M_n generated from Equation [3-5] and M_{n_calc}. It clearly states that M_{n_calc} is always lower than M_n. However, with longer hydrocarbon chains the difference becomes smaller and eventually it is not detectable anymore.

CALCULATIONS / OUTPUT VALUES

C_{1-4}	16,8%					
	mass% [kg_{Cn}/kg_{CO}]	M_{Cn} [kg/kmol]	O/P	paraffin %	olefin %	mol% [$kmol_{Cn}/kmol_{CO}$]
CH_4	8,1%	12	0	100,0%	0,0%	43,45%
C_{2-}	0,7%	24				1,99%
$C_{2=}$	0,1%	24	0,09	91,7%	8,3%	0,17%
C_{3-}	1,1%	36				1,94%
$C_{3=}$	2,0%	36	2,01	33,2%	66,8%	3,66%
C_{4-}	1,5%	48				2,04%
$C_{4=}$	3,4%	48	2,28	30,5%	69,5%	4,51%

Source: Rane, Borget al (2012), p. 16 average values

Formulas

$\alpha = [A*(\gamma_{CO}/(\gamma_{H2} + \gamma_{CO})) + B] * [1- 0{,}0039*(T-533)]$

$M_n = (1-\alpha)*\alpha^{n-1}$ **α 0,85**

$W_n = \alpha^{n-1} (1-\alpha)^2 n$ **Selectivity S_{C5+} 83%**

$mol\ flow CO_{,conv} = (CO_{Conv} * n * M_{n\_calc} / Sum(mol_{CO,unstoch\ n})$

$CONV = mol\ flow_{CO,used} / COIN$

Reactions								CO is limiting				
n or CO (stoch) [kmol]	M_n [-]	M_{n_calc}	W_n [-]	CO (unstoch) [kmol]	O/P	paraffin %	olefin %	$flow_{CO,conv}$ [kmol/s]	$flow_{CO,used}$ Paraffin [kmol/s]	$flow_{CO,used}$ Olefin [kmol/s]	CONV Paraffin	CONV Olefin
1	15,07%	43,45%	8%	0,435	0,000	100%	0%	0,068	0,068	0,000	3,7%	0,00%
2	12,80%	2,17%	1%	0,043	0,090	92%	8%	0,007	0,006	0,001	0,3%	0,03%
3	10,87%	5,59%	3%	0,168	2,010	33%	67%	0,026	0,009	0,018	0,5%	0,96%
4	9,23%	6,56%	5%	0,262	2,280	30%	70%	0,041	0,013	0,029	0,7%	1,56%
5	7,84%	6,37%	6%	0,318	0,287	78%	22%	0,050	0,039	0,011	2,1%	0,61%
6	6,66%	5,41%	6%	0,324	0,223	82%	18%	0,051	0,042	0,009	2,3%	0,51%
48	0,01%	0,01%	0%	0,003	0,000	100%	0%	0,000	0,000	0,000	0,0%	0,00%
49	0,01%	0,00%	0%	0,002	0,000	100%	0%	0,000	0,000	0,000	0,0%	0,00%
50	0,01%	0,00%	0%	0,002	0,000	100%	0%	0,000	0,000	0,000	0,0%	0,00%
1265	100%	100%	100%	5,390				0,846		0,994		

W_n to M_n calculation		
M_{Cn} [kg/kmol]	W_n/M_{Cn} [$kmol_{Cn}$/ Σ kg_{Cn}]	M_{n_calc} [$kmol_{Cn}$/ Σ $kmol_{Cn}$]
12	0,007	43,45%
24	0,000	2,17%
36	0,001	5,59%
48	0,001	6,56%
60	0,001	6,37%
72	0,001	5,41%
576	0,000	0,01%
588	0,000	0,00%
600	0,000	0,00%
	0,015	
M_{Ctot}	64,67	

Figure 4-9: Carbon distribution calculation and Output part of the Excel calculation file

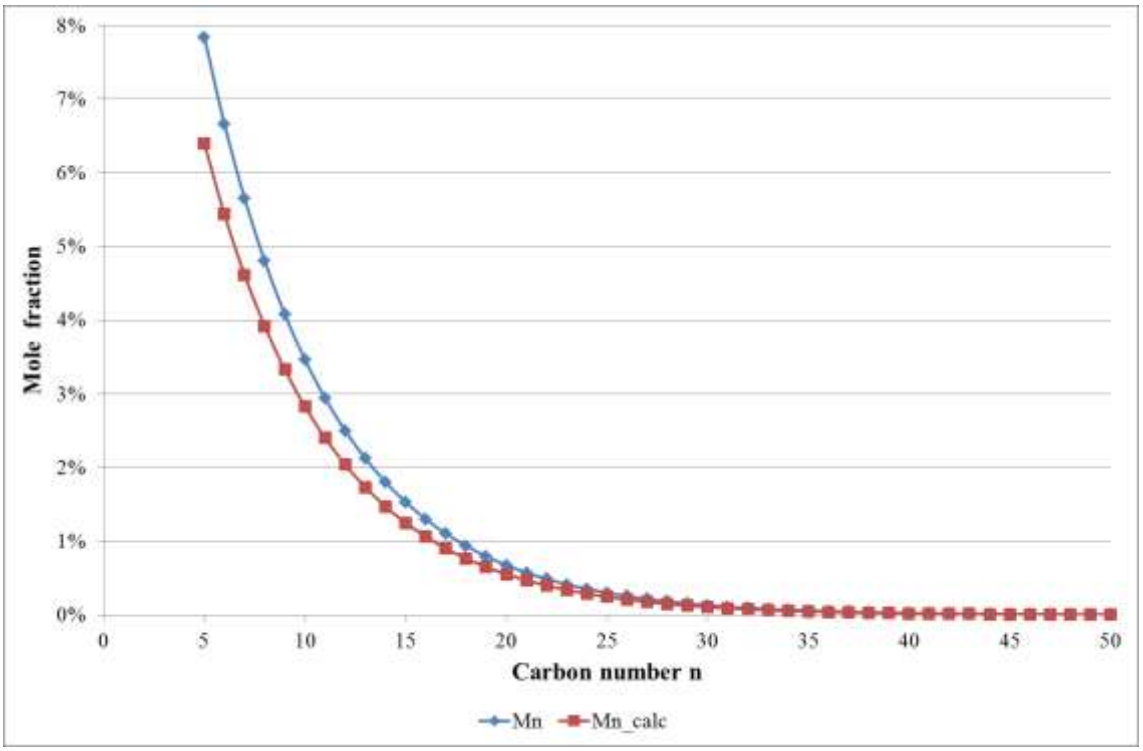

Figure 4-10: Comparison of formula derived M_n and calculated M_{n_calc}

With the value of M_{n_calc} the mole flow of the CO converted for each reaction can be calculated:

$$Flow\ CO_{conv,n} = \frac{Flow\ CO_{in}}{\sum_{n=1}^{50} n * M_{n\_calc}} * \left(n *\ M_{n\_calc}\right) \qquad [4\text{-}16]$$

This flow represents the CO_{conv} for the paraffin and olefin for each C_n, however, to export the fractional conversion back to Aspen Plus, the separate value for the paraffins and olefins is needed. The stoichiometry for these two possible reactions is shown below:

Paraffins: $n\ CO + (2n+1)\ H_2 \rightarrow C_nH_{2n+2} + n\ H_2O$

Olefins: $n\ CO + 2n\ H_2 \rightarrow C_nH_{2n} + n\ H_2O$

To distinguish the extent to which each of these reactions occur the olefin over paraffin ratio O/P, as introduced in Section 2.1, is needed. Since C_{1-4} does not follow that correlation once again the average values from Rane (2012) are applied.

As for the other hydrocarbons the relation expressed in Equation [3-4] is considered with the assumption of a constant c = 0.25.

From these ratios it is possible to obtain the percentage of both olefins and paraffins:

$$P\% = \frac{P}{O+P} = \frac{1}{\frac{O}{P}+1} \qquad [4\text{-}17]$$

$$O\% = 1 - P\% \qquad [4\text{-}18]$$

Each flow of CO converted can be divided into the flow yielding the paraffin species and the one yielding the olefin by multiplying the total flow by the percentages of paraffins and olefins determined before:

$$\%CO_{conv} = \frac{Flow\ CO_{conv}}{Flow\ CO_{in}} \quad [4\text{-}19]$$

$$\%CO_{conv\ P} = \frac{Flow\ CO_{conv\ P}}{Flow\ CO_{in}} \quad [4\text{-}20]$$

$$\%CO_{conv\ O} = \frac{Flow\ CO_{conv\ O}}{Flow\ CO_{in}} \quad [4\text{-}21]$$

4.2.4 Higher Heating Value calculation

One important characteristic of any feedstock or product within chemical plants is the heating value which can be distinguished between higher and lower heating value.

For this thesis the higher heating value (HHV) is chosen as a comparison value. To determine the HHV for the syngas a simulation as shown in Figure 4-11 is used.

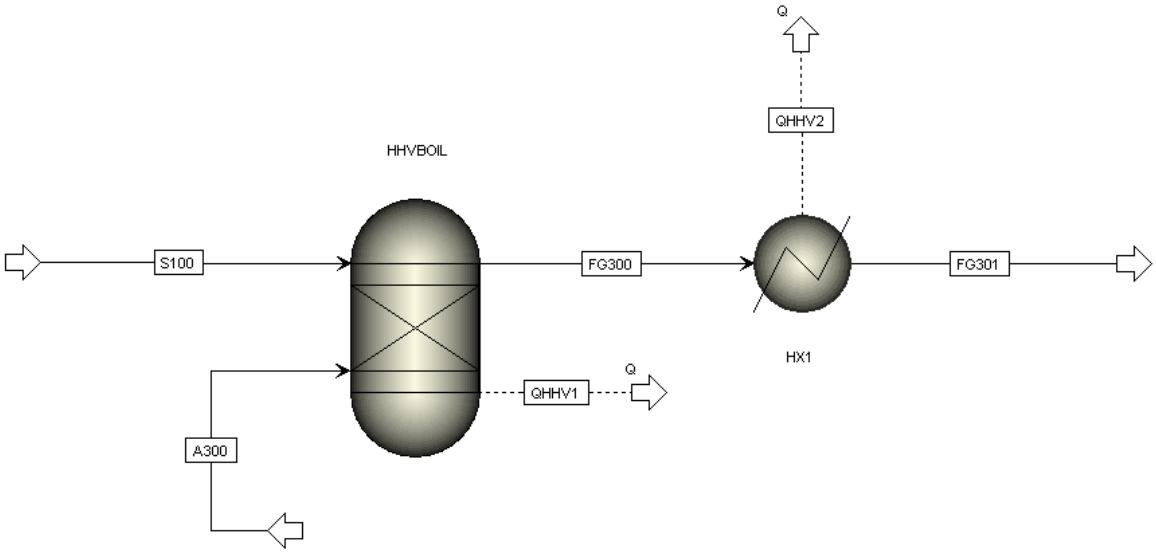

Figure 4-11: Simulation for HHV determination

The S100 enters the HHVBOIL at 25 °C and 1 atm. To ensure that a complete combustion takes place the air flow is calculated with a calculator block in the background by calculating the oxygen moles needed for stoichiometric combustion of H_2, CO and CH_4. The HHVBOIL is modelled with a Gibbs reactor model assuming that only O_2, H_2O, CO_2 and N_2 can be products and the operation conditions being 1000 °C and 1 atm. After the boiler the flue gas in FG300 is cooled back down to 25 °C which accounts for the convection heat flow of a boiler combustion. For calculating the HHV the two heat streams QHHV1 and QHHV2 have to be considered:

$$HHV = \frac{QHHV1+QHHV2}{\dot{m}_{S100}} = 21.48\ \frac{MJ}{kg} \quad [4\text{-}22]$$

The same approach is used for calculating the HHV of the FTL stream.

4.3 Overview of studied cases and parametric study

To study general performances of the different configurations each one undergoes a parametric study. In particular, it was chosen to investigate the effect of temperature, pressure and desired conversion through one reactor passage. The temperature and pressure are varied from 200 to 250 °C and 20 to 30 bar respectively. The CO conversion within the FT-reactor is increased from 50 to 70 %. A graphical overview of how the simulations of the various cases are performed is given in Figure 4-12.

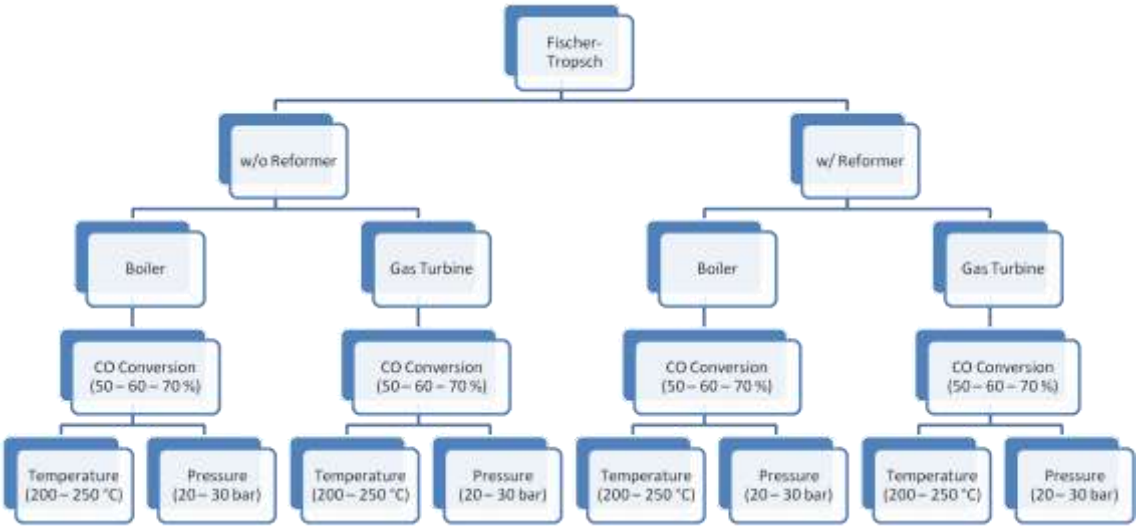

Figure 4-12: Overview of the studied cases and parametric study

In order to compare the different configurations the values of the following indicators for the different cases are considered in this study:

- Product distribution of the FT-liquids
- Catalyst amount and FT-reactor volume
- Electricity balance for boiler and GT configurations
- Efficiencies
- Exergy in the heat streams

Aspen Plus gives the possibility to perform parametric study and to define stream and unit output values as well as comparison factors.

The product distribution within the FTL stream determines the amount and composition of FT-fuel that can be produced. On the one hand this indicator is of interest to distinguish between paraffins and olefins but also to further divide the paraffins and olefins into carbon number ranges. It is common practice to cluster paraffins of the length C_5 to C_{11} as naphtha, C_{12} to C_{19} as diesel and everything longer than C_{20} as waxes. The olefins are clustered in the same way however they are not called naphtha, diesel or waxes. All of these carbon ranges are further combined to C_{5+} hydrocarbons to figure out the remaining amount of unwanted C_{1-4} hydrocarbons in the FTL stream.

The kinetic modelling approach to determine the catalyst amount and reactor volume is introduced in Section 4.1.4. Generally the CO conversion is calculated according to Equation [4-4]:

$$-R_{CO} = \frac{a \cdot p_{CO} \cdot p_{H_2}}{(1+b \cdot p_{CO})^2} \qquad [4–4]$$

The values for a and b are calculated with the approach of Krishna (2000) according to the Equations (4-7) and [4-8] which show the dependency of the CO conversion on the temperature together with pressure and mole fraction of CO and H_2 after the FT-reactor.

The kinetic theory for Continuous-Stirred Tank Reactors (CSTR) is taken into consideration for sizing the reactor. When considering a CSTR steady-state conditions can be assumed, and temperature, concentration and reaction rate are considered homogeneous in all the reactor and equal to those of the product stream. The design equation for CSTR is based on a function of the CO converted as well as of the reaction rate r_{CO} [mol/dm^3 s] (Fogler 1999).

$$V = \frac{CO_{in} - CO_{out}}{r_{CO}} \qquad [4\text{-}23]$$

As the numerator of the previous formula can be expressed as $CO_{in} \cdot \chi_{CO}$, Equation [4-24] can be easily rearranged into Equation [4-25]. In this way it's possible to calculate the volume of reactor necessary to achieve a certain CO conversion, in addition since the conditions inside the reactor are the same as in the exit, r_{CO} is calculated at exit conditions.

$$V = \frac{CO_{in} \cdot \chi_{CO}}{r_{CO,\ exit}} \qquad [4\text{-}24]$$

As the R_{CO} previously introduced is the carbon monoxide consumption rate in mol/(s kg_{cat}), the amount of catalyst needed in order to reach χ_{CO} is given by the equation below:

$$g_{cat} = \frac{\chi_{CO} \cdot CO_{in}}{R_{CO}} = \frac{CO_{conv}}{R_{CO}} \qquad [4\text{-}25]$$

The catalyst amount is afterwards used to calculate the FT-reactor volume according to the following equation:

$$V_{FTREA} = \frac{g_{cat}}{\rho_{cat}} \qquad [4\text{-}26]$$

in which ρ_{cat} stand for the catalyst density within the reactor in $kg_{cat}/m^3_{Reactor}$.

A further indicator considered in this work is the electricity balance which is of special interest for the GT configurations which include both electricity producer and consumer. For the boiler configurations, however, only the electricity consumption has to be considered since no electricity producer is present. In general the electricity balance is calculated as:

$$W_{e,net} = \left| \sum W_{e,produced} - \sum W_{e,consumed} \right| \qquad [4\text{-}27]$$

In the followings, $W_{e,net}$ is always shown as a positive value and clearly highlighted whether it is consumption or production.

Within this thesis three efficiencies are also calculated to thermodynamically evaluate how efficiently the raw materials or the input energy rate is converted into valuable products.

At first the conversion efficiency is an indicator of how efficient the syngas is converted into the FTL and is calculated according to the following equation:

$$\eta_{conv} = \frac{HHV_{FTL} * \dot{m}_{FTL}}{HHV_{Syngas} * \dot{m}_{Syngas}} \qquad [4\text{-}28]$$

in which the HHV is expressed in kJ/kg and the mass flow $\dot{m}$ in kg/sec.

In the literature conversion efficiencies for FT-liquid production can be found in the range of 40 – 50 % (Hamelinck 2004).

An overall system efficiency is also considered in order to take into account additional heat and work flows that are needed or produced. Depending on the technology used for further using the purge gas different versions of the system efficiency equation are used:

$$\eta_{system,GT} = \frac{HHV_{FTL} * \dot{m}_{FTL} + W_{e,net}}{HHV_{Syngas} * \dot{m}_{Syngas} + \dot{m}_{NG} * HHV_{CH_4}} \quad [4\text{-}29]$$

$$\eta_{System,Boiler} = \frac{HHV_{FTL} \cdot \dot{m}_{FTL}}{HHV_{Syngas} \cdot \dot{m}_{Syngas} + W_{e,net}} \quad [4\text{-}30]$$

in which $W_{e,net}$ stands for power production in the GT case and for consumption in the boiler case.

At last the cold gas efficiency η_{CG} is a figure which goes one step further than the conversion efficiency by calculating the ratio of the usable product and the actual process feedstock since the syngas is usually produced through reforming or gasification of various solid feedstock. In this thesis the primary energy source is considered to be biomass. Since the gasification process hasn't been considered within this thesis a conversion efficiency of 0.7 is assumed for the production of syngas from biomass (Zwart and Boerrigter 2005). Therefore the cold gas efficiency η_{CG} of the process can be calculated as shown below (Heyne and Harvey 2013):

$$\eta_{CG} = \frac{HHV_{Product} * \dot{m}_{Product}}{\frac{(HHV_{Syngas} * \dot{m}_{Syngas})}{0.7}} \quad [4\text{-}31]$$

Due to the highly exothermic reaction in the FT-reactor it is also of interest to consider the amount of excess heat of the process. Generally there are two ways of valuing the amount of heat available: either by combining the heat streams into a grand composite curve (GCC) followed by the integration of a steam cycle to calculate the power that could be produced within a steam turbine or by calculating the theoretical exergy of the excess heat. Generally, exergy is a theoretical value to describe the maximum available amount of work that can be extracted by a reversible process from a system in exchange with the environment (Wall 2004). Therefore, exergy-based indicators are more suitable to compare the theoretical potential of work/electricity production of a thermodynamic process since the energy efficiency of the system units do not have to be considered.

The exergy of a heat stream is calculated according to the following:

$$\dot{E}_q = \Theta \cdot \dot{Q} = \left(1 - \frac{T_0}{T}\right) \cdot \dot{Q} \quad [4\text{-}32]$$

in which T_0 describes the ambient temperature in Kelvin. This value is here set to 298.15 K (25 °C).

One possible way to graphically show the amount of exergy included in all the heat streams within a system is the Carnot GCCs. These curves can be created with the Excel AddIn "pro_pi" which was developed at the Heat and Power Technology Division at Chalmers. The Carnot GCC shows the Carnot factor over the available heat and therefore the exergy can be calculated as the area underneath the GCC.

5 Modelling Results and Discussion

In this chapter the results of the parametric study of the various configurations introduced in Section 4.3 are shown and discussed. Note that the configurations only vary by the utilization of the purge stream. Furthermore, the models are distinguished in two cases: one with reformer and the other one without reformer.

5.1 Product Distribution

Fel! Hittar inte referenskälla. Table 5-1 shows the small increase of the FTL stream with an increase in pressure. Even though the α-model does not consider a pressure dependency the flashing process to separate the FTL from the FTC stream is influenced by an increase in pressure. Therefore, the amount of FTL changes with pressure. The table also shows that the product stream can increase to around 4.6 kg/s for the case with reformer and at 220 °C and 30 bar. This value equals approximately 5 200 bbl/day which is in the range of the maximum reactor capacity of the SSPD reactor by Sasol (cf. Section 3.3.2).

Table 5-1: FTL stream [kg/s] at a constant temperature of 220 °C

FT-pressure [bar]	w/o Reformer			w Reformer		
	χ_{CO} = 0.5	χ_{CO} = 0.6	χ_{CO} = 0.7	χ_{CO} = 0.5	χ_{CO} = 0.6	χ_{CO} = 0.7
20	3.04	3.17	3.28	3.21	3.78	4.42
22	3.07	3.20	3.30	3.24	3.82	4.43
24	3.09	3.22	3.33	3.26	3.88	4.46
26	3.11	3.24	3.35	3.29	3.91	4.49
28	3.13	3.26	3.37	3.31	3.95	4.52
30	3.14	3.28	3.39	3.33	3.96	4.58

As explained in the theory about the FT-synthesis an increase in the temperature of the reactor promotes the synthesis of light hydrocarbons to a higher extent than those with longer chain (cf. Section 4.1.3). This is shown in Figure 5-1 for a CO conversion of 50 % where the products in FTL are clustered according to the carbon ranges of interest. It can be further noticed that the hydrocarbons in the typical ranges for biofuels production (Diesel and Waxes) decrease significantly whereas the olefin content grows in a small percentage. The increase of the olefin amount with the temperature can be explained with the model used for the olefin/paraffin ratio.

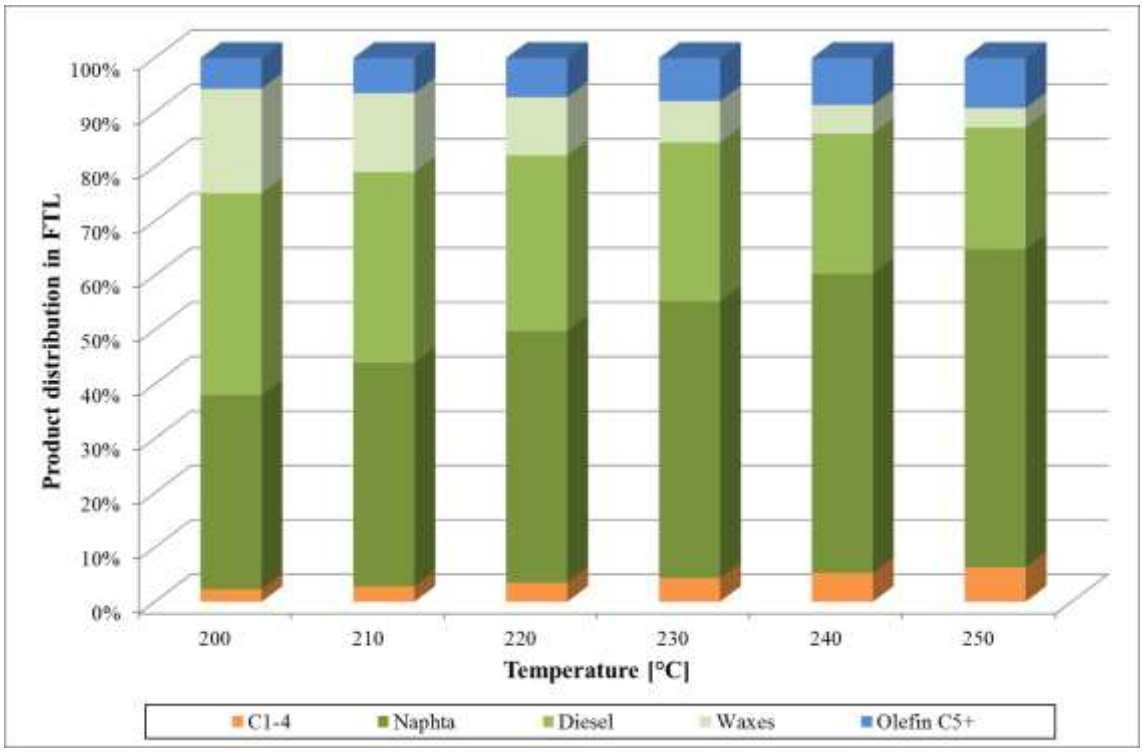

Figure 5-1*: Product distribution in FTL for the case without reformer at 20 bar and a CO conversion of 50 %*

Since the amount of olefins and paraffins is predicted with an exponential model a higher paraffin amount of naphtha also leads to a higher amount of olefins in the range of $C_{5\text{-}11}$. The tendency just described can also be illustrated in absolute mass flows (cf. Figure 5-2).

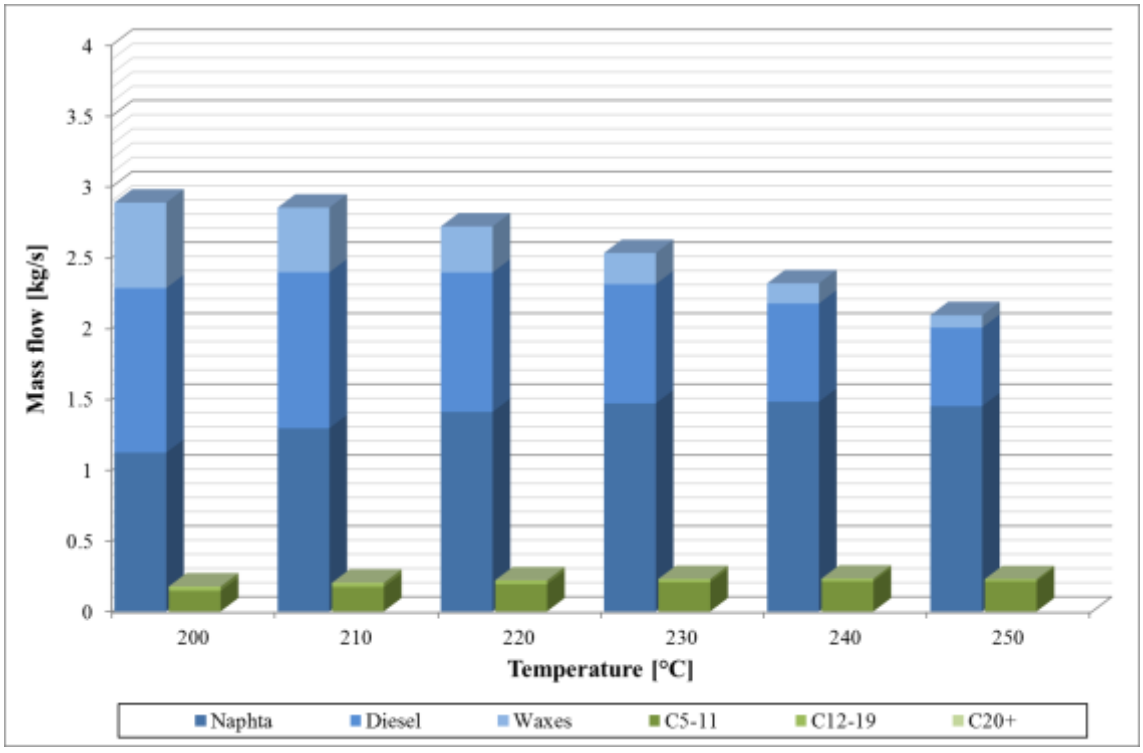

Figure 5-2: Mass flow of the FTL stream [kg/s] and the product distribution at 20 bar and a CO conversion of 50 %

Figure 5-2 shows the more pronounced decrease in the paraffin content with increasing temperature compared to olefins yield which remains almost constant with the temperature and thus make their percentage increase as well.

The general distribution in Figure 5-1 is similar for all configurations from a percentage perspective however the absolute values increase for the case with reformer as shown in Figure 5-3. It is striking that the FTL flow increases more rapidly for the case with reformer while changing the CO conversion. This can be explained by having a closer look at the recirculating flow for both cases. For the case with reformer the recirculating flow entering the CO2SEP unit consists of mainly H_2 and CO whereas for the other case this stream also includes hydrocarbons to some extent. This already decreases the amount of H_2 and CO which can be converted in the FT-reactor. In addition to this the H_2/CO ratio is fixed at S203 for the case without reformer and therefore decreases after mixing with the recirculating stream with an increase in temperature and CO conversion. These two phenomena lead to a smaller increase in the FTL flow for the case without reformer.

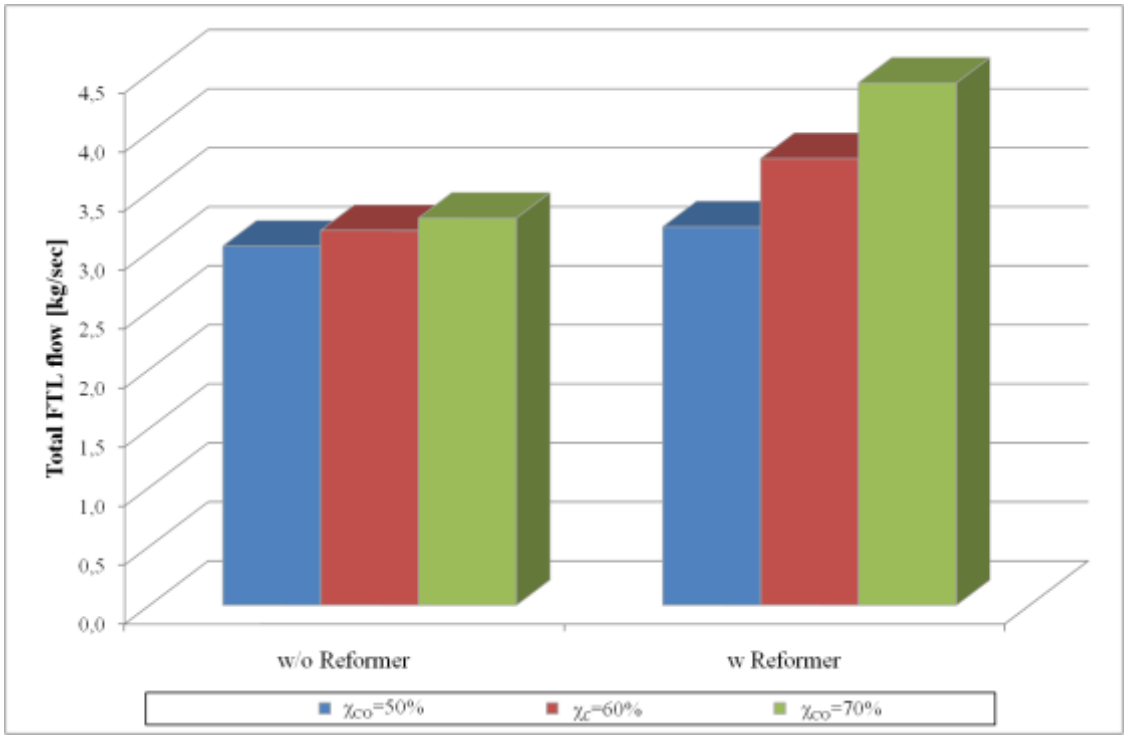

Figure 5-3: FTL flow for both cases at 220 °C and 20 bar

A further validation of the reasons stated above to explain the product distribution is given in Figure 5-4 Figure 5-4 in which S_{C5+}, S_{C1-4} and H_2/CO are shown in function of the temperature. As verified in Section 4.1.3 the alpha chain growth decreases with the temperature and so does the selectivity S_{C5+} towards long chain hydrocarbons as a consequence. Therefore the selectivity for light hydrocarbons behaves symmetrically since it is defined as 1- S_{C5+}. The growth of S_{C1-4} should go together with an increase of the H_2/CO ratio according to Hamelinck et al. (2004) as well as Ng and Sadhukhan (2011) due to the higher probability in chain termination. This is not what can be gathered from Figure 5-4 below which shows an increase of the C_{1-4} selectivity whilst the H_2/CO ratio decreases. This tendency can be justified by underlining the higher impact of the temperature on the chain growth probability α. Therefore, an increase in temperature leads to a lower α-value and consequently to a higher S_{C1-4}. These trends for the selectivities are valid for all the

configurations. The H_2/CO ratio, however, will not change for the case with reformer since the "Design Specification" in Aspen Plus fixes the ratio in stream S300.

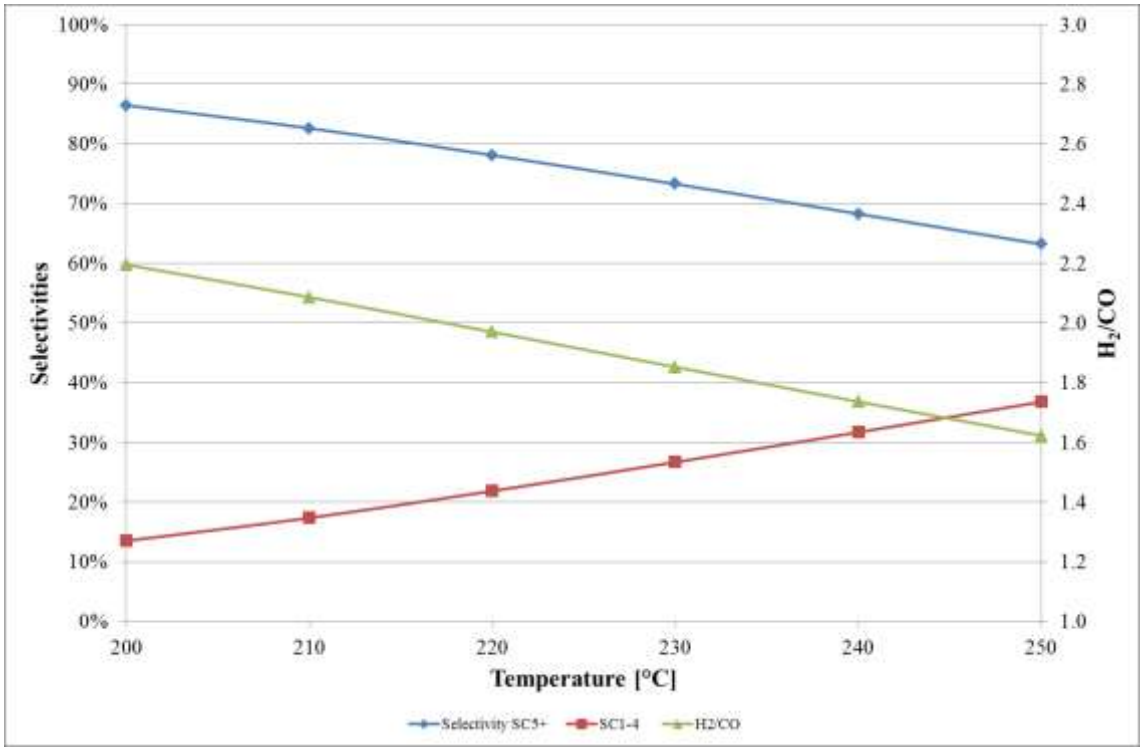

Figure 5-4: Selectivities and H_2/CO ratio in S300 for the case without reformer at 20 bar and a CO conversion of 50 %

5.2 Catalyst amount and reactor volume

The estimation of the catalyst amount needed to obtain a specified conversion of the reactants shows different trends for the cases with and without reformer.

In the first place the kinetic model depends stronger on the temperature and the CO conversion than on the pressure therefore this indicator is analyzed by looking at the different CO conversions fixed in the reactor. From Figure 5-5 it can be stated that the catalyst amount generally decreases exponentially with the temperature but if high conversions like 60 and 70 % are targeted the reactor volume has a local minimum at temperatures within the range investigated and more precisely around 240 °C for 60 % conversion and at 220 °C for 70 % conversion. In particular for 60 % conversion a small increase is observed at higher temperatures while at 70 % the increase in reactor volume is noticeable and even seems disproportional compared to the other values. The reason that no value is shown for a CO conversion of 70 % and a temperature of 250 °C is the occurrence of a lack of H_2 to carry out the FT-synthesis for the case of no reformer. This is due to the low H_2/CO ratio that is reached in stream S300. Table 5-2 shows that the ratio decreases to a level below 2 with an increase in temperature. This fact constrains the progression of the synthesis unless a huge amount of catalyst is applied. The amount of catalyst determined with Equation [4-26] gives results that are comparable with the quantity specified by Fogler (1999) for a FT-synthesis reactor by Sasol.

Table 5-2: H_2/CO ratio in Stream S300 for cases without reformer at 20 bar

CO Conversion[1]	Temperature [°C]					
	200	**210**	**220**	**230**	**240**	**250**
50 %	2.20	2.09	1.97	1.85	1.74	1.62
60 %	2.20	2.08	1.94	1.80	1.67	1.53
70 %	2.21	2.06	1.91	1.75	1.60	1.49

[1] CO conversion within FT-reactor

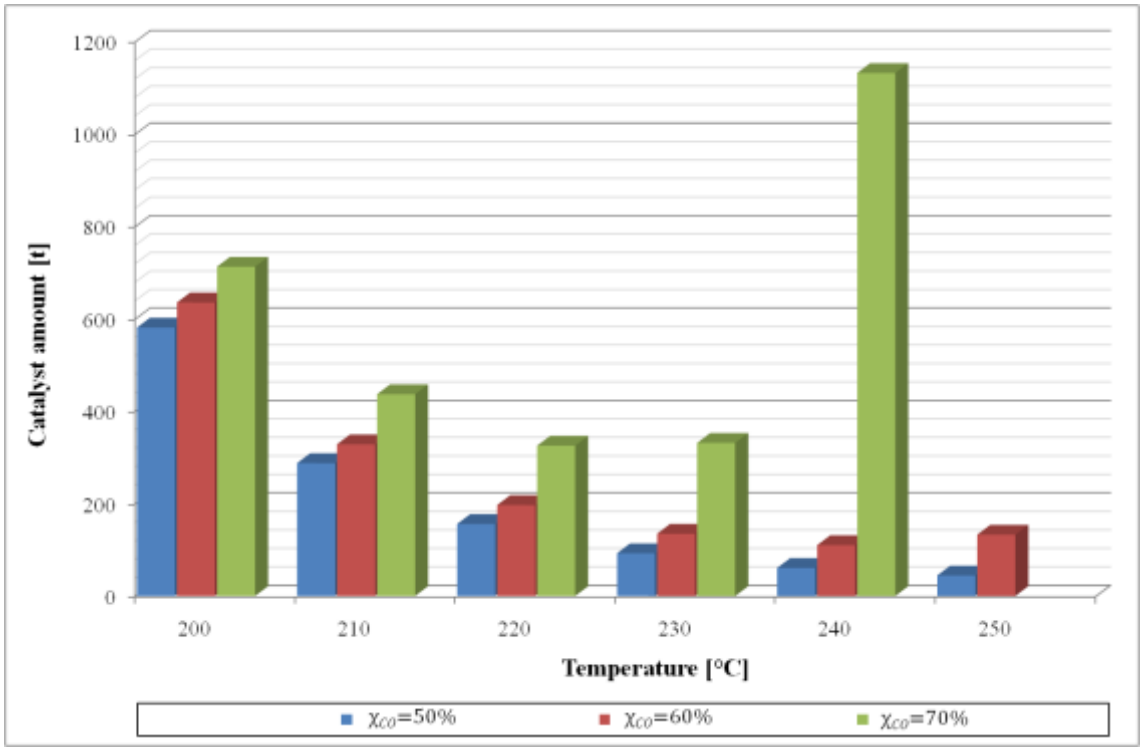

Figure 5-5: Catalyst amount needed in FTREA for the case without reformer at 20 bar calculated with Equation [4-26]

Comparing the catalyst amount needed for both cases it is striking that the amount is higher at 200 °C for the case with reformer but decreases faster with an increase in temperature as shown in Figure 5-5 and Figure 5-6. This again can be justified by having a look at the H_2/CO ratios when entering the FT-reactor at this temperature. The ratio for the basic case is higher than 2 as shown in Table 5-2 whereas it is 2 for the other case. This apparently leads to a lower demand since CO can be converted more easily. However, the advantage of having a higher H_2/CO ratio is overcome at a temperature of 210 °C at which the H_2/CO ratio for both cases is around 2. Another possible reason for the higher amount of catalyst needed can again be based on the higher absolute value of H_2 and CO within the stream to the FT-reactor which is due to the complete reformation of all recirculating components to H_2 and CO.

Figure 5-6 also shows that the necessary catalyst amount decreases steadily for the case with reformer since the H_2/CO ratio is kept at a constant level. This shows that keeping the H_2/CO ratio at a constant value is advantageous to avoid a lack of H_2 and therefore an exponential increase of the catalyst amount.

Table 5-3: Reactor volume in m^3 at a constant pressure of 20 bar calculated with Equation [4-27]

Temperature	**w/o Reformer**			**with Reformer**		
[°C]	χ_{CO} **= 0.5**[1]	χ_{CO} **= 0.6**[1]	χ_{CO} **= 0.7**[1]	χ_{CO} **= 0.5**[1]	χ_{CO} **= 0.6**[1]	χ_{CO} **= 0.7**[1]
200	899	983	1104	1097	1324	1614
220	241	321	505	213	262	345
250	69	207	-	27	36	53

[1] CO conversion within FT-reactor

The corresponding reactor volumes which are calculated with Equation [4-27] are listed in Table 5-3. It is shown that the volume of the FT-reactor decreases with the catalyst amounts. The reason that no value is shown for a CO conversion of 70 % and a temperature of 250 °C is the occurrence of a lack of H_2 to carry out the FT-synthesis for the case of no reformer. This occurred for all pressure levels in the case without reformer. This shows that CO builds up within the reactor in this case and therefore higher purge would be needed to achieve the desired conversion but less product yield would be obtained in comparison with low purge ratios.

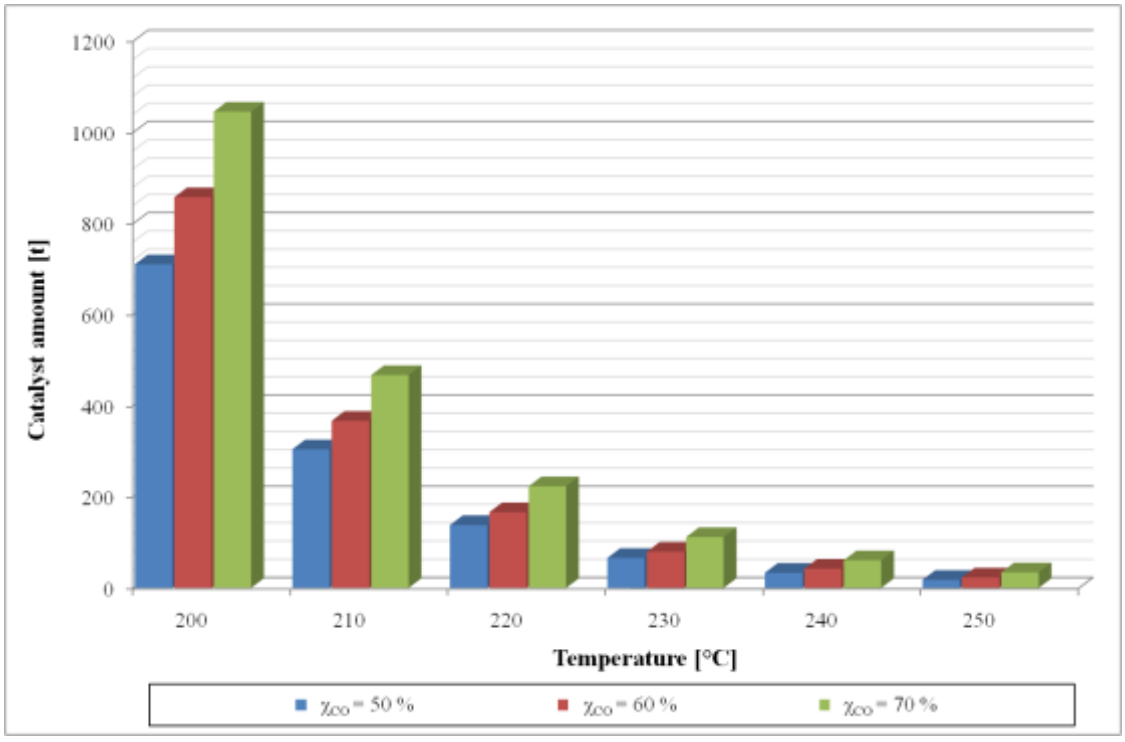

Figure 5-6: Catalyst amount needed in FTREA for the case with reformer at 20 bar calculated with Equation [4-26]

The parametric study also shows a small variation of the volume with pressure even though the α-model is not dependent on the pressure. This fact can be explained by the higher amount of FTL being split in FLASH1 as described in Section 5.1. This leads to a smaller recycle stream and therefore a lower stream has to be handled by the FT-synthesis.

5.3 Electricity balance for the boiler configurations

For the boiler configurations the electricity balance which is calculated according to Equation [4-28] concludes in an electricity deficit since no electricity producer is present in the system. The results show that the electricity deficit and in unison also the electricity consumption is mainly influenced by pressure whereas a change in temperature has less impact on the overall electricity consumption. This is mainly due to the fact that the compressor COMP1 prior to the FT-reactor, which is the primary electricity consumer, is not affected by the FT-operation temperature since the heat exchanger before it cools the stream to a constant temperature. This temperature is around 30 °C in the case without reformer and 0 °C for the case with reformer. This is due to the position at which the recirculating stream and the syngas input stream are mixed (cf. Figure 4-6 and Figure 4-7).

Table 5-4: Electricity deficit [MW] for varying temperature and pressure for the two boiler configurations (the steam from the boiler is not used to produce electricity) according to Equation [4-28]

Pressure	**w/o Reformer**			**with Reformer**		
[bar]	χ_{CO} **= 0.5**	χ_{CO} **= 0.6**	χ_{CO} **= 0.7**	χ_{CO} **= 0.5**	χ_{CO} **= 0.6**	χ_{CO} **= 0.7**
20	0.71	0.66	0.63	1.91	1.54	1.18
24	2.54	2.38	2.25	2.37	2.10	1.83
30	5.72	5.35	5.06	3.09	2.94	2.74

Figure 5-7 shows this behavior for the boiler configurations at a fixed temperature of 220 °C where the net electricity deficit changes between 0.5 to 6 MW. This happens also for the configuration with reformer but the range of variation is smaller (1 - 3.5 MW) as can be seen from the values in Table 5-4. It seems unexpected that in a system with more compressors and pumps the electricity deficit appears to be less depending on pressure variations. Furthermore, a higher pressure seems to lead to a higher electricity consumption increase without reformer compared to the case with reformer even though the latter case has double the consumer units. This fact can be explained by having a closer look at consumers' operation conditions. First of all, the main consumer COMP1 operates at different temperatures and therefore different enthalpy changes appear across the compressor which have a major impact on its electricity consumption. This impact even increases with an increase in pressure that needs to be achieved. The consumption of the additional compressor COMP2 upstream of the ATR in the case with reformer decreases its consumption with an increase in pressure since the default pressure level that it has to achieve is 30 bar. Both pumps included in the process only have a minor contribution to the electricity consumption and therefore an additional pump does not noticeably increase the consumption.

Table 5-4 as well as Figure 5-7 shows furthermore that the CO conversion leads to a decrease of the electricity deficit. This is based on the fact that the long chain hydrocarbon production increases with a higher CO conversion. Therefore, a lower stream is recycled as well as compressed in COMP1.

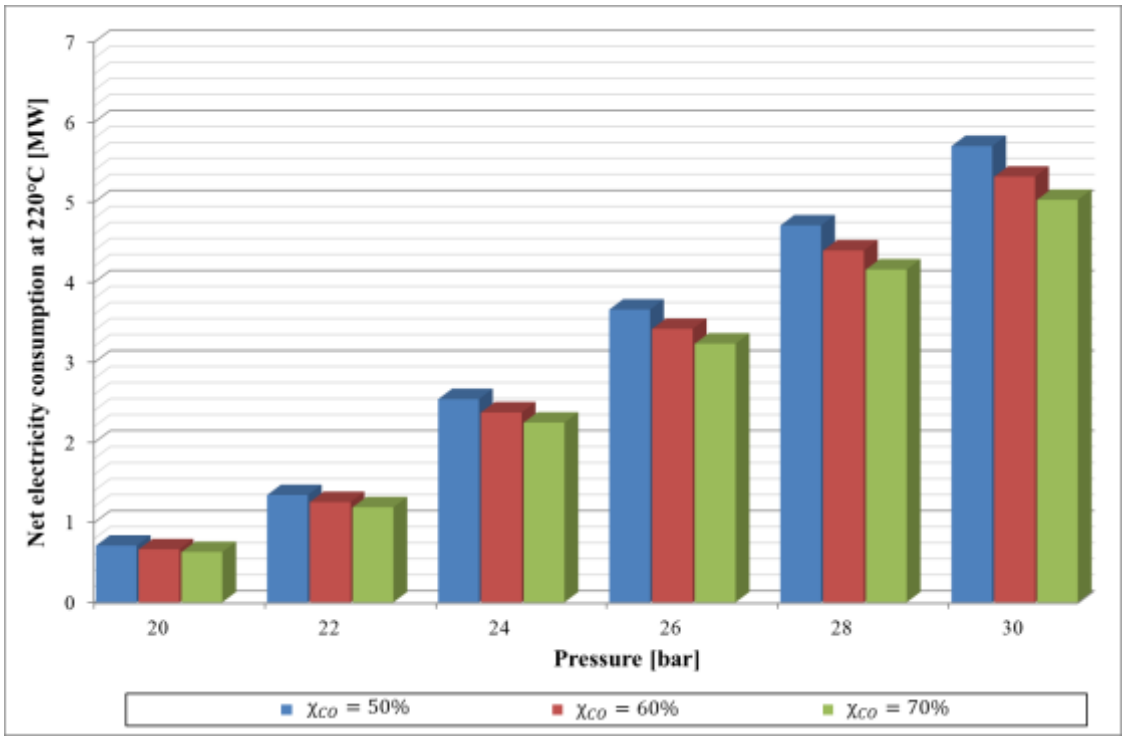

Figure 5-7: Net electricity deficit at 220 °C for the case without reformer calculated with Equation [4-28]

5.4 Electricity balance for the GT configurations

The results for the electricity balance of the GT configurations show an electricity surplus due to the produced electricity in the gas turbine. The electricity consumption for the GT configurations follows the same trends as for the boiler configurations and are therefore not discussed another time.

The electricity production changes with all three parameters. The biggest change is detectable with an increasing temperature. As described before an increase in temperature leads to an increase of light hydrocarbons which conclude in a higher electricity production within the gas turbine. By increasing the CO conversion, however, the electricity production is decreasing which is due to the decreasing amount of light hydrocarbons. Considering the pressure dependence only a minor dependency is detectable. This is due to the fact that the model used in this study is not pressure dependent. However, an increase in pressure leads to a higher flashing performance towards the FT-liquid stream. Therefore, the pressure has a slightly negative effect on the electricity production.

The different dependencies for the electricity consumption and production lead to the electricity surplus being by both pressure and temperature applied in the FT-reactor. A factor that plays an important role in this is the selectivity towards light hydrocarbons which increases at higher temperatures. This results in higher specific mass flows within the recirculating stream FTV110, thus leading to a growing electricity production after the combustion. On the other hand electricity consumption is rising with pressure since the

compressor COMP1 prior to the FT-reactor has to reach a higher pressure level. Therefore, the electricity surplus calculated with Equation [4-28] decreases with pressure as shown in Table 5-5 and Figure 5-7 for the 50% conversion case.

Table 5-5: Net electricity surplus [MW] for varying temperature and pressure for the two GT configurations

Temperature	w/o Reformer			with Reformer		
[°C]	20 bar	24 bar	30 bar	20 bar	24 bar	30 bar
200	68.50	66.27	62.64	16.17	15.66	14.89
220	72.17	69.76	66.00	17.11	16.55	15.71
250	78.26	75.73	71.78	18.73	18.10	17.17

These trends are valid for both gas turbine cases without and with reformer even though the ranges in which the variations occur are different. More specifically, in the former case the net electricity surplus varies between 60 and 80 MW for 50 % conversion whereas in the latter case the interval goes from 10 to 20 MW when moving towards high temperatures and low pressures. The explanation for this big penalty in electricity production when an ATR is applied is connected to the reforming of the recycle stream which increases the fresh syngas converted into FT-products and consequently implies a lower mass flow being purged and going to the combustor.

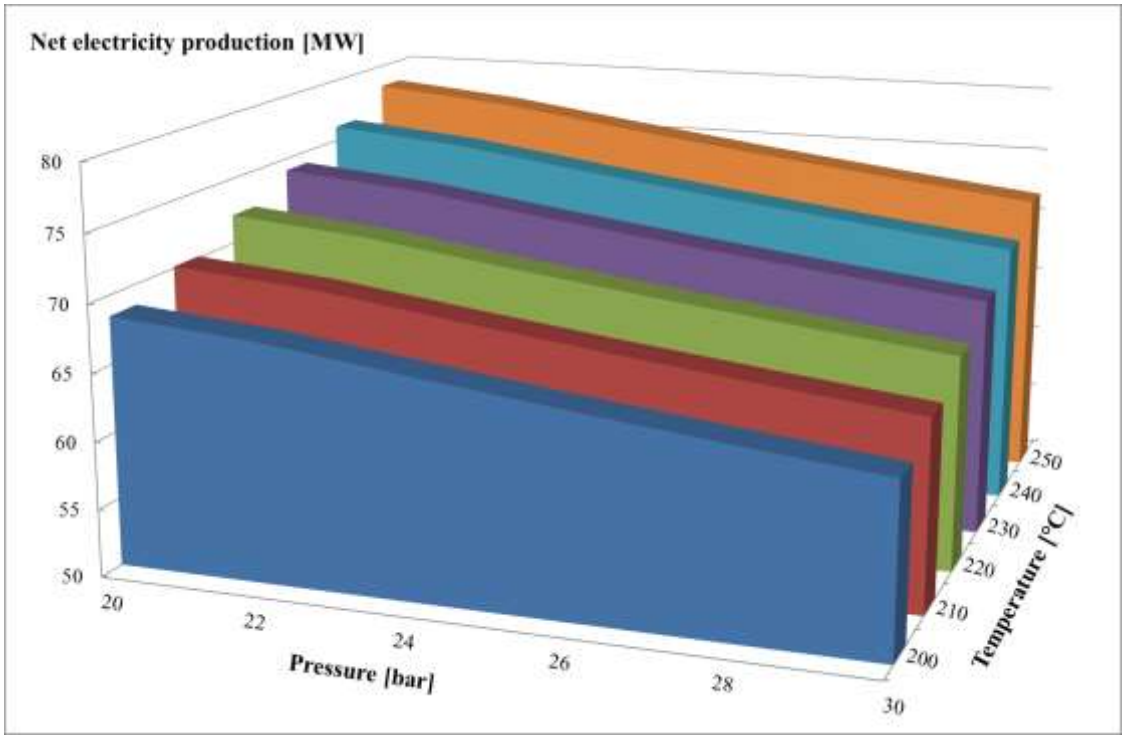

Figure 5-8: Electricity surplus [MW] for the GT base case configuration dependent on the operation pressure and temperature for a CO conversion of 50 %

Furthermore it has been noticed for both cases that the electricity surplus decreases of around 2 MW when CO conversion improves of 10 percentage points. This is mainly due to a higher production of FTL and therefore lower absolute flows diverted to the combustion. The range of variation in the case without reformer is comparable with the results presented in the paper by Ng and Sadhukhan (2011) in which different system capacities are compared. By looking at the plant with 675 MW of capacity, which is close to the energy content of biomass within this thesis, the values for net power generations in Figure 5-7 are in correspondence with the ones obtained by Ng and Sadhukhan (2011). However, this reference includes the power generation from a heat recovery steam cycle which uses the syngas cooling as the main heat supplier.

5.5 Efficiencies

The conversion efficiency η_{conv} (cf. Equation [4-30]) has a slight variation with pressure but a more relevant decrease with the reactor temperature. Figure 5-9 below shows η_{conv} at a constant pressure of 20 bar and for changing temperature. η_{conv} varies in a range between 20 and 35 % which is comparable with intervals for the same conversion efficiency reported in the literature (Iglesias Gonzalez et al. 2011). As expected an increase in temperature decreases the conversion efficiency since the amount of long chain hydrocarbons is lowered.

Figure 5-10 shows the effect of different desired CO conversions on the conversion efficiency. It can be seen that an increase in conversion leads to visible beneficial effects on the efficiency. This is again due to the extended production of long chain hydrocarbons with an increase in CO conversion.

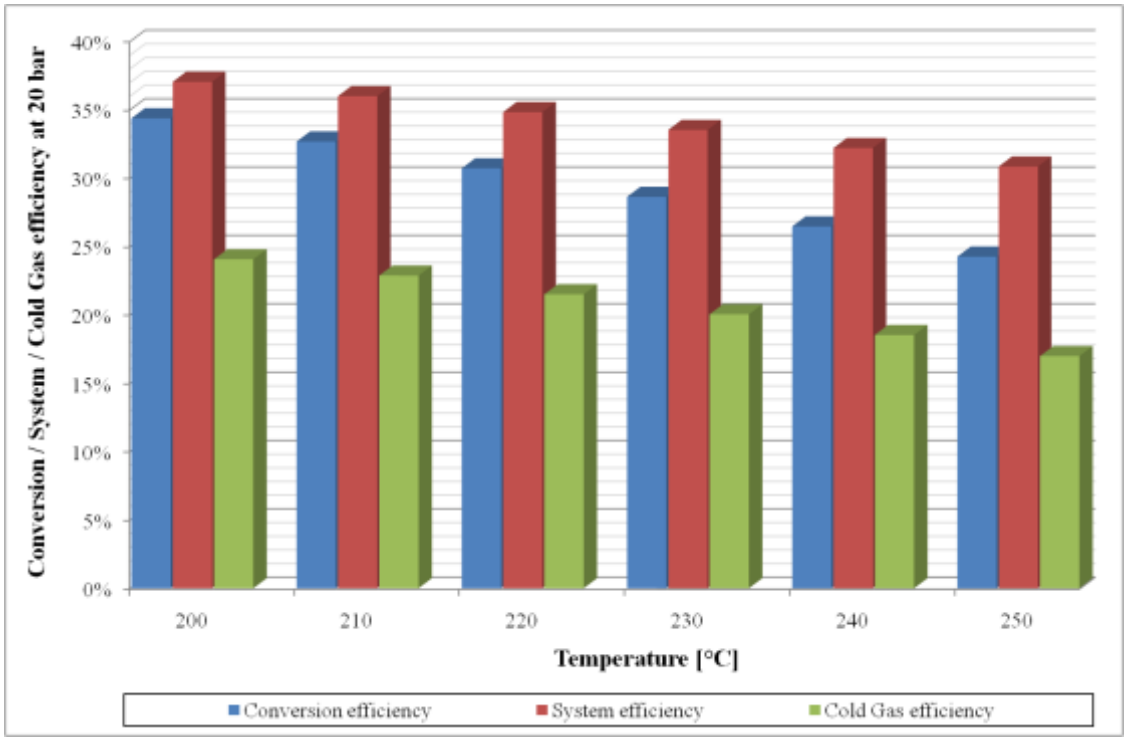

Figure 5-9: Efficiencies of the GT base case for 50 % conversion calculated with the Equations [4-29] to [4-32]

Figure 5-10 furthermore shows that the effect of the CO conversion on the conversion efficiency in the cases with reformer is stronger that in the cases without the reformer. However, it is striking that for a 50 % CO conversion the conversion efficiencies for the two cases are very close to each other and for a temperature of 250 °C the case without reformer even achieves higher conversion efficiency. This can be explained by having a closer look at the definition of the conversion efficiency according to Equation [4-30]. The denominator of this term is a constant value since the composition of the syngas and its mass flow are constant. As a conclusion a change of the conversion efficiency can only be achieved by a change in the mass flow or the distribution of the FTL. As explained in Section 5.1 the amount of produced FTL increases less for the configurations without reformer due to a higher hydrocarbon amount in the recycle stream. Furthermore, an increase in temperature generally concludes in a favored C_{1-4} production. The same facts lead to a steeper increase with CO conversion as well as a stronger decrease with increasing temperature of the conversion efficiency for the configurations with reformer than for the one without.

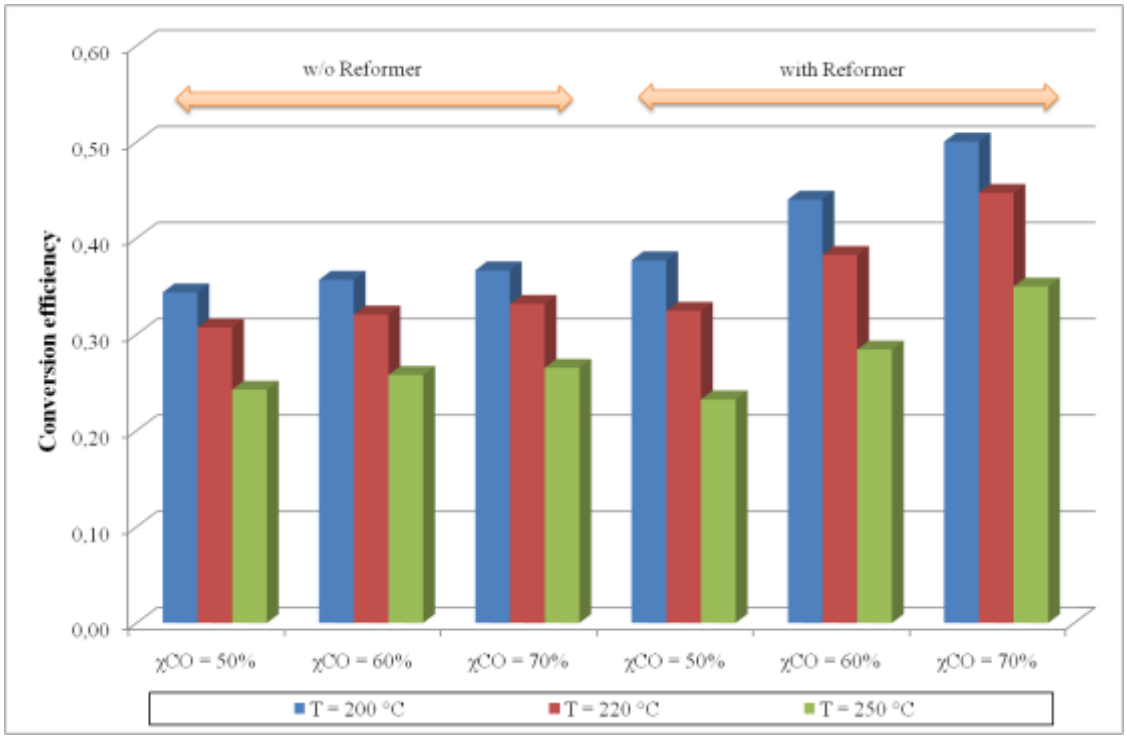

Figure 5-10: Impact of the CO conversion on the conversion efficiency for the GT cases at a 20 bar calculated with Equation [4-32]

A further efficiency closely related to the conversion efficiency is the cold gas efficiency which widens the system boundaries by including the biomass gasification prior to the FT-synthesis (cf. Equation [4-32]). The behavior of the cold gas efficiency with FT-operation temperature, pressure and CO conversion is comparable to the conversion efficiency but at a lower level between 10 – 30 % (cf. Figure 5-9). This is a result of the energy loss during the gasification.

When considering the system efficiency η_{system} (cf. Equation [4-30] and [4-31]) the range for the GT configurations moves to higher levels (30 – 50 %) (cf. Figure 5-9) whereas for boiler configuration it stays in the same range, meaning that the power consumption does not have a big influence on the overall conversion efficiency. Having a closer look at the temperature variation of the system efficiency as shown in Figure 5-11, it is striking that the system

efficiency for the case without reformer is higher than for the one with reformer. This again can be explained by considering the definition of the efficiency according to Equation [4-30]:

$$\eta_{system,GT} = \frac{HHV_{FTL} * \dot{m}_{FTL} + W_{e,net}}{\left(HHV_{Syngas} * \dot{m}_{Syngas} + \dot{m}_{NG} * HHV_{CH_4}\right)_{= \text{const}}} \qquad [4\text{-}30]$$

The denominator of the system efficiency is a constant value since both the syngas and natural gas input are not changing with temperature, pressure or CO conversion. However, the nominator changes a lot. By comparing the values for the energy content in the FTL stream to the net electricity produced it can be concluded that the amount of FTL has a bigger impact on the system efficiency than the net power production which is an order of magnitude smaller. Therefore, a change in temperature leads to a decrease in the amount of FTL and as a result also in the system efficiency. The stronger dependency on FTL is also the reason why the slope is steeper for the case with reformer than without. However, since the values for the energy amount in the FT-crude is close to each other for the two GT configurations the electricity surplus is responsible for η_{system} being higher for the case without reformer since as shown in Section 5.4 the surplus is higher for this case.

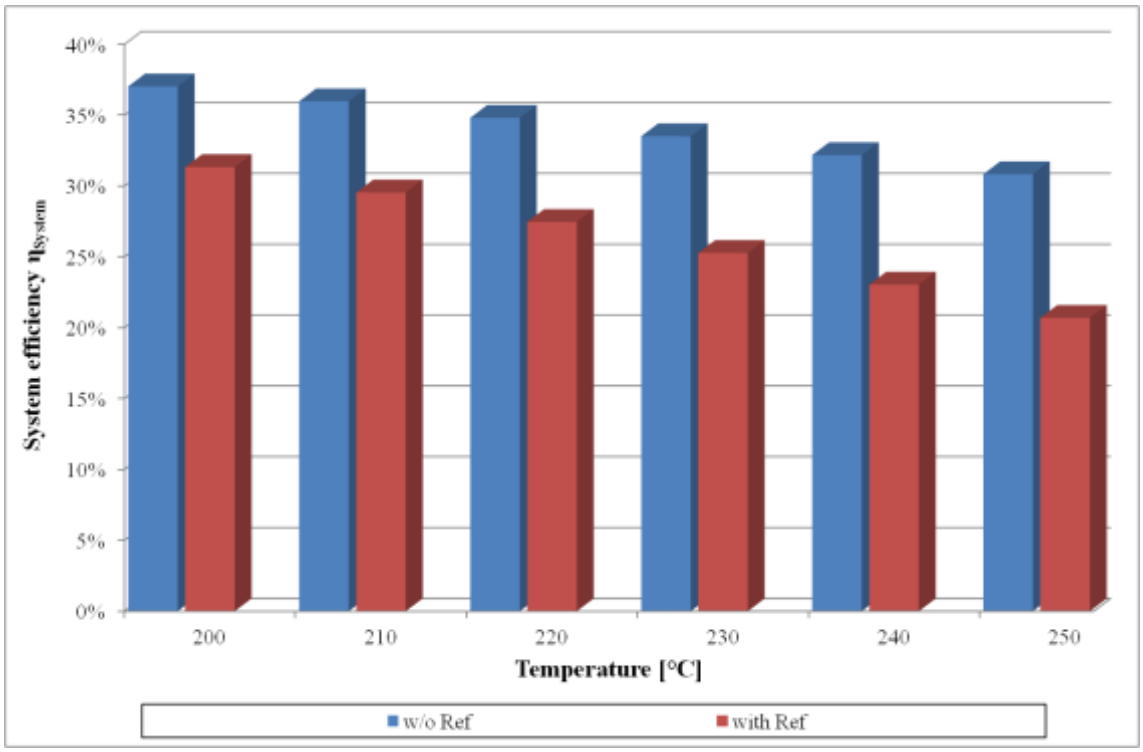

Figure 5-11: System efficiency for both GT configurations and varying temperature

The trend of η_{system} for the boiler configurations which is shown in Figure 5-12 however differs from the one of the GT configurations. It can be seen that η_{system} is first higher for the case with reformer but with an increase in temperature the case without reformer becomes more efficient. This again can be explained by having a look at the equation for η_{system}. The definition for the boiler configurations is once again shown below:

$$\eta_{System,Boiler} = \frac{HHV_{FTL} \cdot \dot{m}_{FTL}}{HHV_{Syngas} \cdot \dot{m}_{Syngas} + W_{e,net}} \qquad [4\text{-}30]$$

The denominator of Equation [4-31] is again constant and only the nominator is responsible for the dependencies of η_{system}. The results for the mass flow of the FT-crude show that the flow is first higher for the case with reformer however it also decreases faster with an increase

in temperature. Therefore, η_{system} for the case without reformer is eventually higher than for the case with reformer.

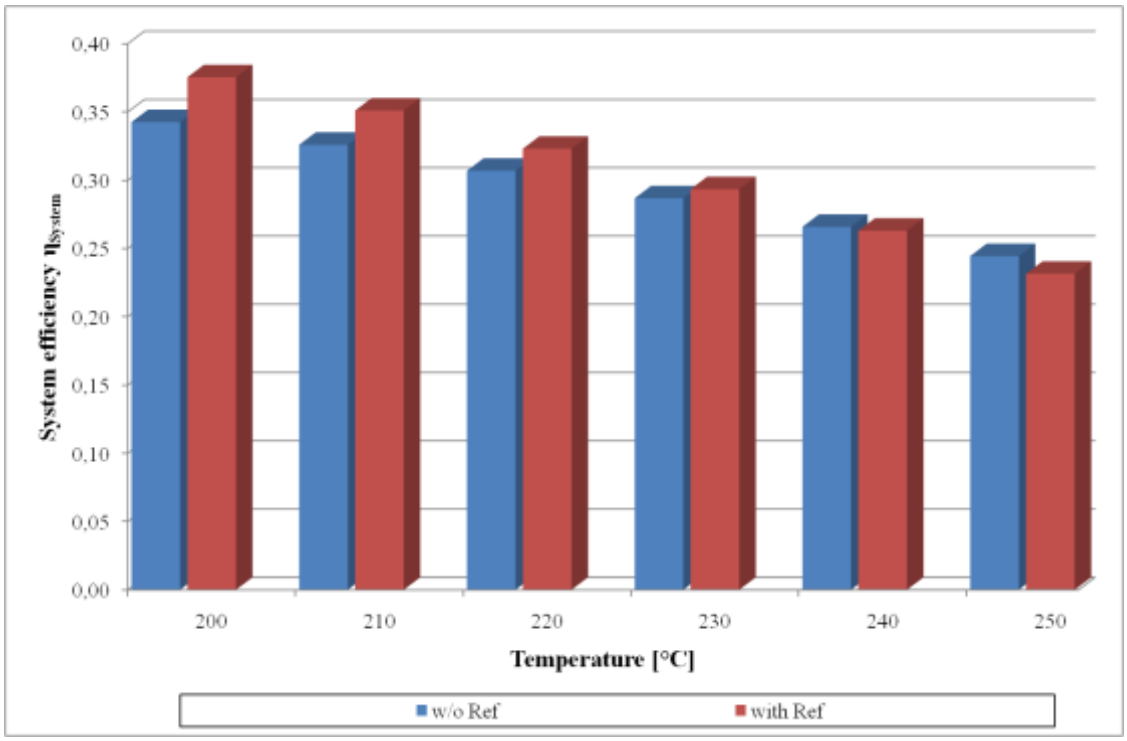

Figure 5-12: System efficiency for both boiler configurations and varying temperature

5.6 Theoretical work potential

To complete the analysis of the system a further investigation of the heat flows of the units in the FT-plant is performed. Therefore, it seems more reasonable to underline the differences between configurations with and without reformer since boiler and gas turbine have similar GCCs and thus Carnot GCCs. From a GCC graph the value of the excess heat produced within the process can be gathered, which also represents the cold utility needed by the process. The Carnot GCC takes into consideration the the maximum theoretical work potential (exergy) of this excess heat as introduced in Section 4.3.

As it can be seen in Figure 5-14 the radiative heat from the boiler (Q_{rad_boiler}) is released at a constant temperature of 1000 °C whereas the convective part is drawn as a line which represents the cooling until 150 °C. The slope of this line varies when other heat streams overlap in the same temperature range.

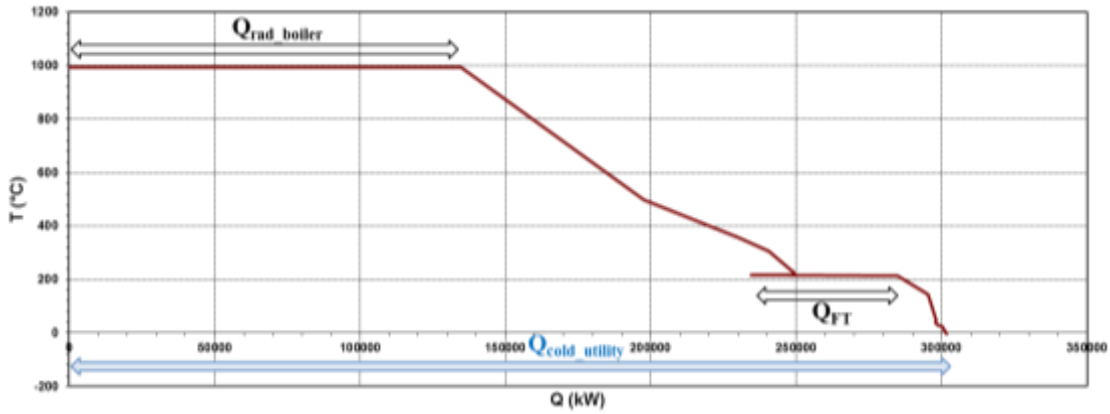

Figure 5-13: GCC for boiler without reformer for the evaluated case 1

From Figure 5-14 it can be noticed that Q_{rad_boiler} is reaching a value of about 130 MW, this quantity decreases to 25 MW for the case with reformer. The higher heat produced in the former case is related to the higher quantity of CH_4 within the recirculating stream. The reason for the CH_4 amount being higher is that it is not reformed to H_2 and CO again and it instead recirculates together with other hydrocarbons thus leading to a higher heating value of the purge stream. On the other hand the heat generated by the exothermal FT-synthesis reaction is increasing in the case with reformer since a higher amount of syngas is converted into FT-products. However, its contribution is less influential on the overall heat excess of the process. This quantity is represented with the blue arrow in Figure 5-14 and its value would be available to produce low pressure steam.

Since this process does not include the gasification which is one of the most relevant sections as far as cooling is concerned, integration of a steam cycle is not considered as an option within this thesis. Theoretical work evaluation is rather evaluated with the Carnot GCC that shows the Carnot factor[5] over the heat.

Table 5-6: Exergy values for the boiler configurations

Evaluated cases	**Exergy**	
	w/o Ref	**with Ref**
χ_{CO} = 50 %; T = 220 °C	**191.95 MW**	**102.74 MW**
χ_{CO} = 60 %; T = 220 °C	187.20 MW	97.74 MW
χ_{CO} = 70 %; T = 220 °C	183.50 MW	93.39 MW
χ_{CO} = 50 %; T = 200 °C	183.64 MW	96.92 MW
χ_{CO} = 50 %; T = 250 °C	206.29 MW	113.84 MW

Furthermore, it is investigated to what extend the exergy is varying with the conversion and temperature in the reactor. Results in Table 5-6 show that in both cases the exergy rate available from the FT-process in form of heat is decreasing with conversion. This is mainly due to lower values for both the radiative and convective heat released by the boiler since a higher mass percentage of FTL products compared to components included in FTV110 is

[5] this factor takes into account the temperature levels of the heat streams and therefore the maximum amount of cold utility that can be applied in other processes.

produced. The temperature increase in the reactor leads to a concurrent increase in the steam production since the heat from both the reaction and the boiler rises. Additionaly, the boiler contribution is higher in this case due to the bigger amount of light hydrocarbons produced at higher temperatures. From Figure 5-15 and Figure 5-16 it can be clearly noticed how the exergy rate, namely the area between the Carnot GCC and the horizontal axis is decreasing for the case with reformer.

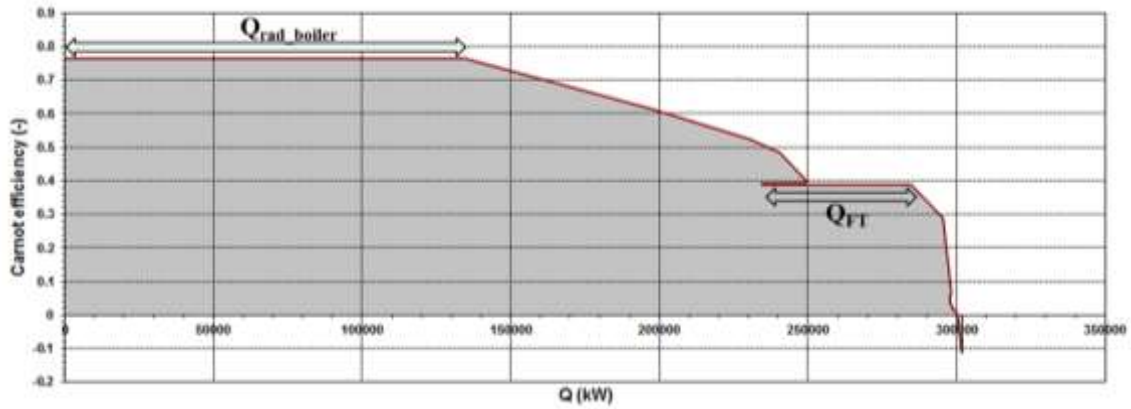

Figure 5-14: Carnot GCC for the boiler configuration without reformer at 220 °C, 20 bar and a CO conversion of 50 %

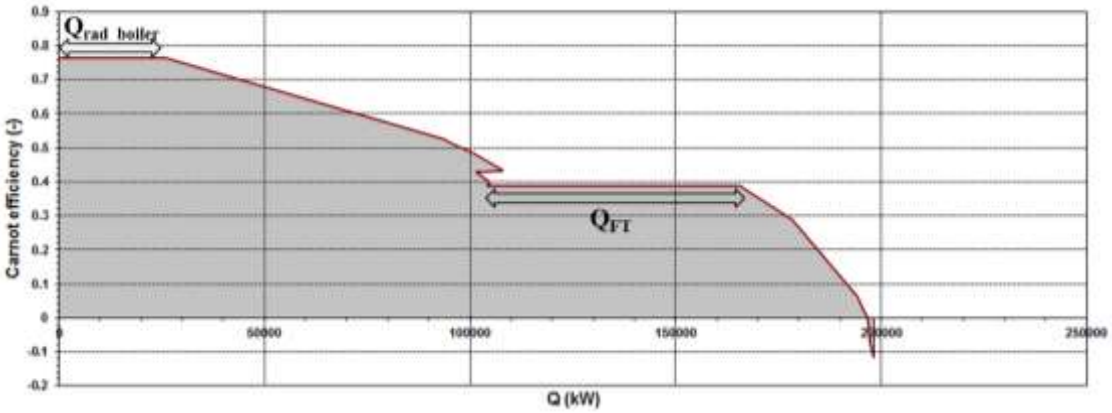

Figure 5-15: Carnot GCC for the boiler configuration with reformer at 220 °C, 20 bar and a CO conversion of 50 %

In the GCC for the GT configurations the heat released is represented as a line that starts from around 800 °C (turbine outlet temperature) and reaches 150 °C with cooler HX8. Figure 5-17 shows the GCC for the GT without reformer configuration. The process excess heat in this case accounts for approximately 214.6 MW which is shown with the blue arrow.

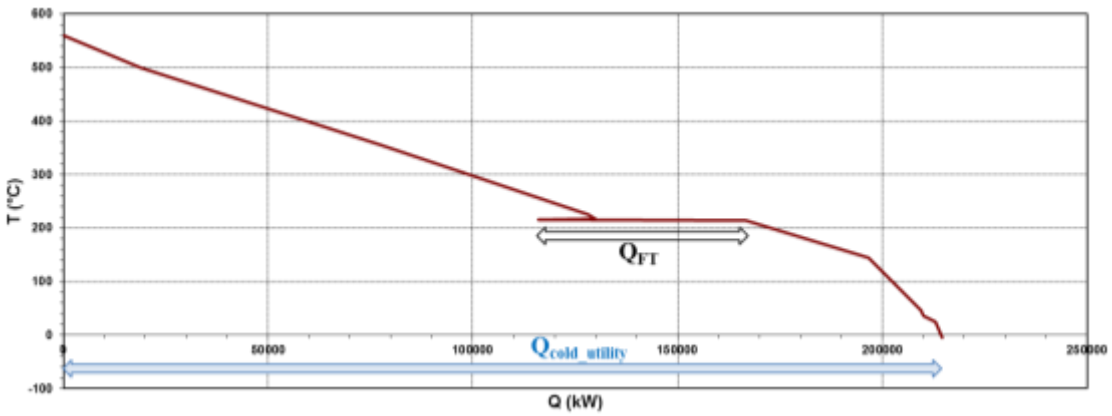

Figure 5-16: GCC for the GT configurations without reformer at 220 °C, 20 bar and a CO conversion of 50 %

Similar to the boiler configurations the amount of excess heat decreases in case a ATR is added. This again is due to the lower amount of CH_4 and other hydrocarbons in the stream entering the GT. However, the variation between these two cases is not as distinctive as for the boiler cases since the major contribution was previously coming from the boiler itself. It can nevertheless be stated that the principal factor that influnces the excess heat is the cooling requirement of the exhaust gases after the turbine which has a smaller mass flow for the case with reformer. This is due to the higher production of FT-liquids and therefore a small flow rate for the recirculating stream.

More meaningful results for these cases are obtained by evaluating the theoretical possible work production. For this analysis the Carnot GCC is again used. The values for the calculated area underneath the Carnot GCC are shown in Table 5-7.

Table 5-7: Exergy values for the GT configurations

Evaluated cases	**Exergy**	
	w/o Ref	**with Ref**
χ_{CO} = 50 %; T = 220 °C	**96.23 MW**	**84.38 MW**
χ_{CO} = 60 %; T = 220 °C	94.91 MW	81.89 MW
χ_{CO} = 70 %; T = 220 °C	93.87 MW	79.89 MW
χ_{CO} = 50 %; T = 200 °C	92.92 MW	80.05 MW
χ_{CO} = 50 %; T = 250 °C	101.94 MW	92.77 MW

Table 5-7 highlights that higher conversions have a negative impact on the exergy due to an increased production of FTL. This leads to a decreasing of the purge stream which concludes in a lower air stream to GT boiler and therefore lower outlet temperature. It can further be observed that a growing temperature for the synthesis reaction generates more heat within the reactor together with a higher amount of C_{1-4} compounds being burnt after the split and reformed in the recycle. These variations in the exergy rate are about 4-6 MW whereas the ones between the case "with" and "without reformer" are close to 12 MW, this can also be noticed from the different areas in the Carnot GCCs in Figure 5-18 and Figure 5-19 below.

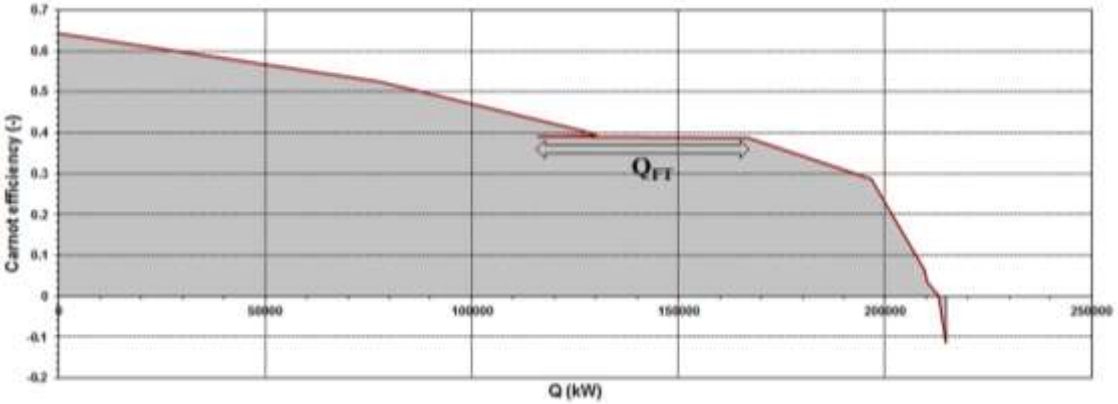

Figure 5-17: Carnot GCC for the GT configuration without reformer at 220 °C, 20 bar and a CO conversion of 50 %

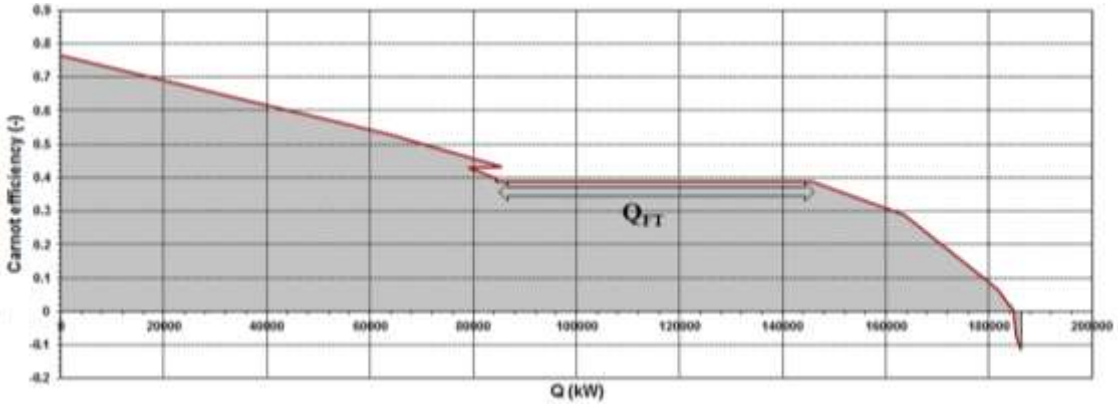

Figure 5-18: Carnot GCC for the GT configuration with reformer at 220 °C, 20 bar and a CO conversion of 50 %

By comparing Table 5-6 and 5-7 it can be noticed that in the boiler configurations there is a really high amount of excess heat which has not been taken into account in the calculations for the efficiencies. However, not all of the excess heat can be converted into work consequently only the theoretical work potential can be included in η_{system} to avoid an underestimation of efficiency. The theoretical maximum system efficiency considering the exergy is calculated as shown below:

$$\eta_{Syst+Exergy,\,Boiler} = \frac{HHV_{FTL}\cdot\dot{m}_{FTL}+Exergy}{HHV_{Syngas}\cdot\dot{m}_{Syngas}+W_{e,net}} \qquad [5\text{-}1]$$

$$\eta_{Syst+Exergy,\,GT} = \frac{HHV_{FTL}\cdot\dot{m}_{FTL}+W_{e,net}+Exergy}{HHV_{Syngas}\cdot\dot{m}_{Syngas}+\dot{m}_{NG}*HHV_{CH_4}} \qquad [5\text{-}2]$$

It is striking from the results in Figure 5-20 below that, when considering also the exergy, boiler configurations have a higher system efficiency compared to GT ones. This value can reach up to 70 % for a reactor temperature of 200 °C. The trends with temperature are the same as explained before for η_{system} and the comparison between the cases with and without reformer can be justified once again by looking at the equations applied. Namely, since the denominator of Equation [5-1] and [5-2] stay constant the major influence is related to the numerator where the magnitude of the exergy is now comparable with the energy content of

FTL. Since the decrease in exergy content in the boiler with reformer configuration is around 90 MW, due to the big difference in Q_{rad_boiler}, whereas the increase in energy content of FTL is around 20 MW, the system efficiency decreases for the case without reformer. The same is valid for GT configurations but to a smaller extent since the difference in the exergy is not as relevant as for the boiler configurations.

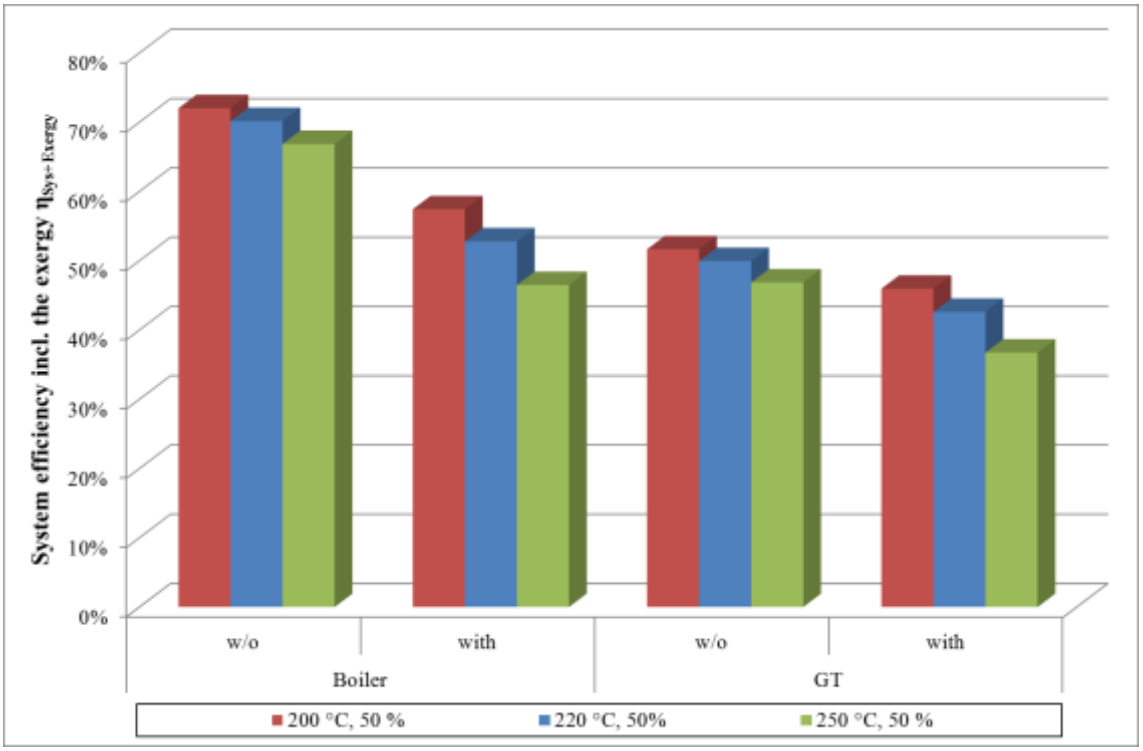

Figure 5-19: Comparison of the theoretical maximum conversion efficiencies for all configurations at 20 bar

5.7 General remarks

In order to be able to evaluate the contribution of the autothermal reformer in avoiding the production of hydrogen through the WGS a further look into the streams around this unit was considered. Therefore the parametric study has included the outlet H_2 stream coming from the WGS and the syngas stream S120 which is split from the initial syngas and reacting in the shift reactor. Their mass flows are indicators of how much shifting is required to achieve the desired H_2/CO ratio at the entrance of the reactor. As expected for the case without reformer the two streams stay constant with pressure and temperature and have the same values both for boiler and gas turbine (cf. Table 5-8). This is related to the required H_2/CO ratio fixed before mixing with the recycle stream.

Table 5-8: Mass flows for H_2 and S120 for the case without reformer at 220 °C, 20 bar and a CO conversion of 50 %

w/o Reformer	
H_2 after WGS [kg/s]	Syngas stream S120 [kg/s]
0.743	71.533

Differently, in case with reformer, the H_2/CO ratio is fixed after mixing with the reformed stream. In this way it is possible to compare the quantity of H_2 produced within the WGS reactor by taking into account the relevant influence of the H_2 produced with the ATR. Table 5-9 below shows the mass flows of the H_2 produced in the WGS and of the syngas guided to the shift reactor. It can be concluded that compared to the case without reformer the values of hydrogen to be produced with the WGS are much lower. Furthermore these flows are increasing when the FT-synthesis reactor works at higher temperatures. This is due to the bigger amount of CO left after FT-synthesis together with higher fractions of light hydrocarbons. Therefore, the contribution of the WGS is required even more in order to achieve the optimal compositions for the syngas. The same phenomenon occurs when the FT-operation pressure increases.

Table 5-9: Mass flows for H_2 and S120 for the case with reformer at a CO conversion of 50 %

Temperature	H_2 after WGS [kg/s]			Syngas stream S120 [kg/s]		
[°C]	p = 20 bar	p = 24 bar	p = 30 bar	p = 20 bar	p = 24 bar	p = 30 bar
200	0.14	0.17	0.20	1.41	1.69	2.04
220	0.26	0.28	0.31	2.64	2.88	3.18
250	0.43	0.45	0.48	4.36	4.59	4.89

When considering the conversions in the reactor a higher amount of hydrogen is needed in order to push more of the reaction towards the products. The results confirm this statement since an increase of about 0.3 kg/s of H_2 from the WGS is required when the conversion is increased of 10 percentage points.

To conclude, the utilisation of a reformer helps to a big extent in avoiding the WGS but its contribution is not high enough to completely avoid this part of the system. The major reason for this is the assumption made for the composition of the syngas which in more favourable cases would be good enough to avoid the implementation of a shift reactor.

6 Conclusions

The production of biofuels via a low temperature Fischer-Tropsch (FT) synthesis could potentially increase the utilization of biofuels without having to change the currently used combustion engines. To gain knowledge about this synthesis four different process configurations have been modelled starting from cleaned biomass derived syngas and ending in a stream of FT-crude. The configurations were further investigated with a parametric study which mainly focused on different FT-operation temperatures, pressures and desired CO conversions and their effects on product quality and process efficiency.

The main differences between the four configurations regard the way the recycled stream is handled and what is the final utilization of the purge gas (which flow was fixed to 10 % of the total flow of light gases obtained at the top of the reactor product condensation). The purge gas is either burned in a boiler or used to fuel a gas turbine. Two different options are also considered for processing the gas recycle into the reactor. The first case recycles the flow without any further treatment, thus including hydrogen, carbon monoxide, carbon dioxide and light hydrocarbons as well as a possible but low amount of water vapour. The second case, however, reforms the light hydrocarbons in the recirculating flow in an ATR. Therefore, only a small amount of methane recirculates and all the rest of it is converted into hydrogen and carbon monoxide. This results in the following four modelled configurations:

- Gas turbine without reformer
- Gas turbine with reformer
- Boiler without reformer
- Boiler with reformer

One major outcome of the parametric study is the product distribution within the FT-liquid stream. It was shown that the case with reformer leads to a higher amount of FT-liquids compared to the case without reformer. However, it is valid for both cases that the amount of FT-liquids increases with an increase in CO conversion and decreases with an increase in operation temperature. Even though the α-model for the FT-reactor, which describes the hydrocarbon chain length distribution within the product stream, does not have a direct correlation to the pressure, a marginal change of the FT-liquid amount was detectable with an increase in pressure due to a favourable flashing process with a higher pressure.

The effect of temperature and desired CO conversion on the required amount of catalyst and the FT-reactor volume has also been studied. The parametric study resulted in no dependence on the pressure but a steady decrease of the catalyst amount and therefore also reactor volume with an increase of reactor temperature. However, this is only rigorously true for the case with reformer since the H_2/CO ratio was fixed right before the FT-reactor and therefore stayed constant at a value of 2. For the case without reformer the ratio was fixed before mixing the recirculating stream which led to a changing ratio from approximately 2.2 down to 1.6. This, furthermore, resulted in a lack of H_2 with an increase in temperature and CO conversion and an exponential increase in the catalyst amount. Considering both the catalyst amount and the quantity of FT-liquids a trade-off between low catalyst consumption and high FT-liquid production appears with a change in temperature.

Another indicator that has been evaluated is the electricity balance which is representing the absolute value of the difference between electricity production and electricity consumption. An electricity production is only present in the GT configurations and is in this study always higher than the electricity consumption for these configurations which results in an electricity

surplus for the GT configurations whereas the boiler configurations only include electricity consumers which leads to an electricity deficit.

While evaluating the electricity consumption it can generally be concluded that the consumption increases with an increase in pressure and CO conversion. The temperature, however, does not have a big impact on the consumption. Furthermore, it was shown that the electricity consumption is higher for the cases without reformer than for the ones with reformer.

The results for the electricity production show that it changes with all three parameters. The biggest change is detectable with an increasing temperature which leads to an increase in the electricity production. A slightly smaller impact is caused by the CO conversion concluding in a decrease of the electricity production. At last only a minor decrease occurs with an increase in pressure. By comparing the GT configurations, the results show that the electricity production reaches a higher value for the case without reformer than for the case with reformer.

The values of three different efficiencies have also been discussed. The efficiencies considered in this work are: conversion efficiency, cold gas efficiency and system efficiency. The conversion efficiency (η_{conv}) varies for the case without reformer from 25 to approximately 40 %. For the case with reformer, it reaches up to 50 %. It can therefore be stated that the cases with reformer seem to be more efficient considering the conversion efficiency. Generally, η_{conv} increases with an increase in CO conversion and slightly with an increase in pressure. However, an increase in temperature leads to a decrease in η_{conv}. The cold gas efficiency (η_{CG}) reaches lower levels compared to η_{conv} since this one includes the conversion within the gasification step and considers as an input the actual biomass that enters the gasification process. These values behave in the same way as the conversion efficiency.

The evaluation of the system efficiency (η_{system}) showed that it does not change noticeable for the boiler case compared to η_{conv}. However, η_{system} changes compared to η_{conv} for the GT configurations. For the case without reformer η_{system} increases compared to η_{conv} whereas for the case with reformer it decreases. It was also noticeable that η_{system} decreases faster with an increase in temperature for the cases with reformer than for the one without. This results in the cases without reformer to be more efficient for high temperature.

The last indicator was the available work from the heat streams. Since this process does not include the gasification which is one of the most relevant sections as far as cooling is concerned, integration of a steam cycle is not considered as an option within this thesis. Therefore, the theoretical work is evaluated with the Carnot GCC. The available thermal exergy rate for the cases with reformer is higher than for the ones without reformer. For the boiler cases this value differs by about 100 MW whereas for the GT cases it only differs by 10 MW. It can also be noticed that the available thermal exergy rate for the GT configurations is always smaller than for the boiler configurations since the boiler adds a big contribution to the available heat. Furthermore, the parametric study showed that the exergy rate is generally increasing with temperature but decreasing with higher CO conversion.

As a conclusion, Figure 6-1 shows a summary of the trends for the indicators studied in the parametric study according to an increase of the parameters. It can be generally said that an increase of the CO conversion has a positive impact on the FT-synthesis since e.g. the long chain hydrocarbons in the FT-crude stream increase and the electricity consumption decreases. The pressure only has minor impact on most of the indicators which is based on the fact that the α-model is not dependent on the pressure. At last, an increase in temperature has a generally negative effect on the FT-synthesis shifting the operation more towards the characteristics of a conventional power plant.

Indicators	Temperature	Pressure	CO conversion
FTL - C_{5+}	↓	↑	↑
FTL - C_{1-4}	↑	↑	↑
Catalyst	↓	–	↑
η_{conv}, η_{GC}	↓	–	↑
η_{system}	↓	–	↑
Consumption	–	↑	↓
Production	↑	↓	↓
Exergy	↑	–	↓

Figure 6-1: Trends for all investigated indicator according to an increase of the parameter temperature, pressure and CO conversion

At last, it was also of interest whether or not the water gas shift prior to the FT-synthesis could be avoided in the cases with reformer. The results show that a big decrease in utilization of the water gas shift reactor was possible but it couldn't be fully avoided.

All in all it can be said that in this study the most significant effects of reactor operating parameters on general performance indicators have been identified and general trends of such effects understood.

The model of the FT-reactor provided by this study can be used in the future to investigate a more complete process where the syngas production, e.g. by biomass gasification, as well as the followed upgrading of the FT-crude to motor fuels is also included. The major advantage of this model with respect to other literature models is that kinetic has been taken into account. This enables the possibility to consider the trade-off between the product quality and quantity and the FT-synthesis reactor volume and catalyst amount.

7 References

Shell MDS Technology and Process - Malaysia. http://www.shell.com.my/products-services/solutions-for-businesses/smds/process-technology.html. Accessed 22 January 2013.

Borg, Ø., Hammer, N., Enger, B. C., Myrstad, R., Lindvåg, O., Eri, S., et al. (2011). Effect of biomass-derived synthesis gas impurity elements on cobalt Fischer-Tropsch catalyst performance including in situ sulphur and nitrogen addition. *Journal of Catalysis, 279*, 163–173.

Calemma, V., Gambaro, C., Parker, W. O. Jr., Carbone, R., Giardino, R., & Scorletti, P. (2010). Middle distillates from hydrocracking of FT waxes: Composition, characteristics and emission properties. *Catalysis Today, 149*, 40–46.

Chang, T. (2000). South African Company Commercializes new F-T process. *Oil & Gas Journal, 98*(2), 42–45.

Da Silva, F. A., & Rodrigues, A. E. (2001). Vacuum Swing Adsorption for Propylene/Propane Separation with 4A Zeolite. *Industrial & Engineering Chemistry Research, 40*, 5758–5774.

de Klerk, A. (2007). Environmentally friendly refining: Fischer-Tropsch versus crude oil. *Green Chemistry, 9*, 560–565.

Dry, M. E. (1981). The Fischer-Tropsch process - Commercial aspects, 183–206.

Dry, M. E. (2004). Present and future applications of the Fischer–Tropsch process. *Applied Catalysis A: General, 276*(1-2), 1–3.

Dry, M. E. (2010). Fischer-Tropsch Synthesis - Industrial. In I. T. Horváth (Ed.), *Encyclopedia of catalysis*. Hoboken, N.J: Wiley-Interscience.

Elbashir, N. O. (Ed.) (2010). *Opportunities for elective control of Fischer-Tropsch synthesis hydrocarbons product distribution*. 2nd Annual Gas Processing Symposium, Qatar, 10.-14. January 2010.

Eldridge, R. B. (1993). Olefin/Paraffin Separation Technology: A Review. *Industrial & Engineering Chemistry Research, 32*, 2208–2212.

Swedish Energy Agency (2013). Energy in Sweden - facts and figures 2012. Energimyndigheten. http://www.energimyndigheten.se/en/Facts-and-figures1/Publications/.

(2007). Regulation (EC) No 715/2007. In *Official Journal of the European Union*, vol. 171 (pp. 1–16).

(2009). Directive 2009/30/EC: EN 590. In *Official Journal of the European Union*, vol. 140 (pp. 88–113).

Fatih Demirbas, M. (2009). Biorefineries for biofuel upgrading: A critical review. *Applied Energy, 86*, S151–S161.

Fogler, H. S. (1999). *Elements of chemical reaction engineering*, 3rd edn. Upper Saddle River, NJ: Prentice Hall International.

Göransson, K., Söderlind, U., He, J., & Zhang, W. (2011). Review of syngas production via biomass DFBGs. *Renewable and Sustainable Energy Reviews, 15*, 482–492.

Guczi, L., & Erdôhelyi, A. (2012). *Catalysis for alternative energy generation.* New York, NY: Springer.

Hamelinck, C., FAAIJ, A., DENUIL, H., & BOERRIGTER, H. (2004). Production of FT transportation fuels from biomass: technical options, process analysis and optimisation, and development potential. *Energy, 29*(11), 1743–1771.

Heyne, S., & Harvey, S. (2013). Impact of choice of CO2 separation technology on thermo-economic preformance of Bio-SNG production processess. *International Journal of Energy Research.*

Iglesias Gonzalez, M., Kraushaar-Czarnetzki, B., & Schaub, G. (2011). Process comparison of biomass-to-liquid (BTL) routes Fischer-Tropsch synthesis and methanol to gasoline. *Biomass Conversion and Biorefinery, 1*, 229–243.

James, O. O., Chowdhury, B., Mesubi, M. A., & Maity, S. (2012). Reflections on the chemistry of the Fischer-Tropsch synthesis. *RSC Advances, 2012, 2*, 7347–7366.

Jin Hu, F. Y. L. (2012). Application of Fischer…Tropsch Synthesis in Biomass to Liquid Conversion. *Catalysts*, 303–326.

Johansson, D., Frank, P.-Å., & Berntsson, T. (Eds.) (2012). *Integration of Fischer-Tropsch Diesel Production with a Complex Oil Refinery*. 7th Conference on Sustainable Development of Energy, Water and Environmental Science, Ohrid, Republic of Macedonia, July 1-7, 2012.

Keyser, M. J., Everson, R. C., & Espinoza, R. L. (2000). Fischer-Tropsch Kinetic Studies with Cobalt-Manganese Oxide Catalysts. *Industrial & Engineering Chemistry Research, 39*(1), 48–54.

Krishna, R., & Sie, S. T. (2000). Design and scale-up of the Fischer–Tropsch bubble column slurry reactor. *Fuel Processing Technology, 64*, 73–105.

Krylova, A. Y., & Kozyukov, E. A. (2007). State-of-the-art processes for manufacturing synthetic liquid fuels via the Fischer-Tropsch synthesis. *Solid Fuel Chemistry, 41*(6), 335–341.

Kågeson, P. (2013). Dieselization in Sweden. *Energy Policy, 54*, 42–46.

Leibbrandt, N. H., Aboyade, A. O., Knoetze, J. H., & Görgens, J. F. (2013). Process efficiency of biofuel production via gasification and Fischer-Tropsch synthesis. *Fuel*.

Luque, R., de la Osa, A. R., Campelo, J. M., Romero, A. A., Valverde, J. L., & Sanchez, P. (2012). Desing and development of catalysts from Biomass-To-Liquid-Fischer-Tropsch (BTL-FT) processes for biofuels production. *Energy & Environmental Science, 5*, 5186–5202.

Lu, Y., & Lee, T. (2007). Influence of the Feed Gas Composition on the Fischer-Tropsch Synthesis in Commercial Operations. *Journal of Natural Gas Chemistry, 16*(4), 329–341.

Maitlis, P. M., & de Klerk, A. (2013). *Greener Fischer-Tropsch Processes for Fuels and Feedstocks*, 1st edn. s.l: John Wiley & Sons; Wiley-VCH.

Milne, T. A., Evans, R. J., & Abatzoglou, N. (1998). *Biomass Gasifier "Tars": Their Nature, Formation and Conversion.* Golden, USA.

Naik, S. N., Goud, V. V., Rout, P. K., & Dalai, A. K. (2010). Production of first and second generation biofuels: A comprehensive review. *Renewable and Sustainable Energy Reviews, 14*, 578–597.

Ng, K. S., & Sadhukhan, J. (2011). Techno-economic performance analysis of bio-oil based Fischer-Tropsch and CHP synthesis platform. *Biomass and Bioenergy, 35*(7), 3218–3234.

Panahi, M., Skogestad, S., & Yelchuru, R. (Eds.) (2010). *Steady State Simulation for Optimal Design and Operation of a GTL Process*. 2nd Annual Gas Processing Symposium, Qatar, 10.-14. January 2010.

Rane, S., Borg, Ø., Rytter, E., & Holmen, A. (2012). Relation between hydrocarbon selectivity and cobalt particle size for alumina supported cobalt Fischer–Tropsch catalysts. *Applied Catalysis A: General, 437-438*, 10–17.

Rapier, R. (2008). Renewable Diesel. In D. Pimentel (Ed.), *Biofuels, Solar and Wind as Renewable Energy Systems*: *Benefits and Risks* (pp. 153–171): Springer Netherlands.

Reichling, J., & Kulacki, F. (2011). Comparative analysis of Fischer–Tropsch and integrated gasification combined cycle biomass utilization. *Energy, 36*(11), 6529–6535.

Schulz, H. (1999). Short history and present trends of Fischer-Tropsch synthesis. *Applied Catalysis A: General, 186*, 3–12.

Shi, B., & Davis, B. H. (2005). Fischer-Tropsch synthesis: The paraffin to olefin ratio as a function of carbon number. *Catalysis Today, 106*(1), 129–131.

Sie, S. T., & Krishna, R. (1999). Fundamentals and selection of advanced Fischer–Tropsch reactors. *Applied Catalysis, 186*, 55–70.

Song, H.-S., Ramkrishna, D., Trinh, S., & Wright, H. (2004). Operating Strategies for Fischer-Tropsch Reators: A Model-Directed Study. *Korean Journal of Chemical Engineering, 21*(2), 308–317.

Steynberg, A., & Dry, M. (2004). *Fischer-Tropsch Technology*. Chemical, Petrochemical & Process: Elsevier.

Tijmensen, M. J., Faaji, A. P., Hamelinck, C. N., & van Hardeveld, M. R. (2002). Exploration of the possibilities for production of Fischer Tropsch liquids and power via biomass gasification. *Biomass and Bioenergy, 23*, 129–152.

van der Laan, G. P., & Beenackers, A. A. C. M. (1998). Alpha-olefin readsorption product distribution model for the gas-solid Fischer-Tropsch synthesis. *Studies in Surface Science and Catalysis, 119*, 179–183.

van der Laan, G. P., & Beenackers, A. A. C. M. (1999). Kinetics and Selectivity of the Fischer-Tropsch Synthesis: A Literature Review. *Catalysis Reviews: Science and Engineering, 31*(3-4), 255–318.

van Steen, E., & Claeys, M. (2008). Fischer-Tropsch Catalysts for the Biomass-to-Liquid (BTL)-Process. *Chemical Engineering & Technology, 31*(5), 655–666.

van Vliet, O. P., Faaij, A. P., & Turkenburg, W. C. (2009). Fischer–Tropsch diesel production in a well-to-wheel perspective: A carbon, energy flow and cost analysis. *Energy Conversion and Management, 50*(4), 855–876.

Vassilev, S., Baxter, D., Andersen, L. K., & Vassileva, C. G. (2010). An overview of the chemical composition of biomass. *Fuel, 89*(5), 913–933.

Wall, G. (2004). Exergy. In C. J. Cleveland (Ed.), *Encyclopedia of Energy* (pp. 593–606). Amsterdam: Elsevier.

Yates, I. C., & Satterfield, C. N. (1991). Intrinsic Kinetics of the Fischer-Tropsch Synthesis on a Cobalt Catalyst. *Energy & Fuels, 5*, 168–173.

Yermakova, A., & Anikeev, V. (2000). Thermodynamic Calculations in the Modeling of Multiphase Processes and Reactors. *Industrial & Engineering Chemistry Research*, *39*(5), 1453–1472.

Yuan, W., Vaughan, G. C., Roberts, C. B., & Eden, M. R. (2011). Modeling and Optimization of Supercritical Phase Fischer-Tropsch Synthesis. *21st European Symposium on Computer Aided Process Engineering*, *29*, 1929–1933.

Zimmerman, W. H., & Bukur, D. B. (1990). Reaction Kinetics over Iron Catalysts used for Fischer-Tropsch. *Canadian Journal of Chemical Engineering*, *68*, 292–301.

Zwart, R. W. R., & Boerrigter, H. (2005). High Efficiency Co-production of Synthetic Natural Gas (SNG) and Fischer-Tropsch (FT) Transportation Fuels from Biomass. *Energy & Fuels*, *19*, 591–597.

CHALMERS UNIVERSITY OF TECHNOLOGY
SE 412 96 Göteborg, Sweden
Phone: + 46 - (0)31 772 10 00
Web: www.chalmers.se